MODELING HEAT TRANSFER IN MASS CONCRETE FLOORS WITH RADIANT HEAT FROM GROUND SOURCE SYSTEMS

By

MOHAMMAD TAHERSIMA

Bachelor of Science
University of Tehran
Tehran
2008

Master of Science
Iran University of Science and Technology
Tehran
2011

Submitted to the Faculty of the
GraduateCollege of the
OklahomaStateUniversity
in partial fulfillment of
the requirements for
the Degree of
DOCTOR OF PHILOSOPHY
May, 2017

MODELING HEAT TRANSFER IN MASS CONCRETE FLOORS WITH RADIANT HEAT FROM GROUND SOURCE SYSTEMS

Dissertation Approved:

Paul J. Tikalsky

Bruce W. Russell

M. Tyler Ley

Jeffrey D. Spitler

ACKNOWLEDGEMENTS

The research has been conducted at the Bert Cooper Laboratory, Oklahoma State University. I would like to thank Dr. Bruce Russell, Director of Bert Cooper Laboratory and OSU long range planningfor cooperating with the experimental protocols in this building from the first day of construction until the present time.

I would like to express my appreciationto my advisor, Dean. Paul Tikalsky, for his great support during my research and it is an honor to work as his PhD student. I would like to thank Dr. Tyler Ley who helped me during my research with his great recommendation and job site instrumentation.

Further thanks goes to facilities managerat Oklahoma State University, Patrick Wheeler and former facilities manager, Yvonne Roberts who kept me connected to control the building systems. I would like to thank Roshan Revankar from the International Ground Source Heat Pump Association for his counsel.

I really want to thank the expert HVAC controls technician, Robert Bradley, for his great collaboration in operating the different heating or cooling systems throughout the past 3 years. Also, David Porter and Jake Leflore for their help to provide me different devices for my test.

Finally, I would thank my family for giving a wonderful energy and motivation toward my career in my life.

Name: MOHAMMAD TAHERSIMA

Date of Degree: MAY, 2017

Title of Study: MODELING HEAT TRANSFER IN MASS CONCRETE FLOORS WITH RADIANT HEAT GROUND SOURCE SYSTEMS

Major Field: CIVIL ENGINEERING

Abstract:Thermal properties of concrete have been extensively studied for the design of mass concrete structuresregarding cracking and stress development considerations. The rise in blended cement with limestone and fly ash as a sustainable building material is one approach to reducing the exothermic release from cement and significantly reducing the greenhouse gas signature of the building materials while maintaining the technical properties needed for building design. Concrete containing limestone blended cement with limestone and fly ash have noticeably different thermal properties that are not well predicted by commercially available software. The purpose of first phase of this project is to provide thermal property data for designers or software developers. The second phase of the research demonstrates the sustainability and energy savings of a ground source system paired with a mass radiant floor constructed of concrete containing blended cement. This phase built and conducted controlled experiments on an instrumented 33,000 square foot industrial facility. The scope of second phase of this project is improving the efficiency of radiant floor in the buildings with a geothermal system. Large areas of heated slab can provide sufficient heat flux needed to maintain the indoor temperature at a comfortable level. The Cooper Laboratory features a strong floor, which is a massive concrete element that can store heat due to its large heat capacity and low thermal conductivity. Stored heat can later be releasedto the laboratory atmosphere through convective transfer. Using the mass heated radiant floor in the covered structures such as laboratories with large bay area with controlled condition of internal air temperature can moderate the air conditioning need at cool or warm seasons. For both parts of this project, a finite element (FE) model was applied to simulate the temperature rise due to cement hydration in the mass floor and thermal behavior of the radiant floor in different loading conditions of the piping system. The third phase of the research was to optimize the electricity used by utilizing an off-peak rate structure for the radiant heating and cooling the mass concrete floor during low cost times and use the convective transfer from the mass concrete to the air during peak rate hours with the radiant system shut off.

TABLE OF CONTENTS

Chapter Page

I. INTRODUCTION 1

1.1 Introduction 1
1.2 Key Elements of Study 2
1.3 dissertation Outline 3

II. HYDRATION HEAT IN A CONCRETE SLAB-ON-GRADE FLOOR WITH LIMESTONE BLENDED CEMENT 4

2.1 Overview 4
2.2 Introduction 5
2.3 Experiment 7
2.3.1 Site 7
2.3.2 Concrete Mixture Design 10
2.3.3 Instrumentation 11
2.3.4 Calorimetry 14
2.4 Heat Transfer Modeling 15
2.4.1 Finite Element Modeling 15
2.4.2 Temperature Prediction 18
2.5 Results and Discussion 19
2.6 Conclusion 29

III. HEATING PERFORMANCE OF MASS CONCRETE RADIANT FLOOR SYSTEM WITH GROUND SOURCE GEOTHERMAL SYSTEMS 31

3.1 Overview 31
3.2 Introduction 32
3.2.1 Green Building 32
3.2.2 Thermal Mass 33
3.2.3 Heat Pumps 34
3.2.4 Ground Source Heat Pump 37
3.2.5 Radiant heat Floor 40
3.3 Experiment 41
3.3.1 Instrumentation 41
3.3.2 Geothermal system with Radiant Floor 42

Chapter Page

3.4 Heat Transfer Analysis 46
3.5 Result and Discussion 49
3.5.1 Site Results.....49
3.5.2 Finite Element Model Results.....58
3.6 Conclusion 62

IV. COOLING PERFORMANCE OF THICK AND THIN CONCRETE RADIANT FLOOR SYSTEM WITH GROUND SOURCE SYSTEMS 63

4.1 Overview.....63
4.2 Introduction.....64
4.3 Experiment.....66
4.4 Results and Discussion 70
4.4.1 Site Result 70
4.4.2 Modeling Result.....89
4.5 Conclusion 94

V. AN EFFICIENT APPROACH FOR USING THE MASS RADIANT FLOOR WITH GROUND SOURCE HEAT PUMPS.....95

5.1 Overview.....95
5.2 Introduction.....96
5.3 Experiment.....97
5.4 Results and Discussion 100
5.5 Conclusion 115

VI. CONCLUSION.....116

6.1 Hydration Heat in a Concrete Slab-on-Grade Floor with Limestone Blended Cement 116
6.2 Heating Performance of Mass Concrete Radiant Floor System with Ground Source Pipe Systems.....117
6.3 Cooling Performance of Thick and Thin Concrete Radiant Floor System with Ground Source Pipe Systems 118
6.4 An Efficient Approach for Using the Mass Radiant Floor with Ground Source Heat Pumps.....118
6.5 Future Work 119

REFERENCES 120

APPENDICES 127

LIST OF TABLES

Table Page

2.1 Mix design of the job site.....10
2.2 Mix proportions of calorimetry samples.....14
2.3 Chemical composition of Holcim cement IL, I-II 15
2.4 Density and thermal properties of concrete 18
2.5 Concreteworks input parameters.....18
2.6 Error Estimation of modeling accuracy 28
3.1 FEM Material properties.....49
4.1 Cooling schedule for summer season 67
4.2 Comparison between 19 days of cooling vs 19 days of night cooling.....82
4.3 Average Temperature in the mass floor (Edge) for 19 days of continuous cooling and 19 days of night cooling.....89
4.4 Average Temperature in the mass floor (Center) for 19 days of continuous cooling and 19 days of night cooling.....89
5.1 Comparison of average indoor and outdoor temperature between Test 1 and Test 2 108
5.2 Comparison of average supply and return ground temperature between Test 1 and Test 2.....108
5.3 Electricity usage comparison of night heating and continuous heating at different supply temperature in the heat pumps 110

LIST OF FIGURES

Figure Page

2.1 Outside view of Bert Cooper Laboratory....8
2.2 Inside view of Bert Cooper Laboratory....8
2.3 Reinforcing detail in the mass floor....9
2.4 Thermocouples location inside of slab (dimension isfoot)....12
2.5 Thermocouples location at 7 in slab (dimension isinch)....12
2.6 Location of Edge and Center point....13
2.7 Thermocouple installation and Data Logger position after casting concrete....13
2.8 Finite Element Algorithm for cement hydration modeling....17
2.9 Temperature development at strong floor after casting concrete....19
2.10 Thermal gradient after casting the concrete (center point)....20
2.11 Thermal gradient after casting the concrete (edgepoint)....21
2.12 Temperature gradient in height of 7 in slab at 12 pm of different days (Center)22
2.13 Temperature gradient in height of 7 in slab at 12 am of different days (Center)22
2.14 Temperature profile at the middle of mass floor for edge and center point....23
2.15 Temperature profile at the under mass floor for edge and center point....23
2.16 Average normalized heat flow result of cement IL, and cement IL + 25% FA samples....24
2.17 Average normalized Heat result of cement IL, and cement IL + 25% FA samples....25
2.18 Comparison of temperature gradient for the mass floor (FEM, Job Site Measurement)....26
2.19 Comparison of temperature gradient for center point (FEM, Concreteworks, Job Site Measurement) software....27
2.20 Comparison of temperature gradient for center point (FEM, Job Site Measurement) job site data....27
2.21 Comparison of temperature history of center point in slab for IL and IL + 25% FA....28
2.22 Comparison of temperature gradient at center point of 4ft slab for IL + 25%FC and I-II + 25%....29
3.1 Condensation and evaporation cycle at the heat pump....37
3.2 Typical Ground-source heat pump parts....39
3.3 Geothermal heat pump and radiant floor system....41
3.4 Water-water Heat pumps at Cooper lab....43

Figure Page

3.5 Water-Water heat pumps at Cooper Lab 44
3.6 Overall set up for geothermal and radiant floor system (heating) 45
3.7 Overall set up for geothermal and radiant floor system (cooling) 45
3.8 Element types (Steel (Link 33), Concrete (thermal solid 70), Pipe (3D th-fl pipe 116)) 47
3.9 Vertical steel anchors and horizontal steel mesh in FE model 48
3.10 Finite element model (concrete, steel, and heating pipes elements) 48
3.11 Temperature measurement at mass floor edge point (80ºF pipe loading) 50
3.12 Temperature measurement at mass floor center point (80ºF pipe loading) 51
3.13 Temperature measurement at thin slab edge point (80ºF pipe loading) 52
3.14 Temperature measurement at thin slab center point (80ºF pipe loading) 52
3.15 Mass floor edge temperature rise (80ºF and two 90ºF heating cycles) 53
3.16 Mass floor center temperature rise (80ºF and two 90ºF heating cycles) 54
3.17 Temperature variation at mass floor edge point at 00:00 (80°F pipe loading and off) 55
3.18 Temperature variation at mass floor center point at 00:00 (80°F pipe loading and off) 55
3.19 Temperature variation at 7 in floor center point at 00:00 (80°F pipe loading and off) 56
3.20 Final Temperature variation at mass floor center point at 00:00 (before and after three heating cycles) 57
3.21 Final Temperature variation at 7 in Slab center point at 00:00 (before and after three heating cycles) 57
3.22 Heat flux measurement at the bottom of thin slab (Edge, center point) 58
3.23 Temperature distribution in the mass floor (FE model) 59
3.24 Temperature variation for mass floor edge (Actual data vs FEM) 60
3.25 Temperature variation for mass floor center (Actual data vs FEM) 60
3.26 Top and Bottom view of temperature distribution in the mass floor (Finite Element model) 61
3.27 Finite element model results for center and edge point (110ºF supply temperature) 62
4.1 Temperature variation during the year 2015-2016 68
4.2 Water Detector Sensor on North (right picture) and South (left picture) 69
4.3 Online monitoring of radiant floor temperature and moisture sensors 69
4.4 Surface heat flux before installation (left) and after installation (right) 70
4.5 Ambient Temperature during the different stages of cooling operation 71
4.6 Temperature profile in the mass floor for 67ºF and 60ºF cooling load 72
4.7 Temperature profile in the thin floor for 67ºF and 60ºF cooling load 73
4.8 The online monitoring system for night cooling 74
4.9 Temperature profile in mass floor for 1 week of night cooling (Center point) 74
4.10 Temperature profile in thin floor for 1 week of night cooling (Center point) 75
4.11 Three Different Cooling mode (continuously 19days, 7, 19 days of night cooling) 76

Figure Page

4.12 The floor cooling for 19days of continuous cooling and night cooling (edge) ...76
4.13 The floor cooling for 19days of continuous cooling and night cooling (7 in slab, ...77
4.14 The floor cooling for 19days of continuous cooling and night cooling (7 in slab, edge)....78
4.15 Heat Flux measurement at the bottom of 7 in slab (Edge, Center points).....79
4.16 Surface heat flux sensors at mass floor and thin slab (center).....80
4.17 Surface heat flux in W/m^2.....81
4.18 The floor cooling for 19days of continuous cooling and night cooling (edge) 81
4.19 Comparison between 19 days of cooling vs 19 days of night cooling.....82
4.20 9.5 days cooling Vs. 19 days Constant Cooling (60°C) 83
4.21 7 days continuous cooling Vs. 7 days night cooling (60°C).....85
4.22 Condensation at the surface of radiant floor system.....85
4.23 The temperature profile across the mass floor before, after (night cooling) 86
4.24 Temperature profiles across the mass floor before and after (continuous cooling) 87
4.25 Average Temperature in mass floor (Edge).....88
4.26 Average Temperature in mass floor (Center) 88
4.27 Finite element results for 60ºF continuous cooling loading at the center.....90
4.28 The floor cooling for 19days of continuous cooling and night cooling (edge) 91
4.29 Concrete slab (left), piping system layout (right) in FE modeling 91
4.30 9.5 days cooling Vs. 19 days Constant Cooling (60°C) 92
4.31 7 days continuous cooling Vs. 7 days night cooling (60°C).....93
4.32 Modeling the floor cooling in 7 in slab for 50ºF (10ºC).....93
5.1 Electricity meter (left picture) and data acquisition system (right picture) 98
5.2 Schematic diagram of heating system.....99
5.3 Supply and return temperature into the radiant floor system.....100
5.4 Indoor and Outdoor temperature (Test # 1) 102
5.5 The average of Indoor and Outdoor temperature during day and night of the test#1 103
5.6 Ground Loop Supply and Ground Loop Return Temperature.....104
5.7 Average Ground Loop Supply and Return Temperature (Test #1) 104
5.8 Difference between supply and return temperature in ground loop system 105
5.9 Electricity usage by two ground source heat pumps (test #1) 105
5.10 Indoor and Outdoor temperature (Test # 2) 106
5.11 The average of Indoor and Outdoor temperature during day and night of the test #2 107
5.12 Ground Loop Supply and Ground Loop Return Temperature (Test # 2) 107
5.13 Average Ground Loop Supply and Return Temperature (Test #2) 108
5.14 Electricity usage by two ground source heat pumps (Test # 2) 109
5.15 COP of heat pumps (Test # 1).....110
5.16 COP of heating system (Test # 1).....111
5.17Temperature profile inside of mass floor (Center) 111

Figure Page

5.18Temperature profile inside of mass floor (Edge).....112
5.19Temperature profile inside of thin slab (Center).....113
5.20Temperature profile inside of thin slab (edge).....114
5.21Temperature profile in the mass floor.....114
A.1. Concrete and piping system modeling (No steel).....127
A.2. Concrete, steel, piping system modeling 127
A.3. Temperature distribution in Concrete and piping system modeling (No steel) .128
A.4. Temperature distribution in concrete, steel, piping system modeling 128
B.1. Piping layout (Case 1).....129
B.2. Piping layout (Case 2).....129
B.3. Temperature distribution in the 7 in slab (Piping layout Case 1).....130
B.4. Temperature distribution in the 7 in slab (Piping layout Case 2).....130
B.5. Temperature distribution in piping system (layout Case 1).....131
B.6. Temperature distribution in piping system (layout Case 2).....131
C.1. Concreteworks temperature distribution with software weather data.....132
C.2. Concreteworks temperature distribution with job site weather data.....133
C.3. Comparison of temperature gradient for center point (different length of 10m or 30m).....133
D.1. Thermal images of radiant floor.....134

CHAPTER I

INTRODUCTION

1.1 Introduction

Concrete slab-on-ground floors with a radiant heat piping system are used for heating/cooling of “smart” or high technology buildings. The radiant floor system can be accompanied with ground source systems for better efficiency in energy saving when compared to traditional forced-air system. Concrete floors perform as the radiant or convective heating or cooling source of the building instead of using a forced air systems. This technology provides thermal comfort for residences and desirable indoor air temperatures.The amount of generated heat after casting the concrete is very important regarding the type of cement in the concrete mixture design. Different cements have different heats of hydration,leading to different temperature risesin concrete with various types of cement. Limestone blended cement is used throughout the worldin building construction because of its sustainable, requires less energy to produce, and it has desirable green properties. Most software programs predict the temperature rise by the portland cement in the concrete based on ASTM C150 Type I, II, or III cements. The calorimetry results of cement hydration for ASTM C595 blended limestone cement and C150 I-II cement is a key to finite element programsin obtaining the initial temperature rise in the of the concrete. The maximum temperature differential in any mass concrete structure is important to avoid thermal stresses or cracking. The scope of second and third part of present project is to improving the efficiency of

radiant floor systems in buildings with ground source systems. The high bay industrial building type is common way for architects to address distribution centers, airport terminals, industrial laboratories, manufacturing plants and controlled temperature storage facilities. Such buildings can be efficiently heated and cooled with concrete floors with embedded pipe radiant heat systems. Larger areas of heated slab can provide sufficient heat flux to maintain the indoor temperature at or near a fixed value. Using the thermal mass of a heated floor can be utilized to save the thermal energy during the surplus time and give it up during peak hours of energy. Using the mass heated floor in acontrolled environment structures such as offices and laboratory can moderate the seasonal energy demands of the building.

The in-situ temperature gradient by piping system can be simulated with a comprehensive finite element modeling. A 3D model of concrete, steel, and pipes is selected to study the thermal behavior of a radiant heated concrete floor in this study to understand the potential for energy optimization.Subsequently, a full size building was constructed with instrumentation to verify the model and test various optimization models.

1.2 Key Elements of Study

The main purposes of this research are presented in the following:

- Investigate the potential of using limestone blended cement with fly ash in a mass concrete floors to reduce the carbon footprint of concrete construction.
- Determine the thermal behavior of limestone blended cement with fly ash.
- Determine the temperature rise in mass concrete floor induced by blended cement hydration.
- Investigate the potential of combining mass concrete floors in large buildings with ground source heating/cooling for low carbon energy efficient buildings.

- Determine the potential for a mass concrete floor to be used as a thermal battery of the building.

- Determine the importance of steel in transmitting radiant heat in conducting heat to the surface for convective heat transfer to the air in the mass floor because of higher thermal conductivity than concrete. Both reinforcing steel and steel anchors were considered.

- Determining the energy savings and environmental sustainability of the building operating within a variable rate electric utility.

1.3Dissertation Outline

In this dissertation, two phases of research will be described in four chapters:

- Chapter 2 demonstrates the importance of heat rise by cement hydration and the differences between limestone blended cement with and without fly ash vs. Type I-II cement. The heat of hydration is modelled with finite element with calorimetry results.

- In the Chapter 3, the properties of mass concrete floor to store heat in the winter will be discussed. The finite element modeling of mass floorand thin slabs on ground are introduced to see the effects of thermal loading on the piping system of the radiant floor system.

- In the Chapter 4, the cooling performance of mass floor and thin slabs on ground in summer season will be discussed. The cyclic cooling load on the radiant floor system and constant floor cooling will be compared.

- In the Chapter 5, an optimizing method demonstrates the saving energy by the mass floor in the heating mode. Two experiments in two weather conditions demonstrates the low cost night heating is sufficient to keep the building warm for multiple days without heating during high cost utilities times . .

CHAPTER II

HYDRATION HEAT IN A CONCRETE SLAB-ON-GRADE FLOOR WITH LIMESTONE BLENDED CEMENT

2.1 Overview

In this study, results of thermocouple measurement at the job site are compared commercially available programs for finite element model and concrete design. Verification of the finite element model (FEM) with experimental data has been completed with cement ASTM C595 Type IL cement with a 25% replacement by mass ofASTM C618 Type C fly ash. This was the same material used for the full scale building investigated in the dissertation. The maximum temperature rise due to heat of hydration for cement I-II+25% FA and cement IL are predicted to compare the results of hydration heat generated by different mixture proportions. The FEM result has a much better compatibility with job site data with respect to the commercial concrete properties software results. The prediction accuracy of finite element results is about 15% more for maximum temperature rise and 30% more for peak time. In addition, applying ambient temperature plays a crucially important role in the prediction model of cement hydration.

2.2 Introduction

Concrete is the second most common used material in the world [1]. It has many useful properties including durability, sustainability, availability, and economy. The initial hydration reactions of cementare exothermic and generate heat.The relatively low thermal conductivity of concrete can cause a thermal gap between the concrete and the ambienttemperature [2]. Oftentimes, these differences in temperature can be quite large and lead to cracking of the concrete as the outer portions of mass concrete cool while interior portions of mass concrete remain heated. Concrete with limestone blended cement leads to carbon footprint reduction and lowers the energy needed to manufacture each ton of cement. Limestone blended cement (IL cement) has 5-20% limestone particles which are replaced by clinker in the cement production. Therefore, the amount of generated CO_2 by cement is reduced when inert limestone particles are added to the cement components.

A supplementary cementitious material (SCM) is a material used in combination with portland cement, contributes to the properties of the hardened concrete through hydraulic or pozzolanic activity or both. The microstructure of cement matrix and durability of concrete are improved because of their pozzolanic effect and physical properties [3]. Fly ash is one of SCMs which is a result of the combustion of pulverized coal. Type C (high calcium) and type F (low calcium) are two most common types of fly ash. The addition of fly ash further reduces the mass of blended cement needed per cubic yard of concrete, reducing the energy density of the overall concrete [4].

Cement hydration is the main causein heat generation inconcrete sections. The amount of cement is the main parameter in estimating the heat generated and resulting temperatures in mass concrete pours. Limestone blended cement can reduce carbon dioxide footprintand the synergistic properties of limestone flour with portland cement are the justifications for its usage. Synergistic properties are related to how (relatively) inert limestone particles interact with cement hydration.

Lower w/c concretes, energy saving, and reduction in CO_2 emission are the main parameters to substitute limestone powder in the cement production [5]. While it is widely available around the world, this kind of cement is not modeled in most temperature prediction commercial software. Therefore, it is necessary to investigate the heat of hydration by limestone blended cement. However, researcher have been studied the heat of hydration of limestone blended cement with calorimetry. The earlier researches have been shown that limestone seems more likely crystallization of monocarbonate rather than monosulfate [6, 7]. Some studies have been completed about replacing the calcium sulfate up to 25% calcium carbonate will not change properties of the system [8, 9]. Rahal V.F et al. studied the influence of compositional and process variables on the early age hydration of limestone blended cement [10].They concluded that limestone filler reduces the heat due to dilution effect. Lothenbach, B. et al. stated that limestone will accelerate the initial hydration reaction and affect assemblage of the hydrating cement pastes [32]. Greater densification of the cement paste improves the strength and durability of the concrete materials [11].

Mass concrete is any volume of concrete with dimensions large enough to require measures to be taken to overcome heat generation from cement hydration, by reducing the volume change in order to minimize cracking [12]. Typically, mass concrete is referred to as any structure with any dimension of greater than 1.0 m. Thick slabs can store more heat of cement hydration due to the low thermal conductivity of concrete. This means it takes time to heat or cool mass concrete, but the concrete also releases the heat or cold slowly as well.

The heat from exothermic reaction of cement hydration may cause early age strain accumulation within concrete contributing to cracks or displacements. Controlling the early age thermal differential strains in concrete and utilizing the other thermal properties of concrete present a potential to utilize concrete as a more sustainable building material. The maximum temperature rise due to cement hydration plays an important role on early

age thermal cracking of the concrete. A lot of research has been done on the subsequent effects of temperature rise in mass concrete construction [13, 14, 15, 16]. The heat of hydration of the cement needs to be predicted by engineers before casting mass concrete. If the peak temperature rise exceeds the maximum allowable temperature to avoid cracking of the concrete structures and delayed ettringite formation, further consideration should be regarded including pre or post cooling of concrete section. The purpose of this chapter is to investigate the modeling of thermal monitoring of the concrete with blended limestone cement after placing the concrete. Cement hydration in a mass of concrete exposed to weather conditions is then predicted by the finite element model. The prediction of heat generated by blended limestone cement hydration is applied to a mass concrete to obtain the maximum internal temperature, time of peak temperature occurrence, and the temperature gradient. The generated heat by the thin slab is used for comparison of temperature gradient results with the mass concrete floor. As a result, finite element modeling is applied for the mass concrete.

2.3Experiment

2.3.1 Site

The experimental platform for this researchwas coordinated with the construction of the Cooper Laboratory at Oklahoma State University. This building was constructed between 2014 – 2015with a mass concrete structural load floor and large areas for fabrication, offices and training. The building is over 33,000 ft^2(3000 m^2) area.

The outside and inside view of this building are shown in Figure 2.1 and Figure 2.2.

Figure 2.1– Outside view of Bert Cooper Laboratory

Figure 2.2 – Inside view of Bert Cooper Laboratory

A 4.0ftthick mass concrete floor was placed on 3 in. mud slab in the center of the laboratory. The mass concrete floor can be viewed in Fig. 2.2 and in plan represents the area supported by the 20

T crane. It's dimensions are 118 ft. by 44 ft. in plan. The mass concrete floor includes the vertical steel, and top and bottom mesh. The reinforcement detail of the 4 ft mass floor is shown in Figure 2.3. The spacing interval of all steel anchor is 4 ft on-center and the diameter of each vertical steel anchor is 1 ½ in. Seven inch slabs were castin the fabrication areas; these wereplaced on 1.0 in polystyrene insulation.

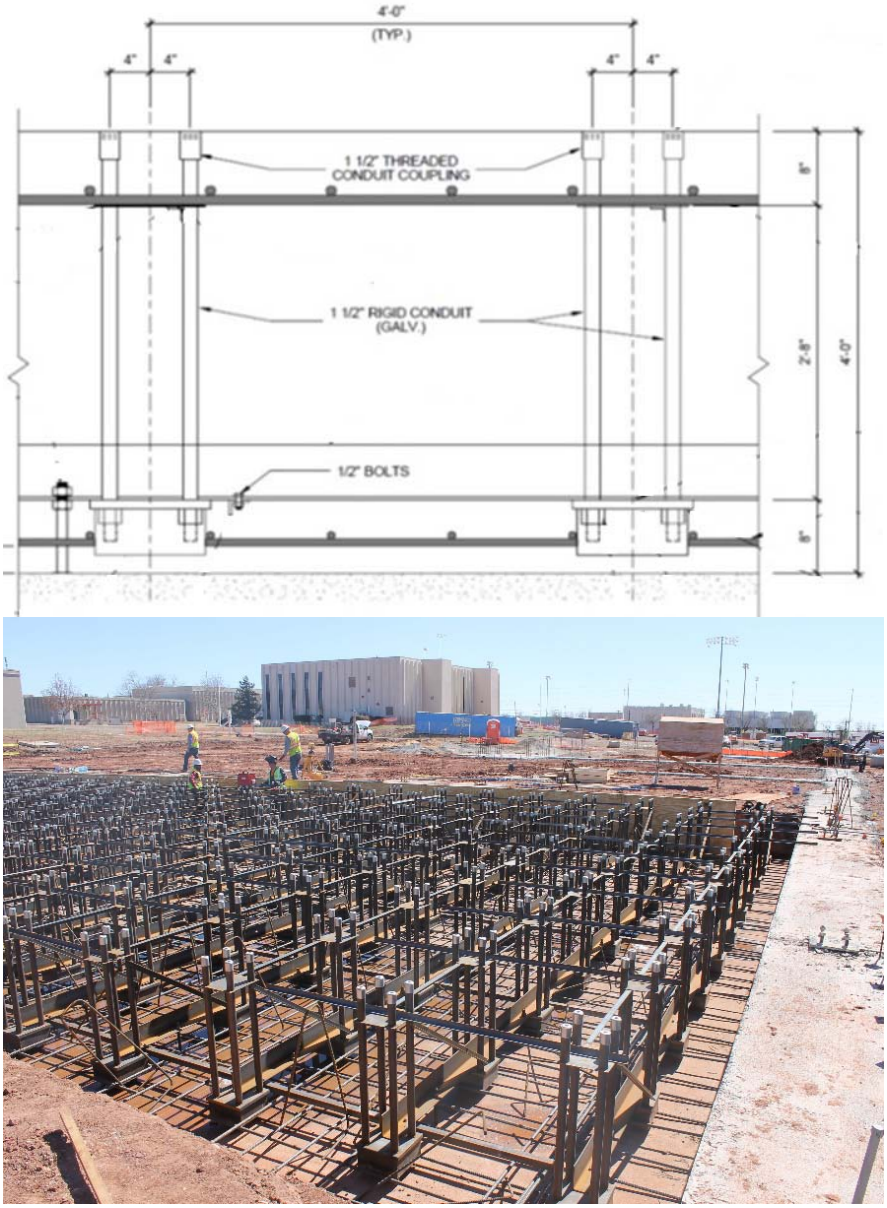

Figure 2.3 – Reinforcing detail in the mass floor

Different radiant heating or cooling systems are categorized into embedded surface system which pipes are placed in a layer of floor, wall, or ceiling [82, 83], thermally activated building system which pipes are integrated into the main building structure [17, 18], and radiant panel system which pipes are integrated to lightweight panels [19]. This slab has a heating tube system which is located 6 in below the surface to provide heating and cooling comfort for the lab. The heating pipe system in the 7 in concrete slab is located on the bottom of the slab right on 1 inpolystyrene insulation.

2.3.2 Concrete Mixture Design

To study the thermal behavior of both concrete floors, concrete mixture proportions need to be recognized. The main factor of generated heat by cement hydration is paste composed of cement, secondary cementitious material (SCM), and water. The mixture proportion design of the concrete slab is presented in Table 2.1., It can be found that job site paste has cement, 25% Fly Ash type C plus water. The water to cementitious material ratio (w/cm) of 0.49 should be considered for heat transfer modeling purposes. The aggregate is composed of natural sand as fine aggregate and limestone coarse aggregate. The Pozzolith 80 is used as water reducer from BASF Company. No calcium chloride or chloride based ingredient is used in the manufacture of Pozzolith 80. Average 7 days strength of concrete sample is 5530 psi.

Table 2.1: Mix design of the job site

Material Type	Design Quantity	Specific Gravity	Volume (ft^3)
Cement	414 lb	3.15	2.11
Fly Ash	103 lb	2.65	0.62
Water	30.5 gal	1.00	4.06
Coarse Agg #57	1730lb	2.80	9.90
Coarse Agg 3/8" #2	415 lb	2.80	2.38
Fine Agg	1234 lb	2.63	7.51
Water Reducer	15.5 lqoz	-	-
Sum			27.00

2.3.3 Instrumentation

Instrumentation at the site to record the temperature inside of concrete slabs is done by T-type thermocouples. Thermocouple wires are attached to a precast column of concrete and are used to read the temperature at different elevations of slab depth before and after casting the concrete. All thermocouple wires are connected to a data logger for measuring the concrete temperatures over time. The aim of setting thermocouples in various elevations of the concrete depth is to have the thermal gradient through the concrete height after casting the concrete. The thermocouples are located at 6 in, 1ft, 1.7ft, 2.7ft, and 4ft below the surface of the mass concrete. One thermocouple is located under the mud slab to measure the soil temperature. Thermocouples are concentrated at the top of the slab to measure more preciselythe heat fromthe radiant pipe system. It means when the radiant floor system working, the greatest variations in temperature are expected at the top of the mass floor around the piping system.There are fewer thermocouples in 7 in slab because of the thinner depth of concrete slab. Thermocouples are located at 1 in below the surface, at middle of the slab, and the bottom of the thin slab. The thermocouples' position in the 4ft floor and 7 in slab are shown in figure 2.4 and 2.5, respectively.

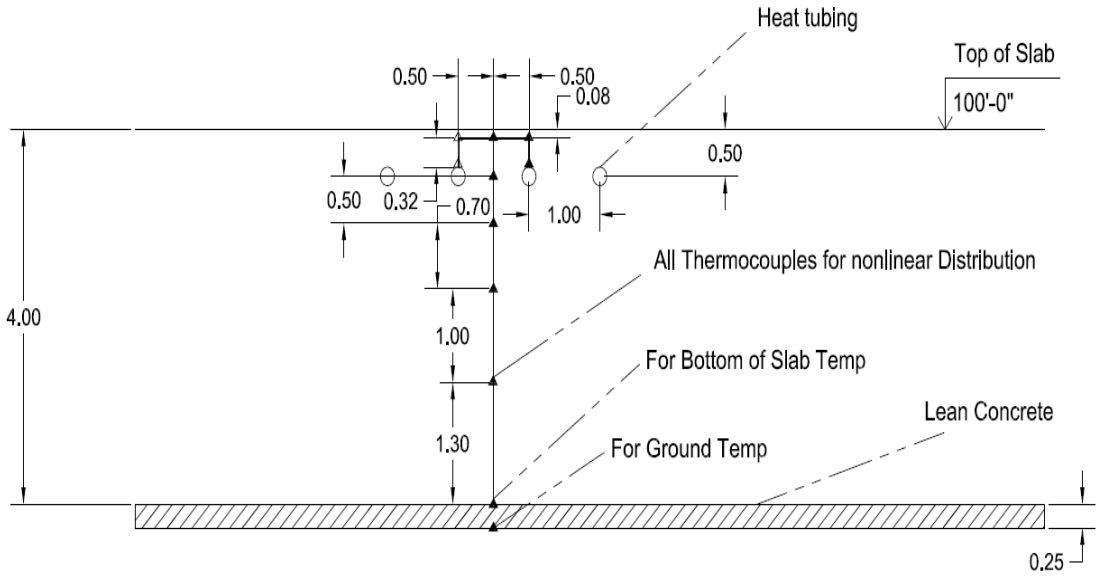

Figure 2.4. Thermocouples location inside of slab (dimension is foot)

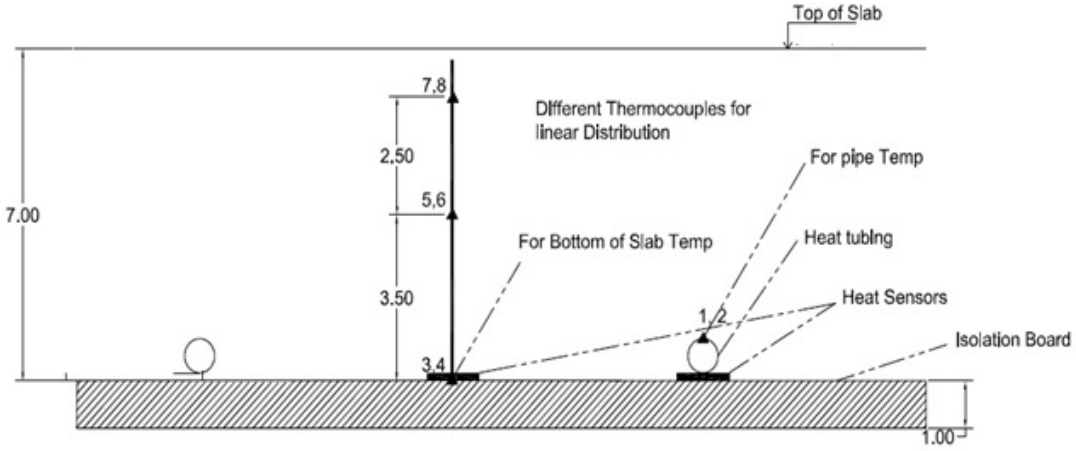

Figure 2.5. Thermocouples location at 7 in slab (dimension is inch)

The average of two thermocouple readings at each locationis used for collecting the temperature data to verify the accuracy of the results. When the concrete is placed, water and cement reactions generate the internal heat of hydration. Thermocouple readings are recorded for the internal heat of hydration every 5 minutes in a data logger. The location of thermocouple installation in the mass floor and the 7 in slab is shown in Figure 2.6.

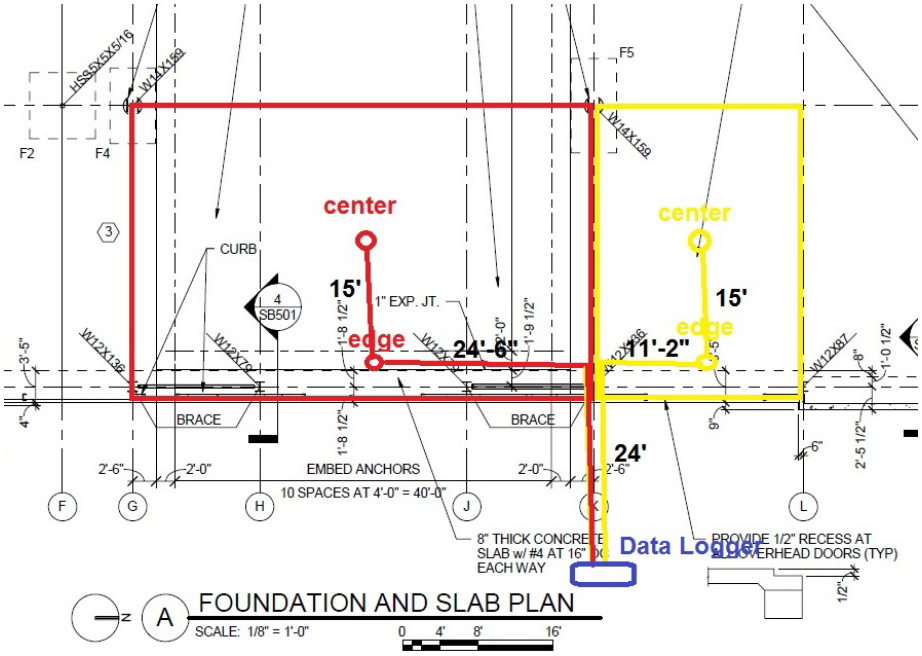

Figure 2.6. Location of Edge and Center point

The edge point is located at 1 ft from the edge of the building and the center point is located at 16 ft from the edge of the building. All wires are extended to the outside of the building and they hooked up to a data logger to collect the data over time. The data logger is connected to a solar panel for charging the battery of data acquisition system. Thermocouple installation and data logger box after casting the mass concrete floor is shown in Figure 2.7

Figure 2.7. Thermocouple installation and Data Logger position after casting the concrete

2.3.4 Calorimetry

Cement hydration behavior can be estimated from an isothermal calorimetry test. In order to obtainthe kinetics of cement hydration, isothermal calorimetry was used to measurethe generated heat. Because isothermal calorimetry is more precise than semi-adiabatic calorimetry for forecasting the heat of hydration, it was used as internal generation heat input for modeling [20]. The Tam Air Isothermal Calorimeter is an instrument used to monitor the long-term behavior of heat of hydration. Three of the same samples of blended limestone cement (IL cement) with 25% fly ash were exposed to water in the calorimeter to gain the heat of hydration curves. Paste mixture proportions are presented in Table 2.2. An average of three samples of (IL+25%FA) was used for modeling the hydration heat in the concrete slab. Cement IL hydration with the same w/cm ratio (0.49) was used to compare fly ash usage in decreasing the heat of hydration.

The samples were prepared with 3 minutes mixing of the sample with a 1000 rpm vibrator machine. Because the calorimetry results are sensitive to prior mixing, the tests should be consistent and all sample preparations have the same condition. The mixing procedure includes pouring weighted cement into a calorimetry vial, adding SCMs, adding water, stiring the mixture with a wooden stick 10 times clockwise and 10 times counter clockwise, putting the cap on the mixture vial, putting the vial on vibrator machine for 3 minutes of 1000 rpm, and placing the vial in the calorimetry machine. The w/cm ratio was 0.49 which matched the job site water to cement materials ratio in order to better cement hydration simulation.

Table 2.2. Mixture proportions of calorimetry samples

Cement IL (gr)	Red Rock FA (%)	Red Rock FA (gr)	Water (gr)	w/cm
5	0	0	2.45	0.49
3.75	25	1.25	2.45	0.49

Two types of cements are selected for the further investigation on the heat of hydration. Cement I-II and cement IL from Holcim, Inc [21] is selected for comparison between the maximum temperature rise if cement I-II is used instead of cement IL. It is necessary to look at the chemical composition of both cements which are shown at Table 2.3.

Table 2.3. Chemical composition of Holcim cement IL, I-II [22]

Cement	Blaine (m^2/kg)	-325	Limestone %	SiO_2	Al_2O_3	Fe_2O_3	CaO	MgO
Type IL	431	97.15	9.43	19.32	5.27	3.26	63.57	2.21
Type I/II	360	96.85	4.09	20.08	5.36	3.33	63.47	2.13

Cement	Na_2O	K_2O	SO_3	C_3S	C_2S	C_3A	C_4AF	NA_{EQ}
Type IL	0.14	0.59	2.97	49.78	16.37	8.54	9.65	0.53
Type I/II	0.13	0.55	2.90	50.80	18.61	8.61	10.02	0.49

2.4 Heat Transfer Modeling

2.4.1 Finite Element Modeling

The Finite Element Method (FEM) is a powerful technique to model the behavior of the heat transfer in different media. A comprehensive finite element analysis tool was used to model the thermal analysis of the concrete floor [23]. Modeling results precision was verified with job site data regarding the thermocouple readings which was described in the experiment section.Thefinite element algorithm for modeling the heat of hydration in the mass floor is shown in Figure 2.8 as a step by step procedure.

Two dimensiontransient thermal analysis was completed to monitor the temperature rise inside the concrete slab as a function of time. Thermal cracking and temperature rise after casting the concrete would happen in the mass concrete structures. Therefore, only the mass floor was used for the modeling of temperature rise due to heat accumulation after concrete casting. Thin slab is not purpose of this 2D modeling. Calorimetry results were applied as internal heat generation by cement hydration. The soil temperature at the bottom of the slab and ambient temperature at the sides and top of the concrete floor were applied as boundary conditions of the modeling. The element used was PLANE55 from the FE tool library, which has a thermal conduction capacity in two dimensions. The element has four nodes and a single degree of freedom at each node for the temperature [24]. The measured initial temperature at the job site right before casting the concrete was applied in the transient analysis because of the impact of initial condition on the next step time. The step time of 10 second was used for first 100 hours of casting. Then, for extended results up to 1000 hours, the step time is changed to 5 minutes. However, shorter step time could increase the computational time. Also, the rectangular mesh with size of 0.1m×0.1m (0.328ft × 0.328ft) was used for the modeling. The convergence of modeling is tested with finer mesh of 0.02m×0.02m (0.65ft × 0.065ft) to confirm that temperature results are not function of mesh size.

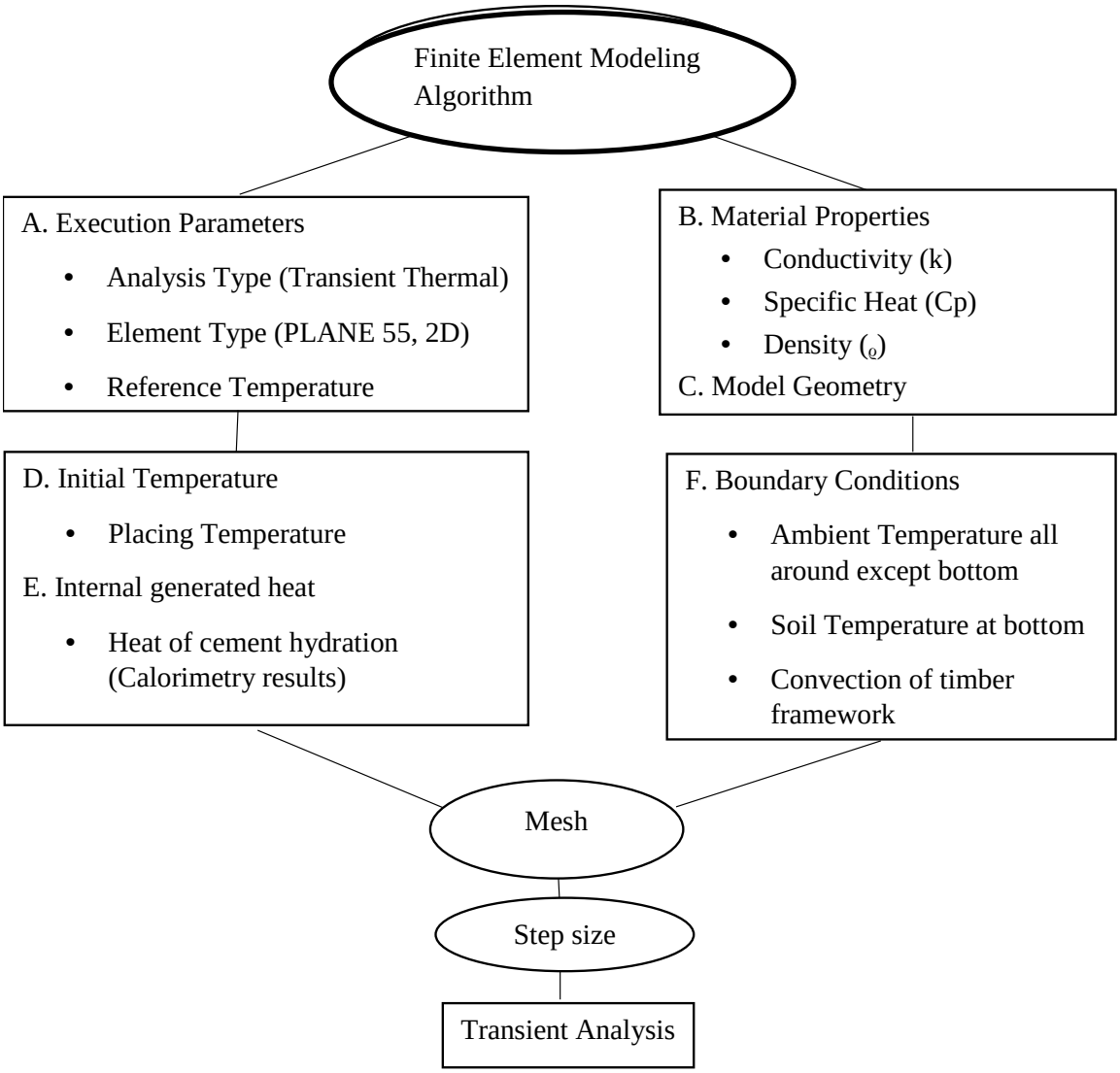

Figure 2.8. Finite element algorithm for cement hydration modeling

In the finite element algorithm, transient analysis is done for 40 days to make sure that cement hydration is substantially complete. The 2D model was chosen because it is a common way to address with heat transfer for cement hydration. The concrete block dimension is 10m×1.22m. Depth is 1.22m (32.8ft×4ft), the same as the mass floor depth, and 10m is selected because it is long enough to replicate the job site length. Increasing the length of the concrete block does not affect the maximum temperature at the middle of the slab because temperature release mainly

occurs at the top and bottom of the section. Density and thermal properties of the slab are shown in Table 2.4.

Table 2.4. Density and thermal properties of concrete [25]

thermal conductivity	1.8 w/m.°k
heat capacity	900 j/kg.°k
density	2466 kg/m^3

2.4.2 Temperature Prediction

There are some software packages that can predict the temperature monitoring of the concrete structures. The 2D finite difference method for thermal analysis of cement and slag was used for a simple structure such as a concrete block [26]. A widely used commercial software was used to model this case of study [27]. Concreteworkssoftware is used as a well-known package for temperature rise predication and new concrete early-age cracking risk and durability [28]. Input parameters in this program are listed below in Table 2.5.

Table 2.5. Concreteworks input parameters

Concrete Type	Mass Concrete
Location	Oklahoma City, OK
Dimension	10 m ×1.33 m
Mixture Design	Job Site mixture design (I-II instead of IL)
Type of Maturity function	Nurse-Saul Method
Data of Placement	03/24/2014, 12 A.M.
Temperature Analyisis Duration	14 days (More days is not available)
Formwork Type	Wood
Concrete Age at form Removal	120 Hours

The temperature prediction program can give us an estimation of amount of temperature rise in concrete structures with input parameters. The accuracy of these software results will be compared with finite element results and job site measurement. Using calorimetry results for cement hydration and measured weather data are two keys for a better estimation of generated heat in the mass concrete structures.

2.5 Results and Discussion

The temperature gradient from 12 hours to 36 hours after casting the concrete across the slab thickness can be seen in Figure 2.9. The vertical axis is the height of the concrete floor above and below the ground surface. The horizontal axis is temperature. Every line shows the temperature distribution inside of the concrete at two hour intervals.

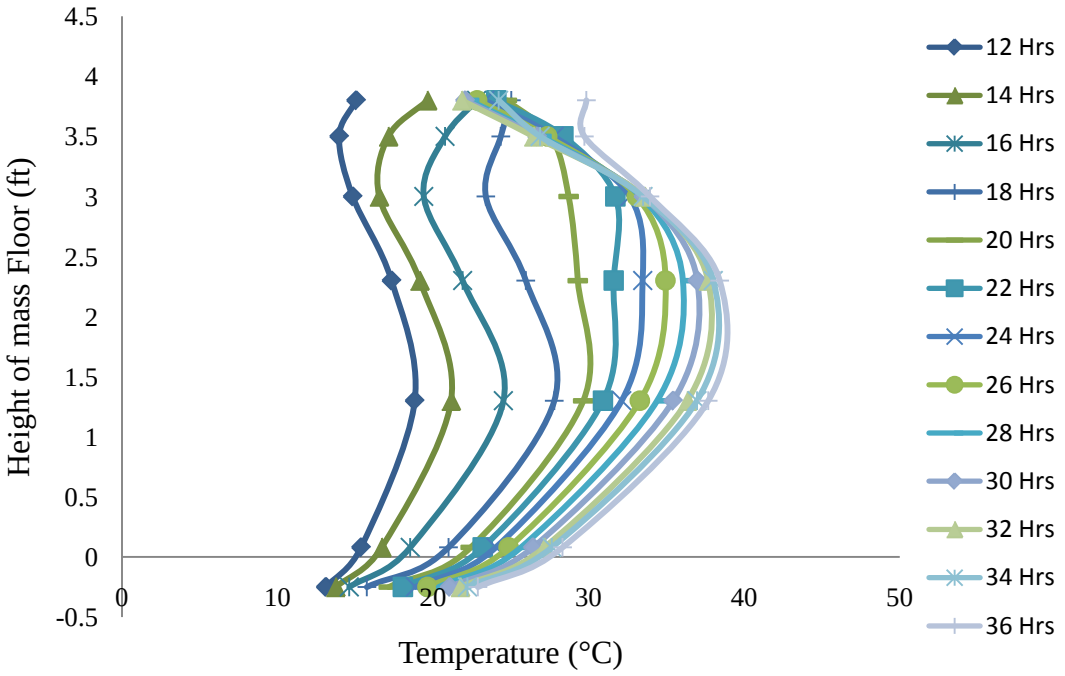

Figure 2.9. Temperature development ofmass concrete floor after casting concrete

The heat of hydration is captured at the middle of the slab because the generated heat at the top and bottom of the slab would escape more easily than at the center of slab. The curvature at the

middle of the slab is increasing during hours of casting concrete, which means that heat is accumulating at the middle of the slab.

The temperature gradient in the mass concrete floor at three different elevations including 2 in below the surface, the middle point and the bottom of the slab (on the mud slab), and ambient temperature are presented in Figure 2.10 and Figure 2.11 over 1000 hours for the center and edge point. The maximum temperature at the middle of the mass floor is 42.9°C (109.22ºF) after 51.75 hours of casting the concrete. The temperature trend is not fully followed by the ambient temperature at a deeper distance from the surface of the slab. For instance, 2 in below the surface is more affected by ambient temperature fluctuation. By increasing or decreasing the ambient temperature, the temperature of 2 in below the surface will be increased or decreased. However, the middle of the slab or mud slab temperature is increased because of temperature rise of cement hydration regardless of ambient temperature fluctuation. Therefore, the surface of the slab is more affected by ambient temperature rather than cement hydration influence. After the hydration peak, the thermal gradient of the middle and mud slab points are fluctuating due to the ambient temperature.

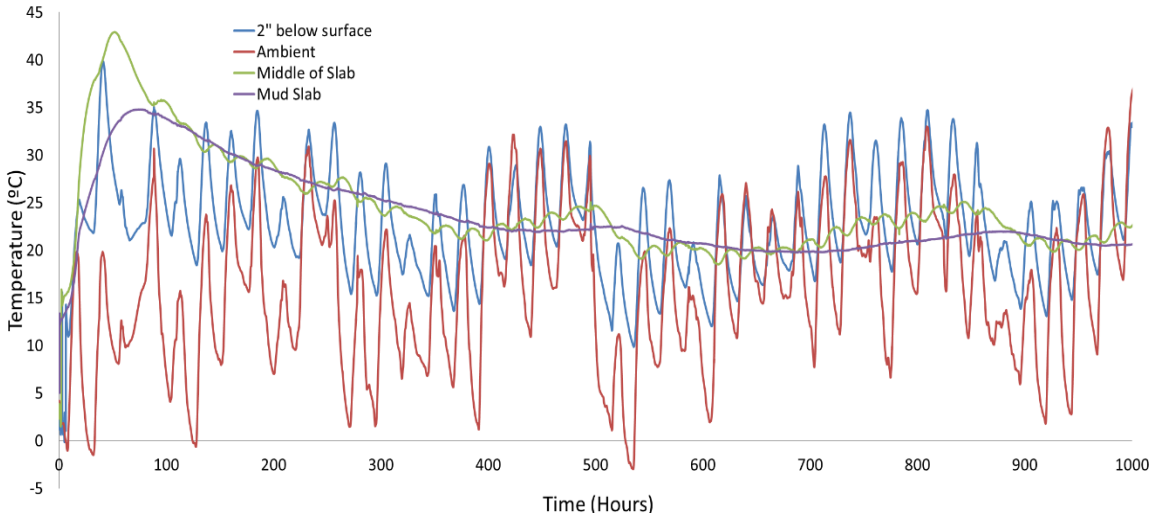

Figure 2.10. Thermal gradient after casting the concrete (center point)

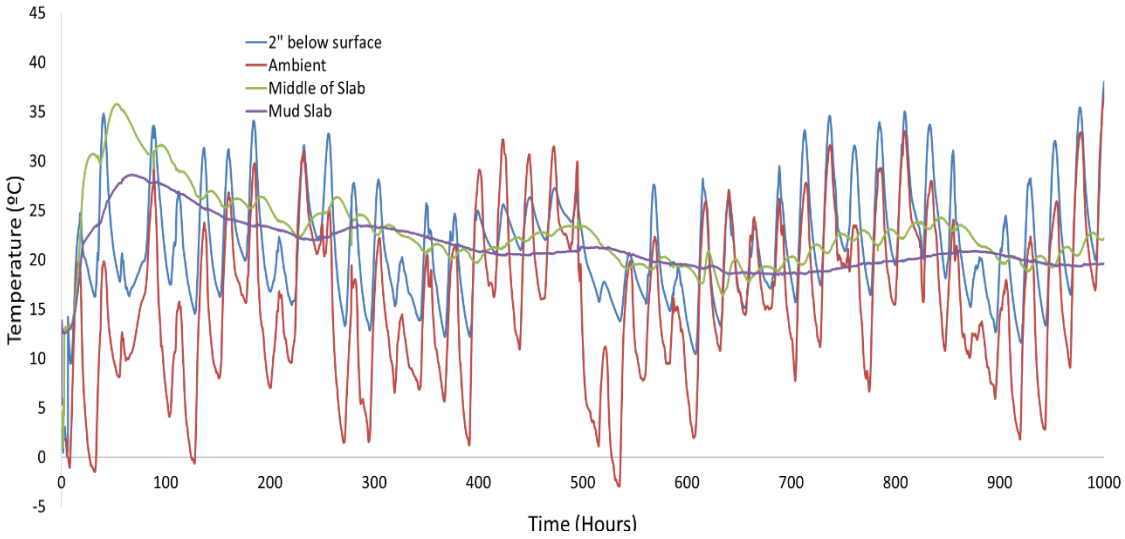

Figure 2.11. Thermal gradient after casting the concrete (edgepoint)

At about 500 hours, the effects of heat of hydration is disappeared. As mentioned before, the thermal behavior of the thin slab regarding the cement hydration is different from the mass concrete floor. Due to the thinness of the 7 in concrete slab, most of the heat of hydration can escape through the top of the slab because the bottom and all around the edges of thin slab is surrounded by 1 in thermal insulation. The temperature gradient at the 7 in slab is shown every day at 12 P.M. and 12 A.M.during one week after casting the concrete in Figure 2.12 and Figure 2.13, respectively.The temperature profiles are shown at a specific time of every day to see the temperature change days after casting the concrete. Concrete was casted on 04/18/2014 at 7:00 A.M. The results are presented in days after casting the thin slab concrete. Regarding the temperature at noon, the surface of the slab has a higher temperature than the bottom of the slab and this variation would be opposite at midnight. Temperature variation inside of the 7 in slab is nearly linear due to the thickness in comparison with the thicker mass concrete floor which has the nonlinear temperature gradient with a peak in the middle of slab. As a result, temperature rising in the thin slab is not a problem regarding temperature accumulation.

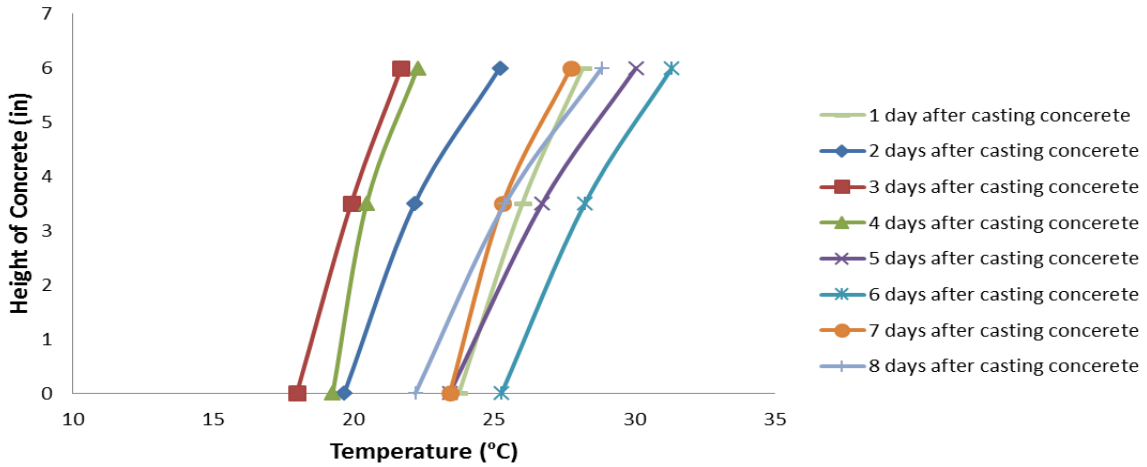

Figure 2.12. Temperature gradient in height of 7 in slab at 12 pm of different days (Center)

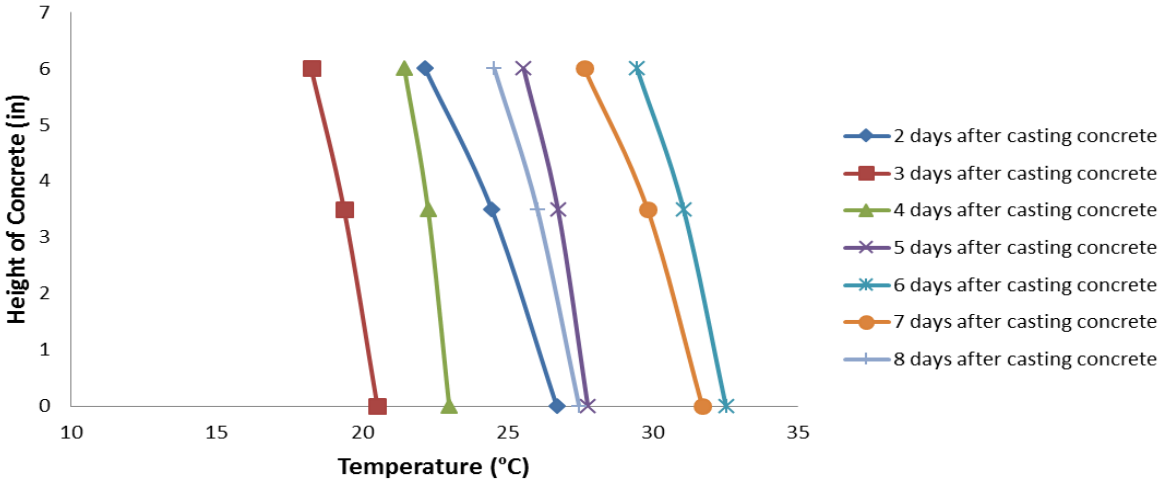

Figure 2.13. Temperature gradient in height of 7 in slab at 12 am of different days (Center)

The temperature rise in the center point and edge point of the slab would be different because the heat could be stored in the center of the slab. This thermal behavior is shown in Figure 2.14 and Figure 2.15 for the middle point of slab (highest thermocouple measurement through the slab

depth) and under the mud slab temperature (ground temperature).

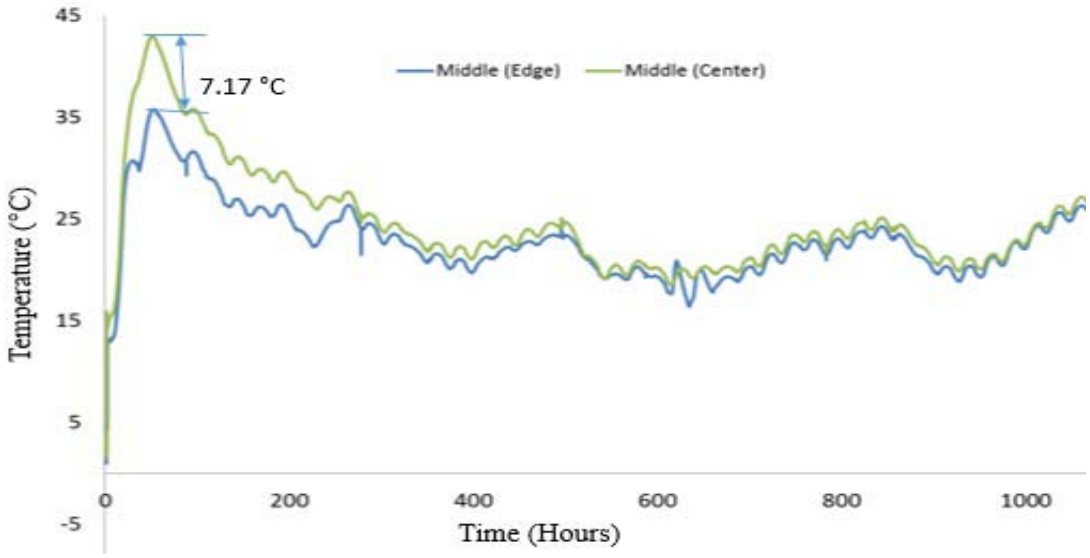

Figure 2.14. Temperature profile at the middle of mass floor for edge and center point

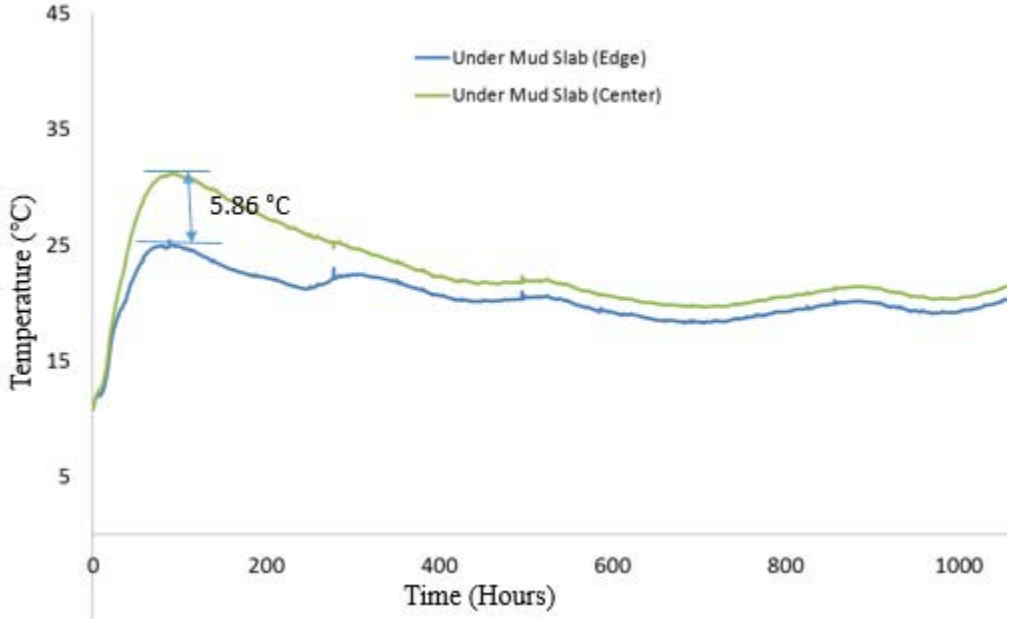

Figure 2.15. Temperature profile at the under mass floor for edge and center point

The difference between maximum temperature reached in the middle of slab for the edge andcenter point is 7.17°C and 5.86°C for ground temperature. It means the heat accumulation in the middle of slab would be in a higher rate than the ground point.

Calorimetry test results of IL and IL+25% Fly ash are presented in Figures 2.16 and 2.17 showing normalized heat flow and normalized heat per gram of cement powder.

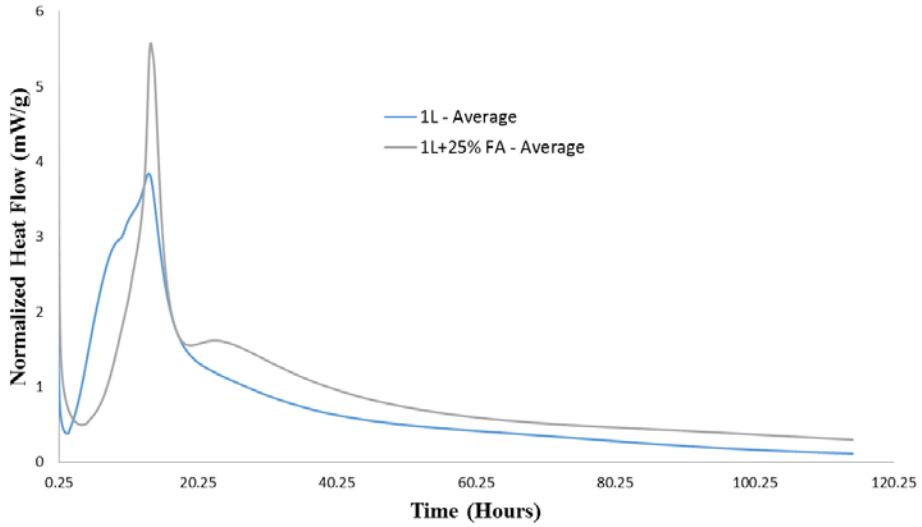

Figure 2.16. Average normalized heat flow result of cement IL, and cement IL + 25% FA samples

These graphs are based on the generated heat per gram of cement. This amount of heat is multiplied by the mass of cement content in the mass concrete to represent the heat of hydration for the total volume of the concrete slab. Figure 2.17 shows the amount of maximum heat flow of IL cement is higher than IL + 25% FA. However, the total heat of hydration of IL cement is greater than IL + 25% FA. Therefore, if it is applied for the whole section, this little difference in this graph would be considerable. This concept will be shown in the modeling result section.

As mentioned before, cement IL + 25% FA was used in the mixture design of the job site but the calorimetry result of cement IL is presented for comparison. Also it is useful to see the effect of SCM on decreasing the maximum temperature. Gurney et al. showed that using limestone cement

can result in an acceleration of set that can alleviate the retarding effects of SCMs replacement [29].

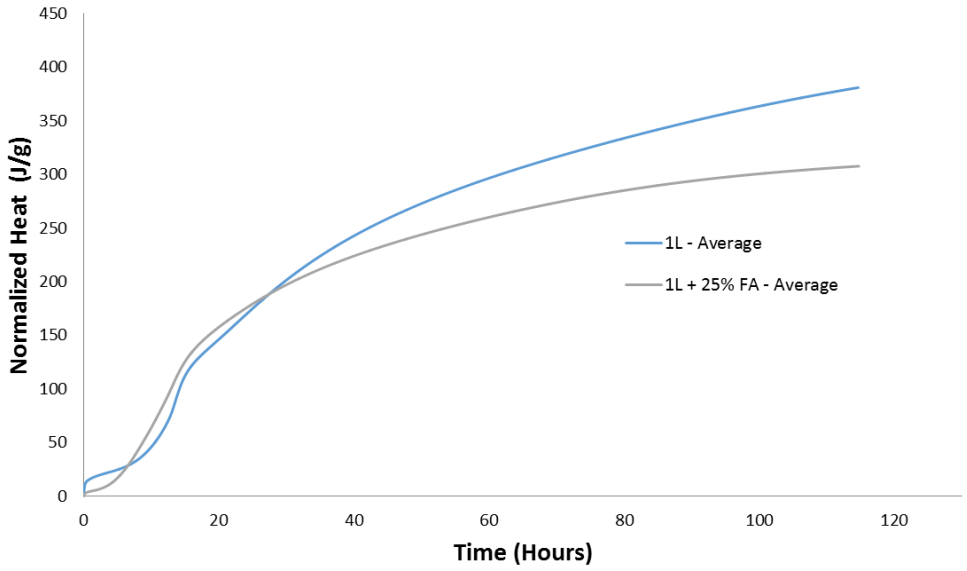

Figure 2.17. Average normalized heat result of cement IL, and cement IL + 25% FA samples

Calorimetry results were used as input for internal heat generation of the model. In addition, the same company cement named I-II was applied for seeing the limestone content on the heat of hydration.

Based on Table 2.3, the limestone cement has 5% more limestone percentage. Blaine fineness is greater than cement I-II similar to what Cost et al said that overall PLC Blaine fineness must be substantially higher than that of OPC [30].Greater blaine fineness or limestone is a representative of greater surface particle area of limestone blended cement. Higher percentage of finer particles provides more filler properties and more surface area which contributes to higher heat of cement hydration.

Based on the results from the site measurement, experimental data was collected. Boundary conditions and calorimetry results are the main parameters to make the model. The aim of modeling was to create a package that can predict the thermal behavior of concrete. Agreement of

job site data with the modeling result is shown in Figure 2.18. The FEM model satisfactory predicts the maximum temperature rise at the peak time.

For further examples, this model could be used for predicting the thermal behavior of different types of cements and making a comparison. For example, another type of cement by Holicm Company can be used to see the difference of maximum temperature rise in the mass concrete floor. By substituting the internal heat of hydration obtained from calorimetry results of different pastes, a new temperature profile will be obtained.

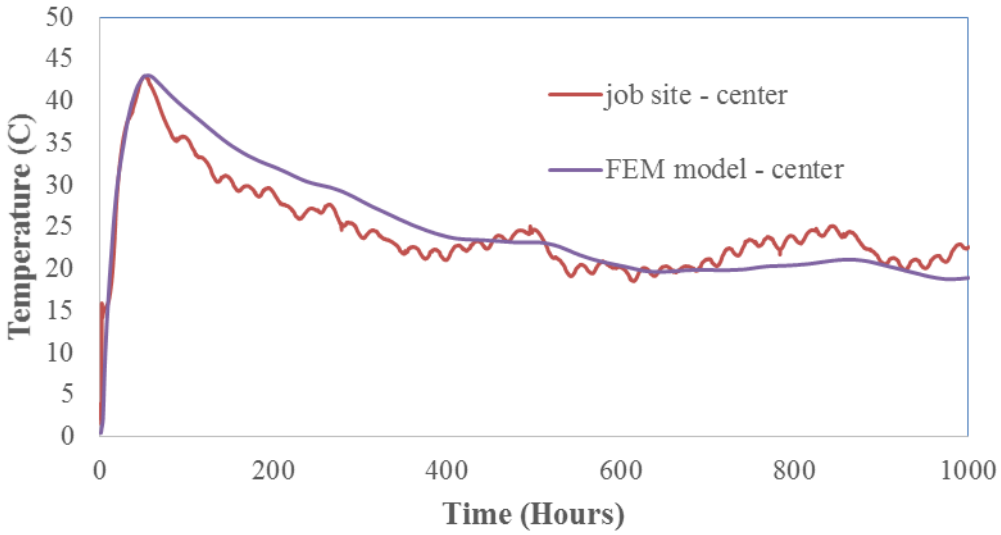

Figure 2.18. Comparison of temperature gradient for the mass floor (FEM, Job Site Measurement)

A commercial software package [27] is used to compare the temperature prediction of the job site with finite element model in two cases. Due to the unavailability of IL cement in the software, cement I-II was selected. If the weather data is applied from software, the results in Figure 2.19 would be obtained. If we use ambient temperature data from the job site, the updated result can be seen in Figure 2.20. Obviously, the ambient temperature is the key point in temperature prediction modeling. Therefore, relying on the weather data from software does not lead to accurate output. Error estimations of these two conditions are presented in Table 2.6. MSE or

mean squared error is the difference between the estimator and what is estimated and it is calculated from the following equation:

$$MSE = \frac{1}{n}\sum_{i=1}^{n}(Yi - \overline{Y}_i)^2$$

Which n is total number of data, Y_i is every data, and $\overline{Y}_i$ is the average of data. R^2 or coefficient of determination is a statistical measure of how close the model data are to the experimental data.

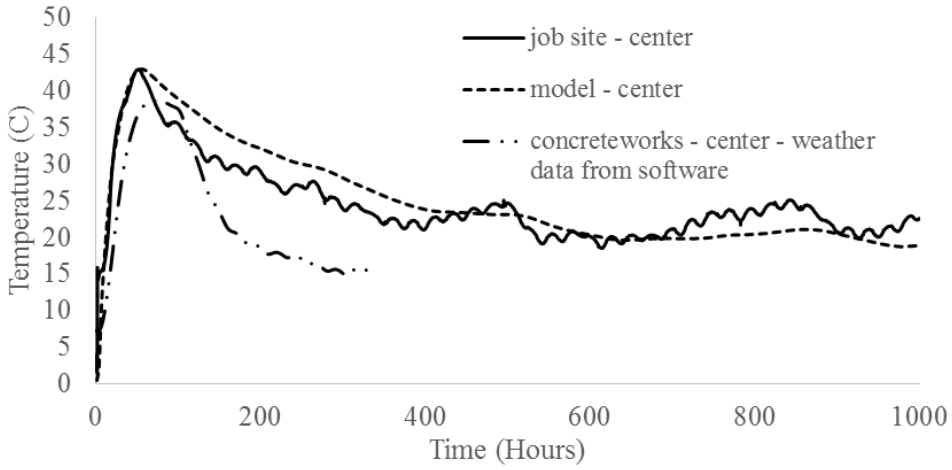

Figure 2.19. Comparison of temperature gradient for center point (FEM, Concreteworks, Job Site Measurement) software data

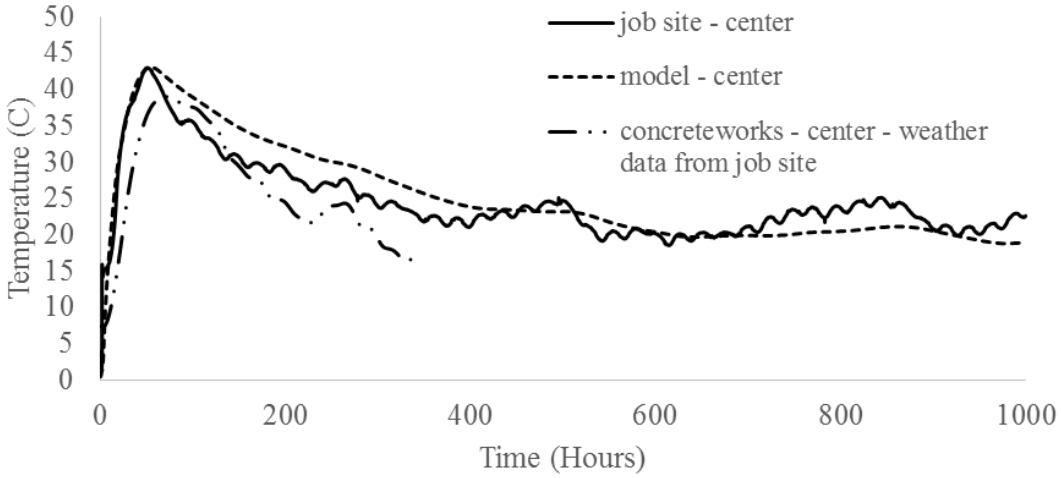

Figure 2.20. Comparison of temperature gradient for center point (FEM, Job Site Measurement) job site data

Table 2.6. Error Estimation of modeling accuracy

Model	MSE	R^2	n
Commercial program (Software ambient temperature)	-6.76	7.97	4032
Commercial program (With job site data temperature)	-3.34	5.02	4032

Considering the calorimetry data, future temperature prediction would be possible. To see the difference of no use of SCMs on the results, Figure 2.21 can elaborate this point of view that the peak temperature difference would be 2% for 10×1.22 m^2 (32.8ft × 4ft) section. It is obvious that with greater depth of concrete section, this difference would be greater. Because heat is accumulated at the middle of mass floor as we have seen it in Figure 2.9.

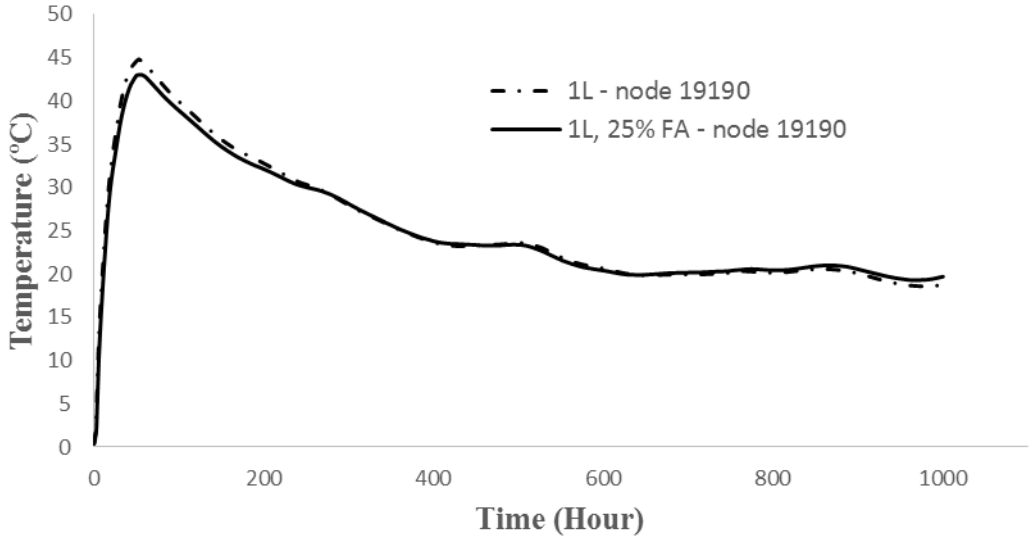

Figure 2.21. Comparison of temperature history of center point in slab for IL and IL + 25% FA

Calorimetry data for cement I-II as internal heat generation input for FE model was used to obtain the temperature rise. The comparison of heat of hydration in IL + 25% FA type C with I-II + 25% FA type C is shown in Figure 2.22. Effects of limestone powder in cement hydration both chemically and mechanically are well documented with respect to synergistic properties, establishment of nucleation sites, formation of calcium carboaluminates, and other interaction mechanisms [31].

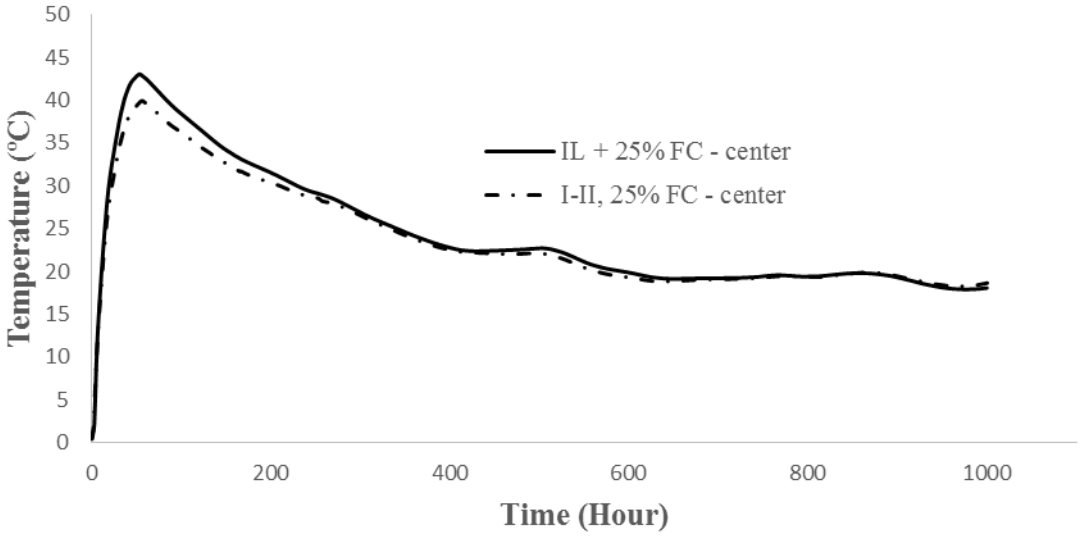

Figure 2.22. Comparison of temperature gradient at center point of 4’ slab for IL + 25%FC and I-II + 25% FC

For this case study, 10% limestone in cement IL and 1.22 m thickness of slab are used, while cement I-II has 5% limestone. Based on the chemical composition of cement IL and cement I-II, cement IL has higher early cement hydration. It should be mentioned that blending of portland cement with limestone is found to accelerate the initial hydration [32]. The difference of maximum temperature potentially would be higher for larger structures and higher limestone percentages.

2.6Conclusion

In summary, prediction of hydration heat in mass concrete structures should be considered because of the possibility for thermal cracking. Limestone blended cement has a different heat of hydration in comparison with other ASTM C150 cements. The researcher need to use calorimetry results and measured weather data if they use different type of cement (like limestone blended cement) rather than standard cements and want more accurate estimation of maximum temperature rise in the mass concrete structures. The maximum temperature at the job site occurred at 42.94°C (109.29ºF) after 51.75 hours. The finite element model is predicted 43.03°C

(109.45ºF) maximum temperature rise after 56.7 hours of casting which is 0.2% close the actual data. However the commercial software predicts 39.08ºC (102.34ºF) after 72 hours for commercial software with ambient temperature of the job site. Using the software weather data leads to 5% less accuracy in temperature prediction results.

In addition, after verification of the model with the job site measurements, the model is applicable for other types of concrete using cement I-II + 25% fly ash type C using the calorimetry results. The maximum temperature of cement IL+25%FC would occur at 43.03°C after 56.7 hours of casting in the mass floor and is about 39.86°C (103.75ºF) after 59.3 hours for cement I-II+25%FC. Higher maximum temperature of cement IL hydration than cement I-II is probably because of high finer particle and greater cement Blaine.

CHAPTER III

HEATING PERFORMANCE OF MASS CONCRETE RADIANT FLOOR SYSTEM WITH GROUND SOURCE GEOTHERMALSYSTEMS

3.1 Overview

Concrete slabs with a radiant heating/cooling pipe system have been used extensively for heating and cooling buildings. Heated or chilled fluid in the radiant floor system originating from a ground source system can substantially increase the energy efficiency of concrete slab floor buildings over both hot and cold seasons. However, the thin slabs or thick slabs perform differently because of the thermal mass and the thermal lag properties. The possibility of storing thermal energy in the mass concrete floor can impact the stability of the temperature in the buildings. Thermal properties of concrete allow thermal energy to be stored in the mass floor after heating or cooling cycles. The thermal performance and energy storage density of a system canbe optimized by controlling the storage-restitution periods, thickness of slab and surface radiative properties which the most practical choice is slab thickness [33].In this chapter, the heating performance of a 4 ft thick mass concrete floor is investigated. A finite element model of the mass concrete floor with an embedded pipe system is performed and validated by the full scale building measurements. The thick slab contains embedded pipes, vertical steel anchors, and horizontal reinforcing steel grids at the top and bottom. A comprehensive finite element analysis is used for the modeling of heat transfer. This model is further expanded to simulate different

thermal loadings on the pipes. Results show that the initial temperature of the thick concrete slab is increased by a few cycles and the mass heated concrete floor acts as a thermal storage battery for the building.

3.2 Introduction

3.2.1 Green Building

The aim of green buildings is to reduce their lifetime carbon footprint. The design of low carbon buildings requires lower operational carbon dioxide emissions either during the construction, including the choice of building materials, during the operation of the building, or both. Building regulations have been changing to lower the effects of climate change on CO_2 emissions, making the application of forced-air air conditioning systems harder to justify, particularly in the face of rising energy costs [34]. The commercial and residential buildings are responsible for 9.9% and 5.4% in production of the global greenhouse gas [35]. In this study, the use of heated/cooled mass concrete floor with limestone blended cement applied with a ground source heat pump is a potentially more sustainable method of heating and cooling.

There are different types of floors with heating/cooling piping systems including the wood, concrete, hollow slabs, etc. The concrete floor is a common type of heated floor for the building with radiant floor system. The thermal conductivity of concrete is low in comparison with other conductive materials. In addition to low thermal conductivity of concrete slabs, concrete elements are inexpensive for building construction. Generally, every pound of concrete costs 2.5 cents in the US. One pound of concrete contributes about 0.2 pound of CO_2 to the environment. In return, that pound of concrete can transmit the 3000 to 5000 lbs of load to the foundation. It also can absorb thermal energy storage, radiation shielding, and protection from natural disasters. The concrete surface would be a finished architecture surface, too. The study described herein reports on the findings of the thermal behavior of a thick mass concrete floor.

Different types of energy in the world can be minimized by optimizing the heating/cooling systems usage. And most heating and cooling systems in the buildings need electrical power to operate. 40% of the primary energy is consumed from the commercial and residential buildings in the United States [36]. To impact the values of green buildings, it is necessary to minimize the energy consumption in the building. Ground source heat pumps (GSHP) are one of the high energy efficiency systems that can reduce the greenhouse gas levels [37]. Generally, there are four basic types of ground loop system including the vertical, horizontal, closed-loop, and pond systems [38]. The GSHP with vertical borehole can extract the geothermal energy for the building because of the constant temperature of the soil regardless the seasonal fluctuation [39]. Ground bore hole installations are higher cost than conventional furnace systems, but using the ground temperature causes energy saving that fully recover construction cost in 5-7 years of normal operation at constant utility rate. Where electricity utility rate are lower at nights or at off-peak hours in the some places like Oklahoma. Therefore, energy usage at nights may cause money saving. The comfort level for the residents can be obtained by air conditioning system or radiant floor system. Radiant floor system with ground source heat pump is used for extracting the heat from the ground source or delivering the heat to the building floor. Also, heating or cooling provided by radiant floor system reduces the size of air conditioning system in the building.

3.2.2 Thermal Mass

The specific heat capacity $C_{p,}$ of the material is ability of the material to absorb or radiate heat defines the effective thermal capacity of a material [40]. The concrete floor with embedded pipes delivers the heat to indoor air through convection and radiation from the surface of the concrete. Concrete has a high volumetric heat capacity and low thermal conductivity properties compare to other materials used in the radiant system like wood. These thermal properties allowthe concrete slab to charge and discharge effectively during 24 hours period [41]. Part of the thermal energy is stored by the mass concrete slab as it’s temperature increases. When the concrete floor is covered

by a roof, the indoor temperature is mostly affected by radiant heat floor. Larger areas of a heated slab can provide the heat flux needed to maintain the indoor temperature. Thermal mass of heated floor would save the thermal energy during the surplus time and give it up during peak hours of energy. Using the mass heated floor in the covered structures such as offices and laboratory with controlled condition of internal air temperature can moderate the heating need at cool seasons.

The in situ temperature gradient by piping system can be simulated with a comprehensive finite element modeling. A three dimension full modeling of concrete, steel, and pipes is selected to study the thermal behavior of heated concrete floor. Several research show that the 3D finite element analysis provides the more detailed modeling of the concrete pavements [42]. Thermal properties of each element during the heat transfer analysis would be specific based on the thermal conductivity, heat capacity and density. Steady state and transient heat transfer analysis of the heated slab with heating pipe systems is done by a widely finite element software [23].

3.2.3 Heat Pumps

A heat pump is an electrical instrument which can extract heat from outside source rather than making the heat. Heat pump technology has been applied in the world for decades. Two common instances of this technology are air ventilation systems and refrigerators. There are some sources of energy that heat pump can use to extract heat like air or water and deliver this heat to another source of air or water. Heat transfer material is fluid (air or liquid). Three most common heat pumps are described as the following:

Air-Air Heat Pumps

An air-air heat pump takes heat from outside air. For example, heat pumps takes the heat from outside air (even cold air) and deliver this heat to inside of the building at winter. On the other hand, this process can be reversible. Heat pump pulls the heat from inside air and delivers it

tooutside to make the building cold. The unique ability of heat pump is very economical and efficient for home purposes because it can operate on the both ways of cooling and heating.

Water-Air Heat Pumps

A water-air heat pump extracts heat from water like a water pool or underground water. The water-air unit is the most common type of heat pump used with ground-source application. The water-refrigerant coil is linked to the outdoor water loop, and it serves as the condenser in cooling and the evaporator in the heating system. The air-refrigerant coil is usually linked to a forced air system.

Water-water Heat Pumps

The water-water heat pump demand isincreasing over the last years based on heating or cooling the system. Water-water units are used for hydronic floor heating, dedicated domestic water heating, outdoor air preconditioning, and hydronic heating and cooling.

An air-air heat pump absorbs the heat from the outdoor air in winter and rejects heat into outdoor air in summer. The ground source heat pump systems which pulls the heat from the ground or ground water is becoming widely used. The efficiency of the ground temperature water with heat pumps would be higher than air-air heat pump because the ground heat pump uses the heat from the ground temperature which is pretty stable during the whole year but air-air heat pump uses the air as a source which include more demand on the heat pump.

Heat pump components

Water-water heat pumps components are generally are as follows:

The refrigerant: The liquid or gas material that circulates through the heat pump, alternately absorbing, transporting and releasing the heat.

The coil: A loop or loops of tubing in which the heat is transferred through. The tubing may have fins to enhance the surface area for heat exchange.

The evaporator: A coil in which the refrigerant absorbs heat from its surroundings and boils to become a low temperature vapor. Some heat pumps include an accumulator which collects any excess liquid that has not been vaporized into a gas.

The compressor: The refrigerant is compressed to increase the temperature refrigerant.

The condenser: A coil in which the refrigerant releases out the heat and converts to liquid.

The expansion valve: A part of the heat pump which reduces the pressure of the refrigerant generated by the compressor. Therefore, the temperature drops and the refrigerant becomes a low-temperature vapor / liquid mixture.

The reversing valve: A valve which controls the refrigerant flow direction in the heat pump from cooling to heating mode or vice versa.

Heat Pumps performance

Generally, heat pumps transfer the heat by circulating a liquid called refrigerant through a cycle of evaporation and condensation. This process can be seen in Figure 3.1.

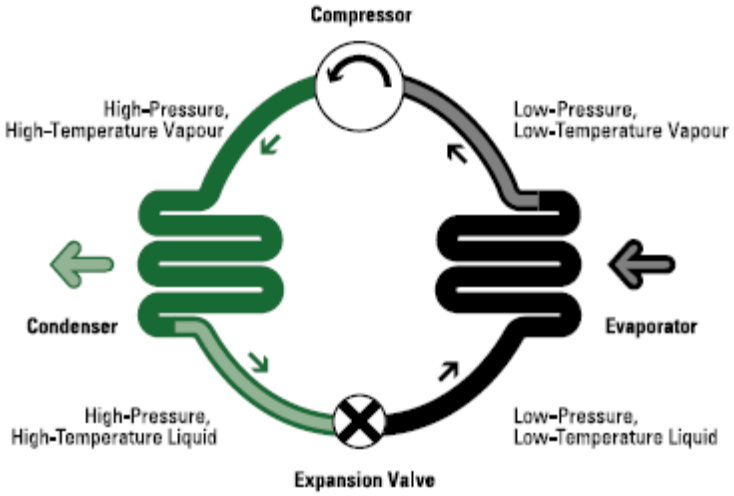

Figure 3.1. Condensation and evaporation cycle at the heat pump [43]

There are two coils for the evaporation and condensation processes which work separately. The compressor pumps the refrigerant from one heat exchanger coil to another coil. In the evaporator heat exchanger, the refrigerant is evaporated at low pressure and the surrounding heat is absorbed by the refrigerant. Then this refrigerant is compressed to the condenser coil and it condenses at high pressure. During this process, it gives up the absorbed heat in the evaporator coil exchanger.

The heat pump fully operates in the cooling and dehumidification mode in summer or heating in winter.The heat pump can generate heat for buildings even from cold air, because the ground and outside air always contain the heat. For example, air at -18°C contains about 85 percent of the heat present in the air at 21°C.

3.2.4Ground source heat pump

The earth energy is extracted inexpensively, green, renewable, and environmentally friendly. They have been applied for more than 60 years in the US. Ground-source heat pumps (GSHPs) usually referred to geothermal heat pumps, were established in the building and residential arena. The advantages of vertical GSHPs are they require less soil area in contact with pipes, need smallest amount of pipe and pumping energy, and they can yield the most efficient GSHPs

performance. The disadvantage is that they are higher in cost including the installation and equipment for drilling [44]. They can work with heat pumps to provide hot or chilled fluid in the piping system of radiant floor for during the heating or cooling process.

Heating

A ground-source heat pump removes the heat from the ground. Several loops of flexible pipes are buried under the ground to use the green energy of the ground. The fluid through the underground pipes can absorb the heat and transfer this amount of heat to the heat pump. The heat pumps pulls the heat from the loop then it distribute this heat through the load pipes which are radiant floor system or a conventional duct system or hot water heating.

In the heating cycle, the geothermal system water or the antifreeze mixture collects the heat from the soil and is brought to the heat pump which is shown in Figure 3.2. The heat from underground water arrives at the refrigerant-filled primary heat exchanger called the evaporator. The cold liquid refrigerant on the other side of heat exchanger, which is colder than the ground water absorbs the heat. This heat from earth source is transferred to the refrigerant and it becomes low temperature vapor. This low pressure and low temperature refrigerant passes through the compressor to be squeezed, then the high pressure and high temperature gaseous refrigerant forms. This high pressure, high temperature refrigerant is fed into a condenser. In the water-water heat pump which performs with the radiant floor system, an antifreeze liquid such as ethylene glycol is used in the tubing system. For next step, the antifreeze liquid, which heats the floor flows through the condenser. Since the refrigerant is warmer than antifreeze liquid, the heat is transferred from the refrigerant to the antifreeze liquid. As the refrigerant loses the heat, the refrigerant's temperature is dropped somewhat and condenses. The high pressure, high temperature liquid refrigerant then flows through an expansion valve. The expansion valve reduces the refrigerant pressure and its temperature subsequently drops. This low temperature

liquid passes to the evaporator, and the cycle repeats. If the heat of ground source water is used to heat the air, the heat pump is called “water-air heat pump”.

The colder water returns to the ground in a closed loop system. It absorbs the ground temperature and returns to the heat pump.

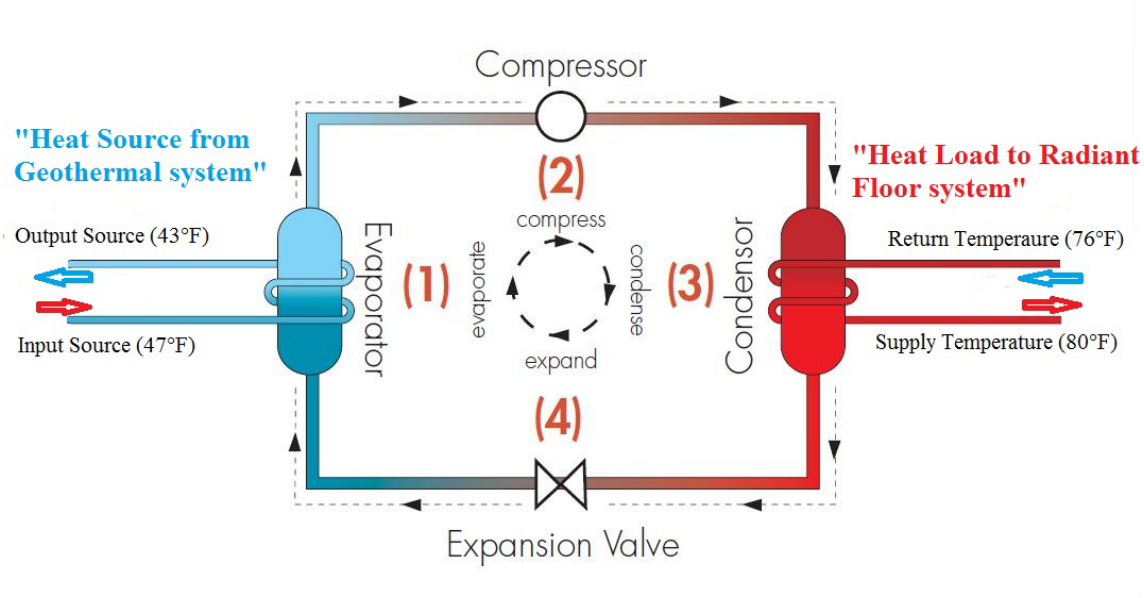

Figure 3.2. Typical Ground-source heat pump parts

Cooling

A heat pump with geothermal system air condition can be used as a cooling generator for building by reversing the heating process. The heat is extracted from the building and either moved back to the ground loop system or used to preheat the water tank in the building. Once the heat is pulled from the air, it will send out to the duct system of the building.

The cooling cycle is completed by reversing the heating process. In the cooling mode, the ground connection to the refrigerant heat exchanger is reapplied within a condenser, and the refrigerant to air heat exchangers reapplied within an evaporator. The refrigerant direction is reversed by the reversing valve. The refrigerant pulls the heat from the inside hot air and transfers it to the antifreeze mixture or geothermal water source. Next the heat is pumped to underground piping in

a closed loop system. This heat can be used for preheating domestic water. The earth energy system does not require the defrost cycle like the air heat pump, because the underground water temperature is pretty stable and the frost problem does not exist.

Typically the cost of ground source heat pumps are higher than air-air system because of drilling and pipe installation but they are most efficient heating system because they use the free, green, renewable energy of the ground for heating of the buildings.

3.2.5 Radiant heat Floor

Geothermal system can provide hot fluid for the radiant application. These pipes are located under the tile, wood or concrete floors. This heat at the surface on the pipes moves to the surface and makes the floor warm and comfortable for residents. This heating system has a better performance in comparison with the conventional air condition system because the heat distribution is more uniform and level of comfort is satisfactory. Heat pump warms a room gradually and it is more uniform temperature distribution rather which is shown in the Figure 3.3. Using radiant heating system has some advantages as following:

- Maximum flexibility in zoning and temperature controls
- Constant and even heat in all areas of the home
- Cozy, warm floor surfaces for bare foot comfort
- No unsightly baseboard heaters to take up wall space
- Completely silent heating
- System can use air handlers with air conditioning, solar heat, or heat pumps [45]

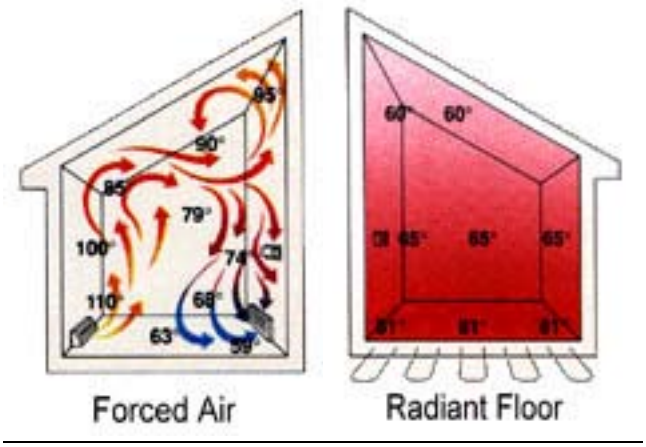

Figure 3.3. Geothermal heat pump and radiant floor system [46]

The main disadvantage is upfront cost of radiant systems and geothermal system. Also, the maintenance regarding the embedded pipes could be expensive. Changing from heating tocooling or vice versa is not as fast as air conditioning systems. Radiant heating/cooling system would need some hours to circulate the heated or chilled water in the tubing system before making the building warm or cold.

3.3 Experiment

3.3.1 Instrumentation

The experimental program has been conducted in full scale at one of Oklahoma State University's researchlaboratory buildings. The concrete slabs with embedded pipes were placed as the foundation of the building. The slabs include the 4-ftthick mass concrete floor with piping system located 6 in under the surface of the slab and the 7-inch-thick slab with embedded piping system at the bottom of slab. There is 1 in of polystyrene insulation under the thin slab and all-around of the mass floor perimeter for better thermal storage capacity of the slab. The mass concrete floor was cast on the 3 in mud slab and there is no insulation underneath.

Therefore, the 1 in of insulation under the thin slab can keep the generated heat by piping system. In addition, due to height of mass floor with concrete materials, the generated heat by piping

system is important to be kept near the surface of the slab. Before casting the concrete slabs, T-type thermocouples have been installed at the positions all through the depth of slab to measure the slab temperature at different elevation. There are two places of thermocouple installation at each kind of slab including the “edge point” located 1ft from the edge of slab and “center point” located 16ft from the edge of slab as shown in Figure 2.6. Thermocouples installation details were presented in Figures 2.4 and 2.5 for the mass floor and the 7 in slab.

Radiant floor system works with ground source heat pump (GSHP). It means the higher temperature of ground water is provided by well system out of the building and the underground water heat will be transferred to the radiant floor fluid by the heat pump operation. Then, heated fluid is inserted to the floor pipes to make the concrete slab warm and it will return to the heat pump in a closed loop. Input supply temperature and return temperature of the pipes are measured over time to control the radiant floor system. An ultrasonic flow meter was used to measure the flow rate of fluid through the pipes. Pressure gauges were inserted to the p-t ports of pipes to measure the return fluid. These measurements were used as input parameters for the modeling of the radiant floor system. All measurements have been carried out over step time of 15 minutes and they are used for modeling of heated slab.

3.3.2 Geothermal system with Radiant Floor

The heat pumps use the source pipes to receive the heat from the well field (ground loop) then transfer this heat to the load pipes which are radiant floor system. Therefore, a heat pump has an entering source pipe which is underground water comes from the ground and a leaving source pipe which is water comes back to the ground from the heat pump. During this process heat is extracted from the underground water then this heat will be used for loading pipes. In addition, the entering load pipe contains the heated fluid which goes to the radiant floor system and leaving load pipe contains the returning fluid from the radiant system.

An online monitoring system is available at Cooper lab which part of the monitoring system is shown inFigure 3.4. With online monitoring system, the all conditioning system and radiant floor system can be controlled by an operator.

It was more efficient to increase the set point temperature gradually on the system. The difference between the temperature of the heat source and the temperature at which the heat is delivered is the basic for the efficiency of the heat pumps. The greater difference leads to the lower efficiency. For the ground heat pump source, the underground temperature is warmer than the outside air at winter and colder than outside air temperature at summer. As a result, using the geothermal system with radiant system should work very well and efficient.

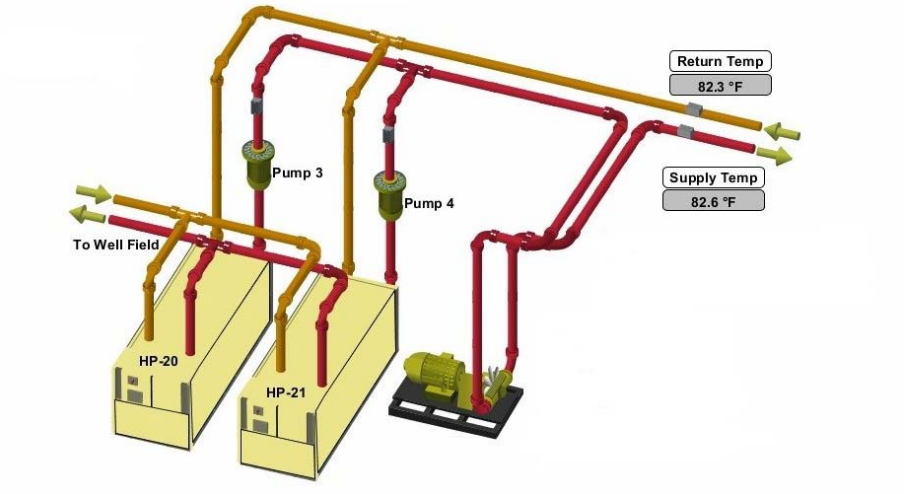

Figure 3.4. Water-water heat pumps at Cooper lab

One of the important terminology in the heating system for the buildings regarding the efficiency and absorbed energy is called “lift” which is the difference between the temperature where the heat is absorbed (“source”) and the temperature where the heat is delivered (the “sink”). The larger the lift, the greater input power is needed by the heat pump. This is the reason why the geothermal system works much more efficient than the air system.

The Cooper engineering lab has two water-water heat pumps which is connected to the radiant floor system as seen in Figure 3.5. As seen before, the supply and return temperatures are measured by the temperature sensors in the online monitoring system. Pumps at the loading pipes make the input water a little warmer than the set point temperature.

For geothermal system the high-density polyethylene (HDPE) pipe is used. This kind of pipe does not corrode or rust and is inert to chemical materials in the soil. Copper or PVC pipe should not be used for the geothermal system. The expected actual life of the pipe is over 200 years.

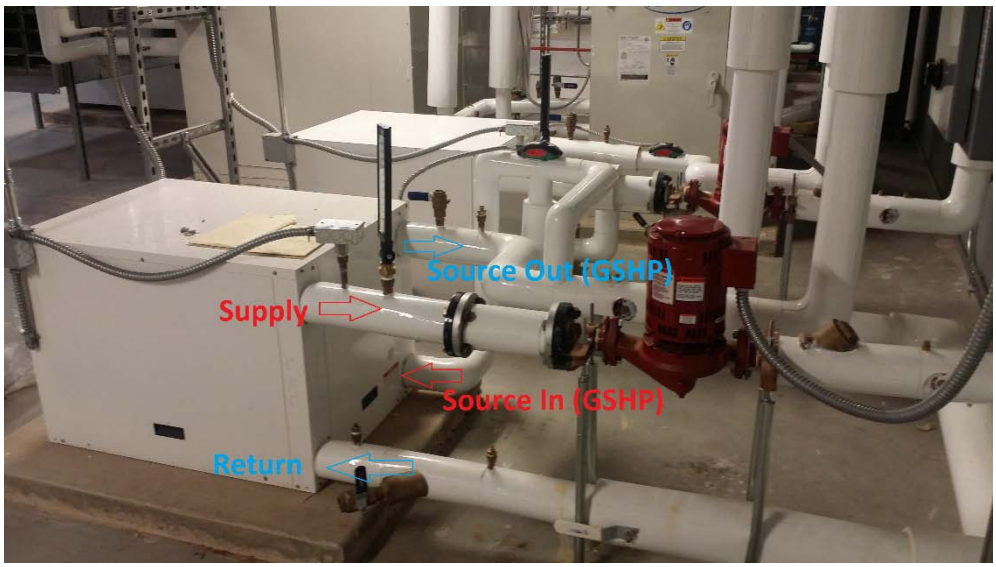

Figure 3.5. Water-Water heat pumps at Cooper Lab

Overall performance of radiant floor system with ground heat pump source is shown in Figure 3.6 for heating cycle at winter season and Figure 3.7 for cooling cycle at summer season. Two heat pumps extract the heat of underground water and use it for heating the radiant floor water. After this water is circulated into the heating pipe system in the slab, it will return to the heat pump as a closed loop.

At the summer season the heat pumps operate in a reverse process (Figure 3.7). The heat pump pulls the heat out of the water and the chilled water will pump to the radiant floor and warmer water will return to the geothermal loop.

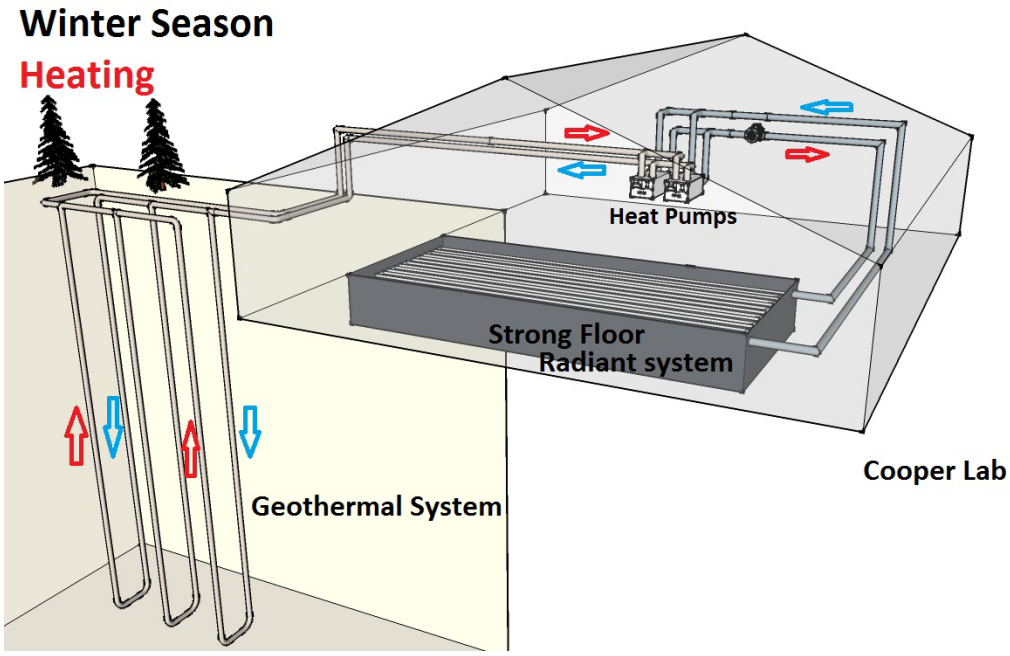

Figure 3.6. Overall set up for geothermal and radiant floor system (heating)

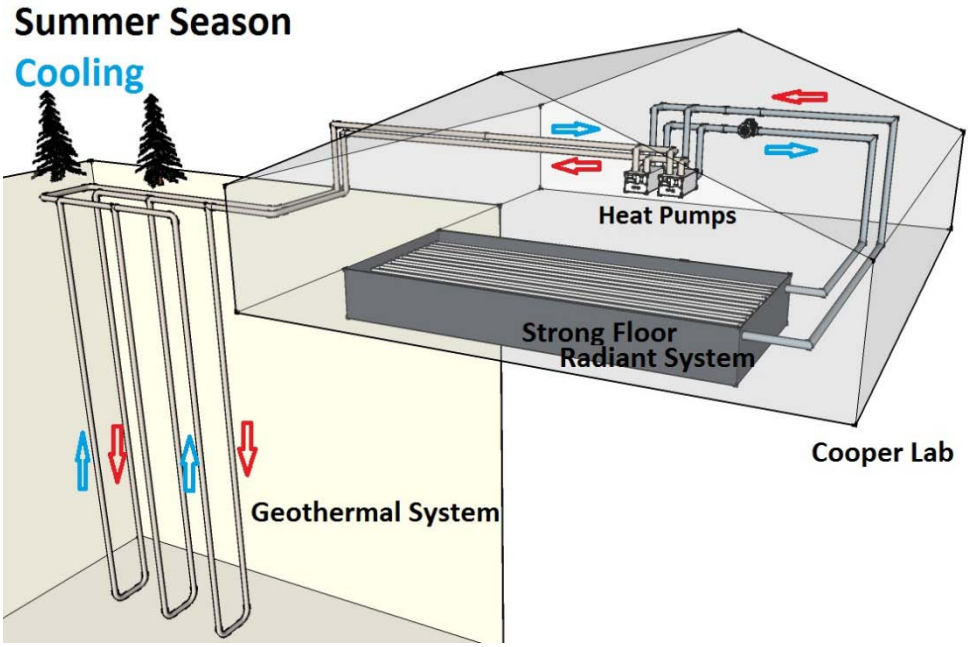

Figure 3.7. Overall set up for geothermal and radiant floor system (cooling)

Based on the sequence of operation at Cooper laboratory, if the radiant floor system is enabled and forced air heat pumps are placed in the cooling mode, after 10 minutes time delay, the radiant floor heating system shall be disabled. If the forced air heat pumps system are placed in the heat position with the radiant floor heating system disabled due to forced air previous condition, after 10 minutes the radiant heating floor system shall be enabled.

3.4 Heat Transfer Analysis

The generated heat from the piping system distributes to the area around it which is concrete, steel anchors, top and bottom horizontal mesh. This heat transfer process happens through the conduction, convection processes. Then, the indoor air would be affected by the heat of embedded pipes in 6 inches below the surface of the concrete by convection and radiation. To describe the air heating process, it should be mentioned that the heat transfers from concrete cover to the surface by conduction, then the heat will distribute to the indoor air by convection and radiation process. The amount of transferred heat through radiation and convection from the surface of the concrete depends on a lot of parameters such as the concrete properties, indoor air temperature, air movement, building insulation, occupants, floor cover, and less on outside weather conditions. The most effective parameters are needed to simplify the model with accurate results.

The in situ temperature gradient by a piping system can be simulated with a comprehensive finite element modeling. A three full modeling of concrete, steel, and pipes is selected to study the thermal behavior of heated concrete floor. Several researches show that the 3D finite element analysis provides the more detailed modeling of the concrete pavements [42].

The fundamental for thermal analysis in this finite element software [47, 48, 49] is a heat balance equation obtained from the principle of energy conservation.

$$k\frac{\partial^2 T}{\partial x^2} + k\frac{\partial^2 T}{\partial y^2} + q = \rho c\frac{\partial T}{\partial t}$$

Where c is the specific heat coefficient [J/(kg.ºC)], k is the thermal conductivity coefficient [W/(m.ºC)], ρ is the density [kg/m^3], q is the heat generation rate [J/(m^3.s)]. The q term can be neglected regarding there is no heat generation after long time of casting concrete.

Regarding the finite element modeling, a three-dimensional 8-node thermal solid element (Solid 70) was used to model concrete thermal properties. A 3D element (Fluid 3-D th-fl pipe 116) used to model the fluid with the ability to conduct heat and transfer fluid between its two main nodes. Finally, 3D conduction bar uniaxial element (Link 33) was applied to model the vertical steel anchors and steel mesh with ability to conduct heat between the nodes at a single degree of freedom of temperature [23]. The element type shape is presented in Figure 3.8.

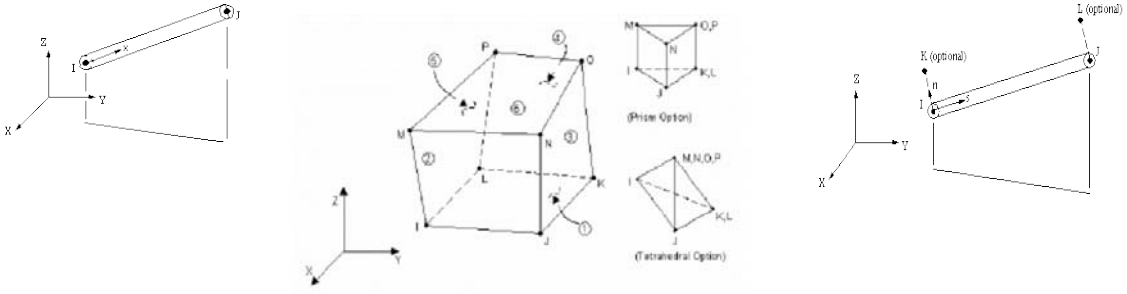

Figure 3.8. Element types (Steel (Link 33), Concrete (thermal solid 70), Pipe (3D th-fl pipe 116))

The steel details and all three elements in FE model are shown in Figures3.9 and 3.10, respectively.

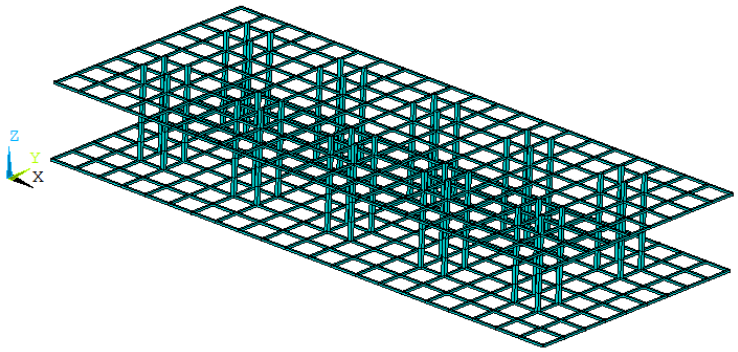

Figure 3.9. Vertical steel anchors and horizontal steel mesh in FE model

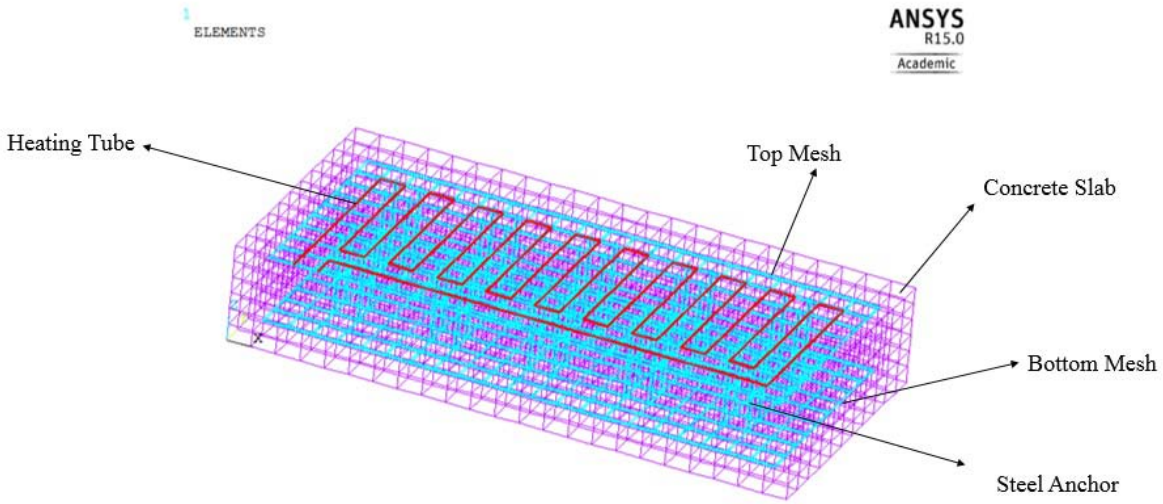

Figure 3.10. Finite element model (concrete, steel, and heating pipes elements)

The concrete slab dimension was 6.9m (22.6 ft) long, 3.3m (10.8 ft) wide, and 1.22m (4 ft) thick in proportion of ¼ of the field mass floor size. The main part of heat transfer from the pipes happened through the top and bottom of slab rather than through the length and width of slab. Horizontal mesh at the top and bottom of slab has diameter of 7/8 in (0.022m). The vertical steel anchors has diameter of 1 ½ in (0.0381m). The pipe diameter is selected ¾ in (0.019m).

Thermal properties of each element during the heat transfer analysis would be specific based on the thermal conductivity, heat capacity and density. Material properties used for the finite element

model are given in Table 3.1. Because of low range of thermal difference in the analysis, it is assumed that the thermal conductivity and heat capacity will be remained constant in this problem.

Table 3.1. FEM Material properties

	Concrete	Steel	Fluid
Density (kg/m^3)	2466	7860	1100
Thermal Conductivity (w/m.°k)	1.8	80	0.258
Specific Heat (i/kg.°k)	900	450	2500

On the other hand, the boundary condition on the heated floor is important to model the heated slab accurately. There is 1 in insulation all around the edges of the slab. The bottom of slab is rested on 3 in of mud slab. The convection at the surface of the slab is assumed h=5.5 W/m^2.K [73]. The emissivity of the surface of the concrete is assumed 0.92 [50]. The mesh convergence is verified by changing the mesh size to make sure that results are independent of quadrilateral mesh.

Steady state indicates the heat transfer equilibrium of the system. To see the thermal behavior of the heated slab over time, transient analysis is needed. The temperature variations in the field were in close agreement with temperature gradient by the finite element simulation. The result of FE simulation will be discussed.

3.5 Result and Discussion

3.5.1 Site Results

As the edge and center of the slab would potentially have different thermal behavior, the results of field data are presented separately. The edge point which is 1 ft far away from the slab is more affected by the boundary condition of the slab including the ambient temperature. The center point which is 16 ft away from the slab side would be less affected by the outdoor air conditions.

The following results will substantiate the difference in thermal behavior of these two points. The results by temperature variation across the mass floor at different elevations over time is shown in Figure 3.11 for edge point and Figure 3.12 for center point. The vertical axis is temperature in degree Celsius and horizontal axis is time in hours. The inlet fluid temperature from ground source heat pumps was set on 80°F (26.7°C). The orange curve shows the thermocouple measurement tied to the embedded tube to read piping temperature at edge and center points.

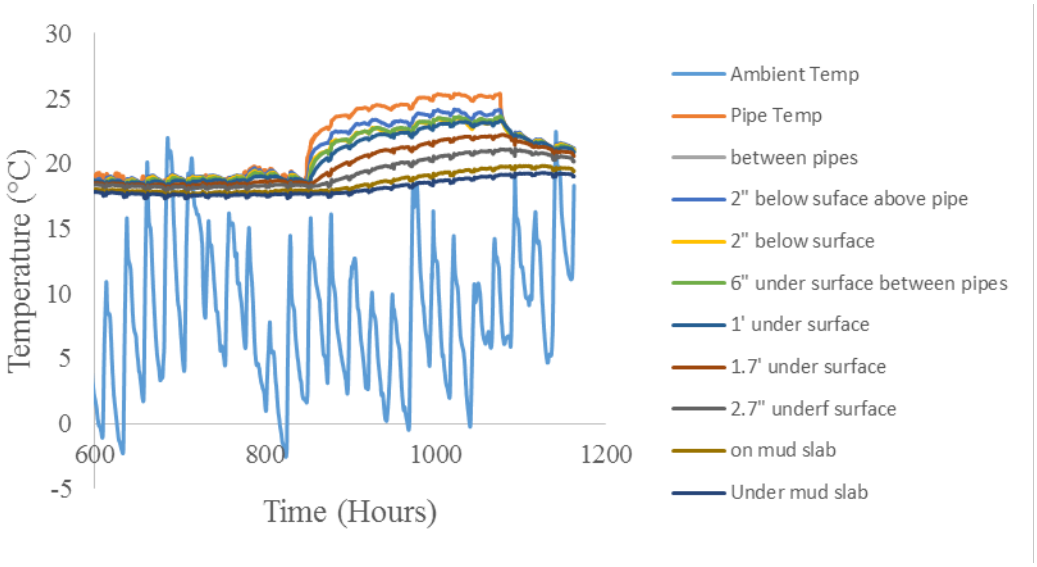

Figure 3.11. Temperature measurement at mass floor edge point (80ºF pipe loading)

Temperature through the slab will be constant after nine days of heating cycle. It means that the slab temperature obtains the equilibrium with indoor air and piping system heat. Zero time is the first day of the year and starting time of the temperature measurements is 600 hours from the origin time to show the initial condition of the mass floor before enabling the heating system at 875 hours. As it can be seen, the initial temperature of the slab before turning the heating system on is about 18-19°C (64.4-66.2ºF) for edge point and 20-20.5°C (68-68.9ºF) for the center point. The blue line indicates the ambient temperature which is between -3 to 22°C (26.6-71.6ºF).

The top of the slab is warmer than the bottom of the slab because of embedded heating pipes under the surface of the concrete. However, the temperature at the bottom of the slab also is affected by the heating pipes because of heat conducted by vertical steel anchors. The temperature trend will be almost stable after 9.5 days of heating cycle. Based on this thermal equilibrium of the system, the next cycle of heating cycles is selected 9.5 days. After turning the heating system OFF at 1090 hours, the temperature trend drops. However, the temperature of the slab after drop would be higher than the initial condition of the slab.

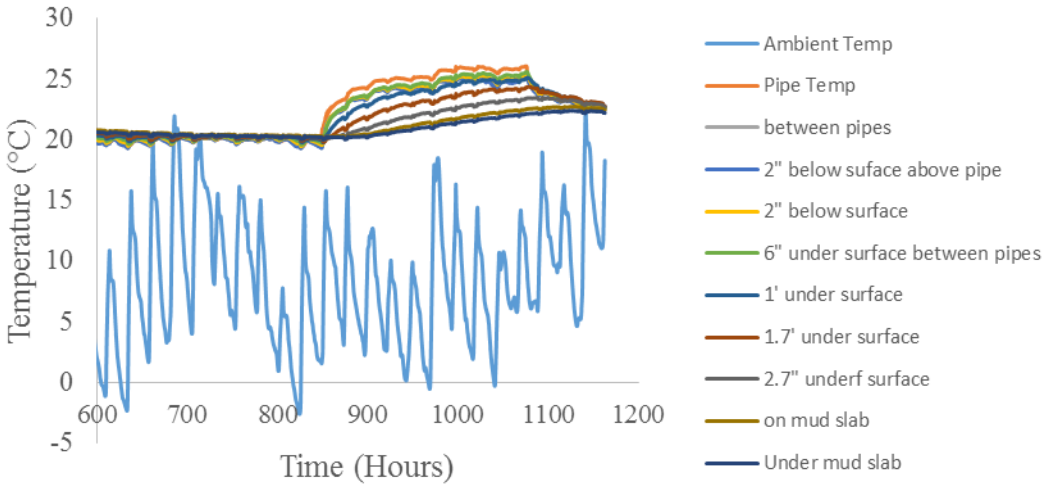

Figure 3.12. Temperature measurement at mass floor center point (80ºF pipe loading)

The temperature variations in the thin slabs are shown in Figure 3.13 and Figure 3.14 for the edge and center points. The thermocouple under insulation of the thin slab at the edge point is less affected by the heating of the floor. The middle of slab and the 1 in below the surface of the slab have the same temperature trend.

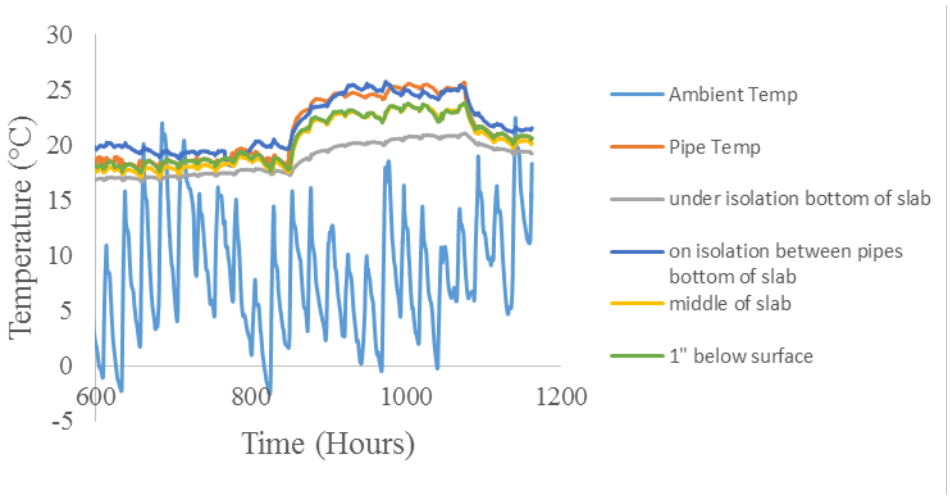

Figure 3.13. Temperature measurement at thin slab edge point (80ºF pipe loading)

The temperature variation in the thin slab at the center point is the same for different elevations of the thermocouples when the heated thin floor is OFF. The heat gain and heat loss from the thin slab would be faster in comparison with the mass floor which heat loss to huge mass of concrete with low thermal conductivity is slower. Radiant floor heating takes advantage of concrete's thermal mass to absorb and store the heat to provide the comfort and efficiency for residents [51].

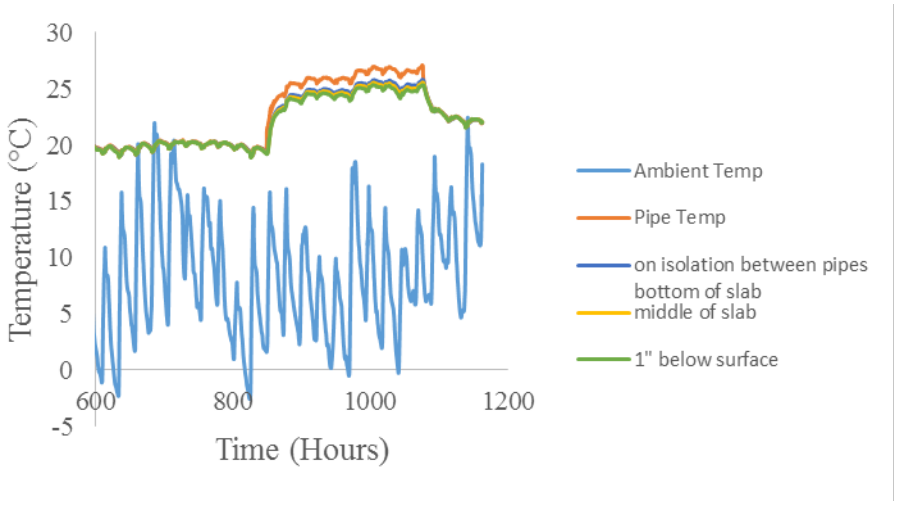

Figure 3.14. Temperature measurement at thin slab center point (80ºF pipe loading)

When the mass concrete floor used in combination with night heating, thermal mass of the concrete floor provides a sustainable technique of heating which saves the electrical energy for air

conditioning system. The sustainable method of heating the building reduces the amount of need for HVAC systems.

The temperature gradient in the mass floor after three heating cycles is illustrated in Figure 3.15 for edge and center points. For more clarity, the legends are not shown. The legend for Figure 3.15 is the same as Figure 3.11. Each heating cycle and rest time lasts 9.5 days. The highest temperature inside of slab is around the heating pipe and the lowest temperature is under the mud slab temperature. Every heating cycle leads to temperature rise in the concrete slab which is a proof of storing heat in the mass floor even regarding the steel role in conducting heat to the indoor air faster. However, the amount of heat storage is clearly seen in Figure 3.16 for the center point.

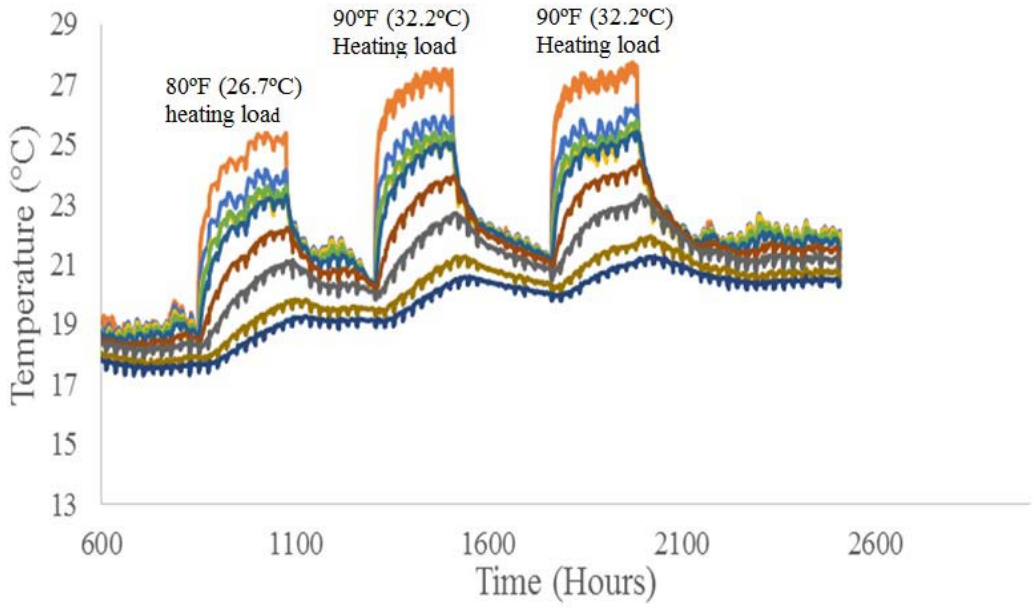

Figure 3.15. Mass floor edge temperature rise (80ºF and two 90ºF heating cycles)

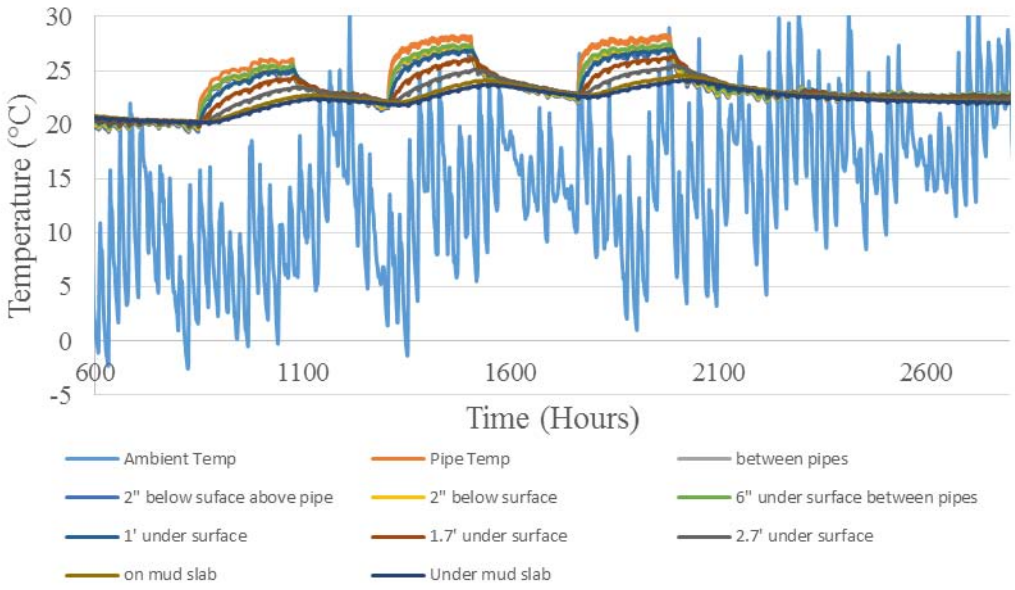

Figure 3.16. Mass floor center temperature rise (80ºF and two 90ºF heating cycles)

The experiments for the heating cycle were carried out at known initial condition of the slab. After three cycles of heating for 80°F, 90°F, and 90°F, the overall temperature of the mass floor is increased for 3ºC. This temperature rise was not reduce after passing the considerable time when the heating system was OFF. It means the thermal energy can be stored in the mass floor with just few cycle of heating system. The amount of thermal energy saved inside of the concrete floor based on the heat capacity of the floor and three degree temperature rise would be 4 MBTU. This overall temperature rise in the concrete slab does not disappear after a long time. It helps to heat pumps efficiency to use less energy to make the heated fluid for the radiant floor.

Temperature gradient in the mass floor along the height of concrete slab is shown in Figure 3.17 and Figure 3.18 at different elevation of thermocouples positions. All temperature measurement shows the temperature of the slab at 00:00 time of each day. The first three lines highlighted by an elliptic indicate the initial temperature of the slab before turning the heating system on. Then, the radiant floor heating is enabled on the fourth day (02/08). The next yellow line at 02/08shows the top of half the slab is heated by the heating pipe. Then, the slab temperature increases

gradually until the heat equilibrium is reached based on thermal loading on the heating pipe after 9 days. The mass floor temperature dropped after disabling the heating system on 02/14.

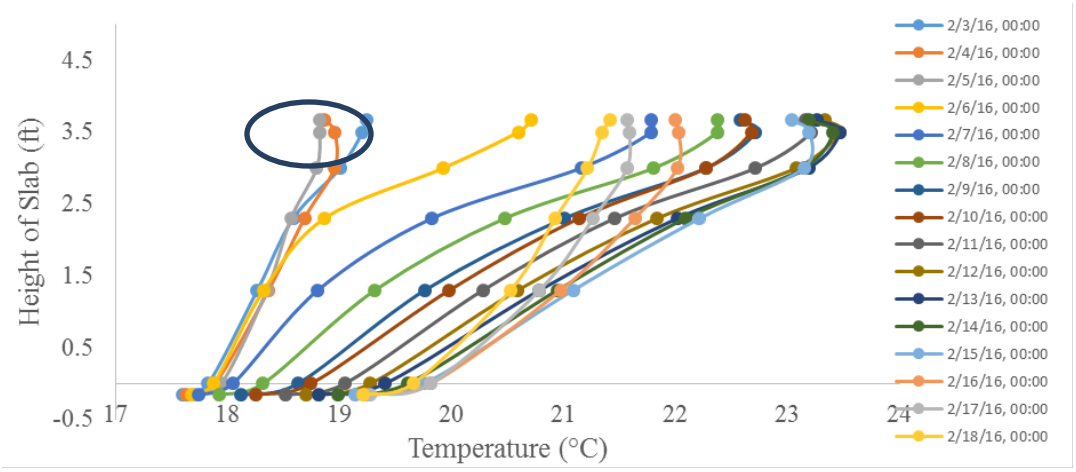

Figure 3.17. Temperature variation at mass floor edge point at 00:00 (80°F pipe loading and off)

The temperature at the center of the mass floor in Figure 3.18 shows that the overall initial and final temperature are greater than the same temperature at the edge point. The top of the slab is affected by the heating pipe from 20°C to 25.5°C (68-77.9ºF). However, the temperature at the bottom of slab is increased from 20°C to 22.7°C (68-72.86ºF). The initial temperature of the slab was not returned to 20°C even after the disabling the heating system.

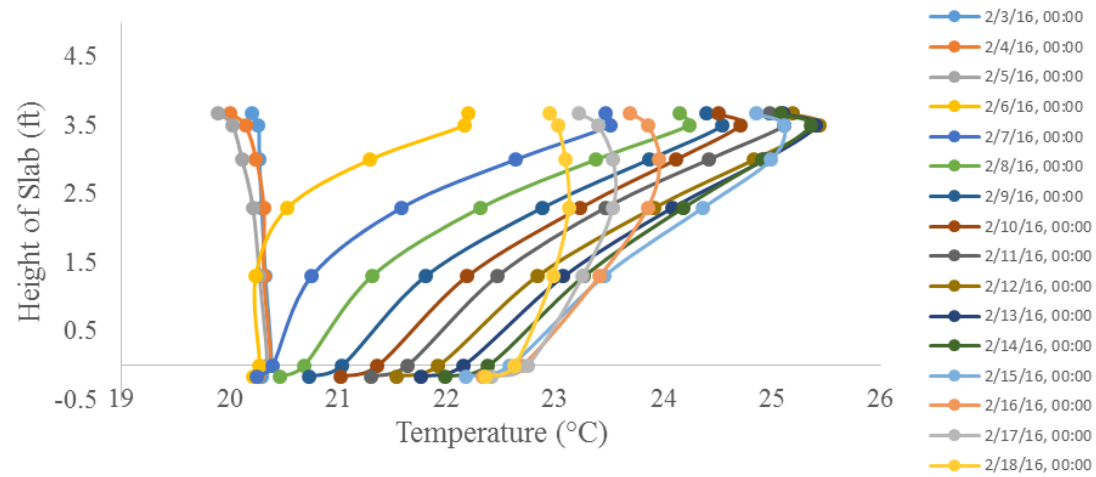

Figure 3.18. Temperature variation at mass floor center point at 00:00 (80°F pipe loading and off)

The temperature variation in the center point of 7 in slab is shown in Figure 3.19 for the same period of time. As it can be seen that temperature profile is almost the same for different three spots through the height of the thin slab. The heat gain and loss for the thin slab would be faster than mass floor due to lower height of the slab. The bottom of slab is warmer than top because of heating pipes located at the bottom.

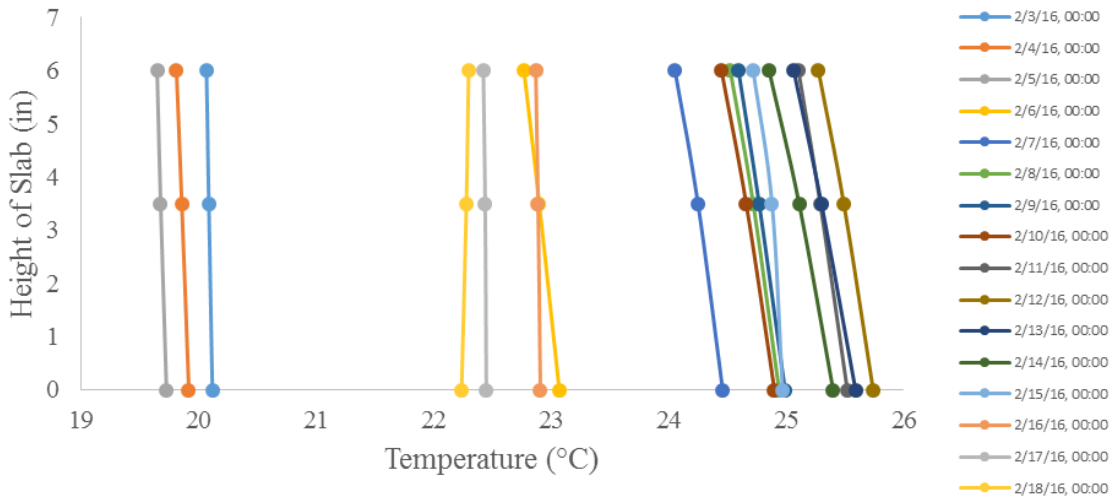

Figure 3.19. Temperature variation at 7 in floor center point at 00:00 (80°F pipe loading and off)

The temperature distributions in the mass floor and thin slab before enabling the heating system and initial and final each 9 days of heating cycle heating are shown in Figure 3.20 and Figure 3.21, respectively.

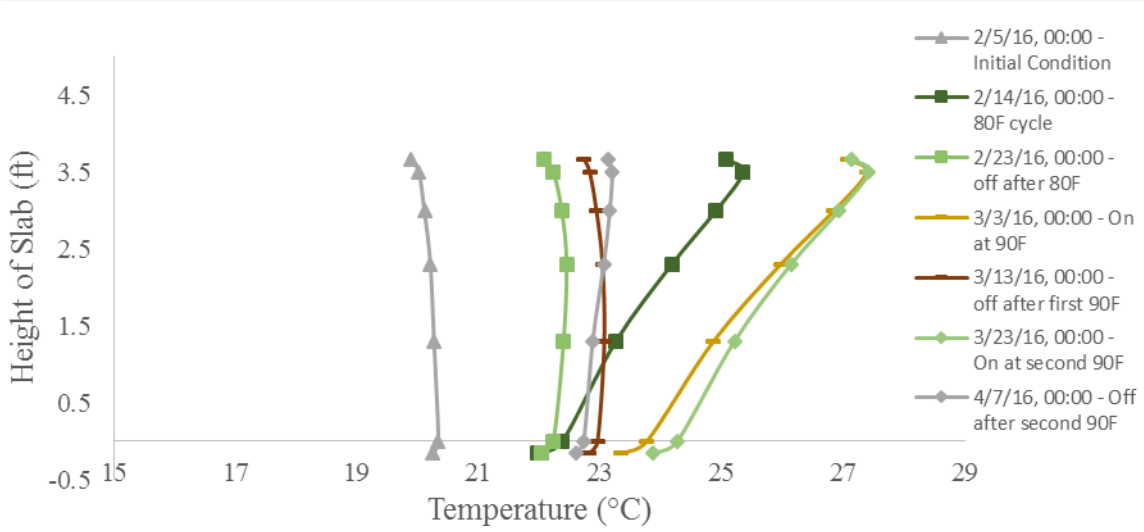

Figure 3.20. Final Temperature variation at mass floor center point at 00:00 (before and after three heating cycles)

The average initial temperature of the mass floor at the center point is 19.7°C (67.46ºF). After every heating cycle, the initial temperature inside of slab for next heating cycle would be greater.

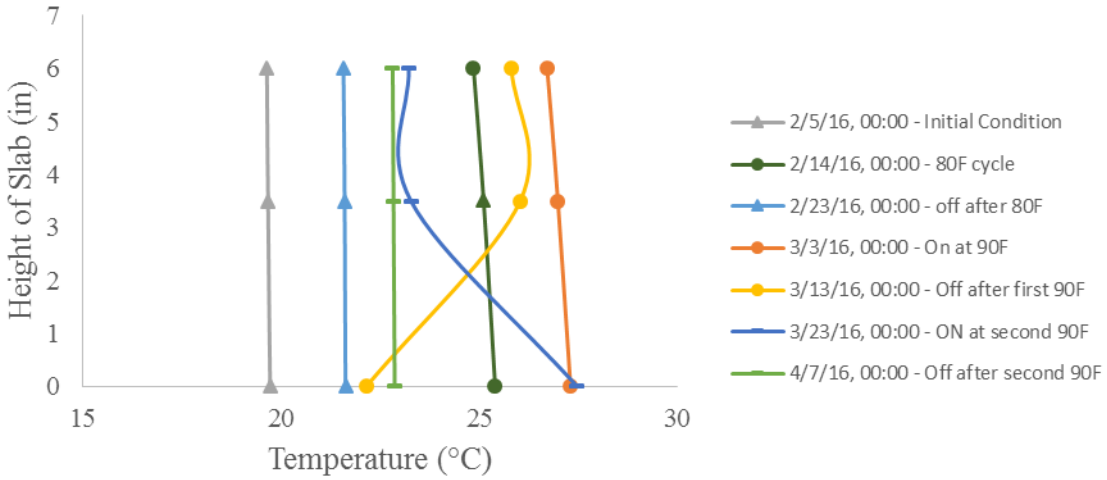

Figure 3.21. Final Temperature variation at 7 in the slab center point at 00:00 (before and after three heating cycles)

The heat fluxes at the bottom of 7 in slab for edge and center point are shown in Figure 3.22. The heat flux at the center point is higher than the edge one when the heating system is on and they are almost the same when the heating pipe system is OFF.

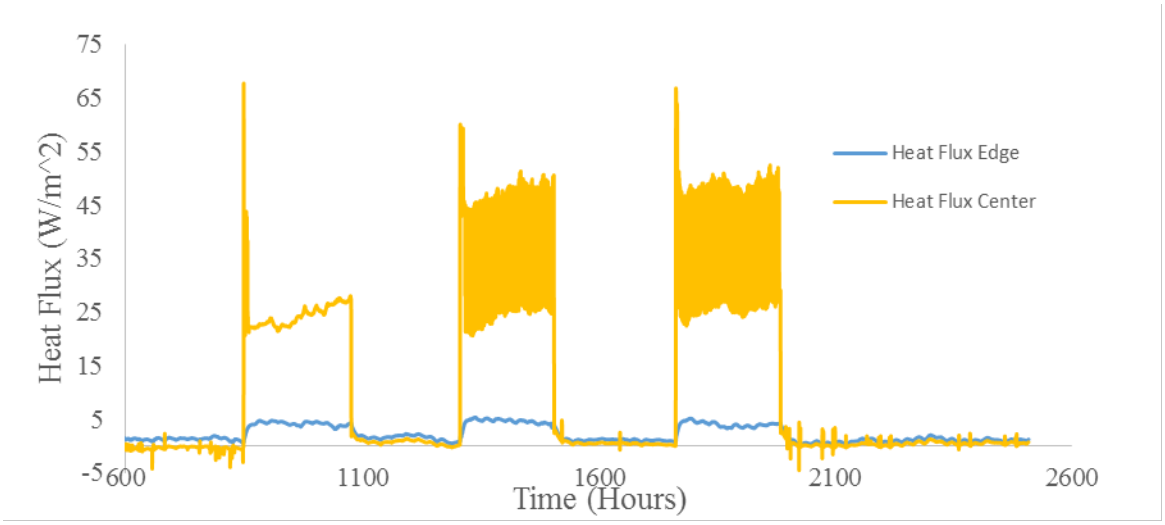

Figure 3.22. Heat flux measurement at the bottom of thin slab (Edge, center point)

3.5.2Finite Element Model Results

The 3D model described in the modeling section withdifferent mesh size range has been analyzed to demonstratethe heat transfer results do not depend on the mesh pattern. The temperature distribution through the concrete slab from the steady state analysis of finite element model are shown in Figure 3.23. Every color show a temperature range which is indicated by the temperature bar under the slab. The four dots on the surface of the concrete show the tip of vertical steel. They are directly in contact with indoor air which means heat at the surface of the slab can be transferred by the concrete and vertical steel.

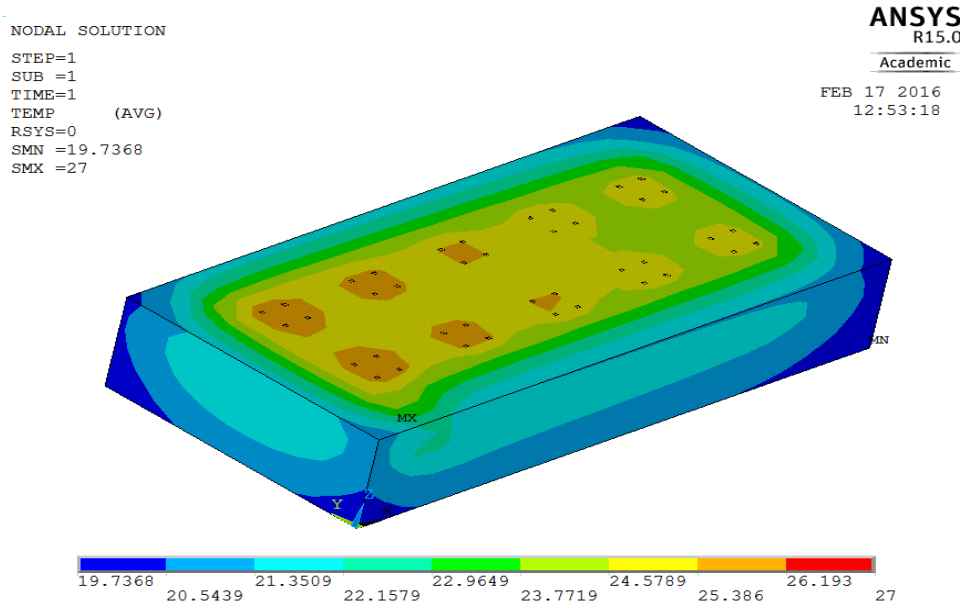

Figure 3.23. Temperature distribution in the mass floor (FE model)

Due to higher conductivity of steel, the generated heat by piping system is transferred by vertical steel faster than concrete slab. This makes the bottom of the slab may receive the temperature difference due to thermal loading of the pipes. The left side of the slab has the higher temperature because the hot fluid is inserted to the slab at the left side.

To validate the model, the full 3-D model, the result of the FE steady state analysis is compared with final temperature profiles through the depth of the concrete block for edge and center points shown in Figure 3.24 and 3.25, respectively. The maximum temperature along the height of concrete slab is occurred at the heating pipe elevation as expected. First three lines indicate the initial condition of mass concrete floor before turning the heating system ON. Good agreement between the model results and experimental data verifies the FE model validation. The temperature prediction at the center of mass floor has the better match to the results of actual data.

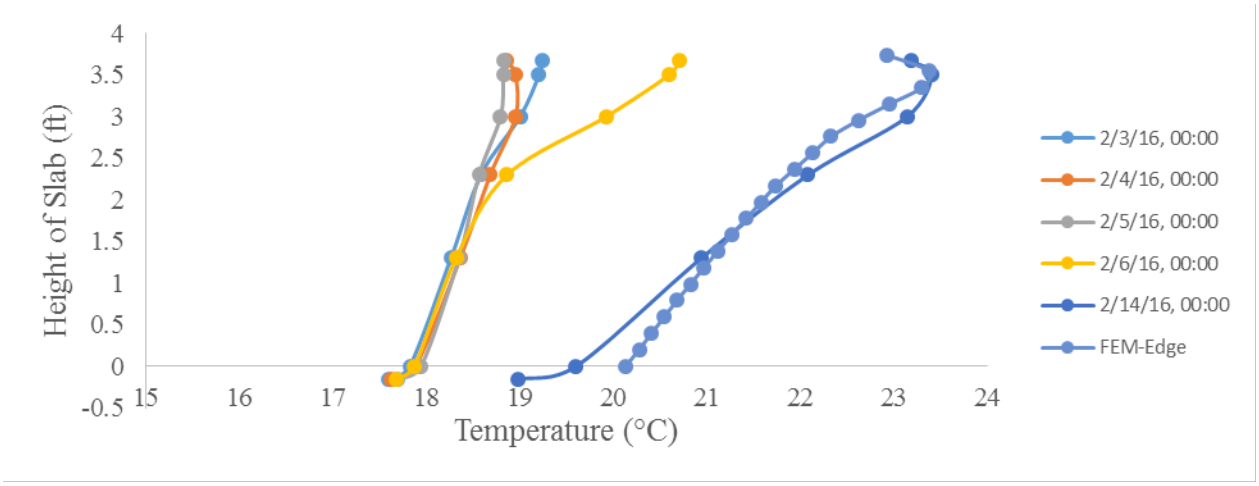

Figure 3.24. Temperature variation for mass floor edge (Actual data vs FEM)

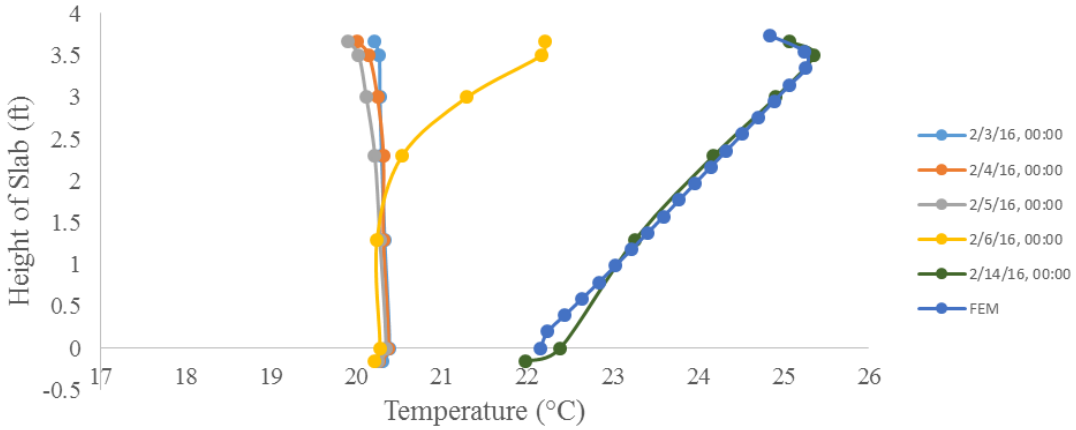

Figure 3.25. Temperature variation for mass floor center (Actual data vs FEM)

After verification of the model with thermocouple measurement at the job site, the model can be extended for another supply temperature by the heat pumps. For example, 110°F (43.3°C) of supply temperature is used to model the mass floor in the heating mode. All other parameters are kept the same as the previous model. Temperature distribution in the mass floor is shown in Figure 3.26 for the top and bottom view.

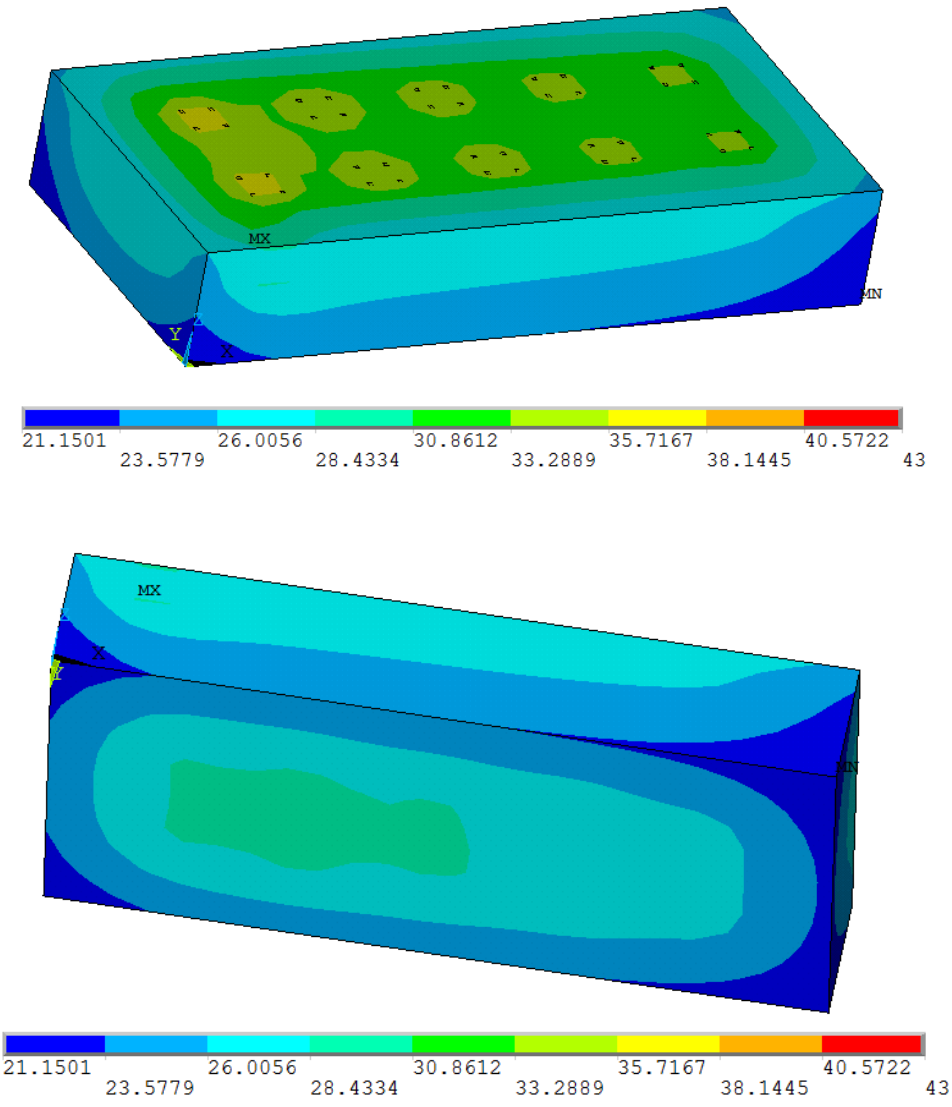

Figure 3.26. Top and Bottom view of temperature distribution in the mass floor (FE model)

From the temperature distribution in the mass floor, the temperature gradient at the center and edge point of slab are extracted and shown in Figure 3.27. There is greater rate of heat loss in higher supply temperature. The temperature at the surface of the slab is much less than piping temperature because of surface convection to the indoor air.

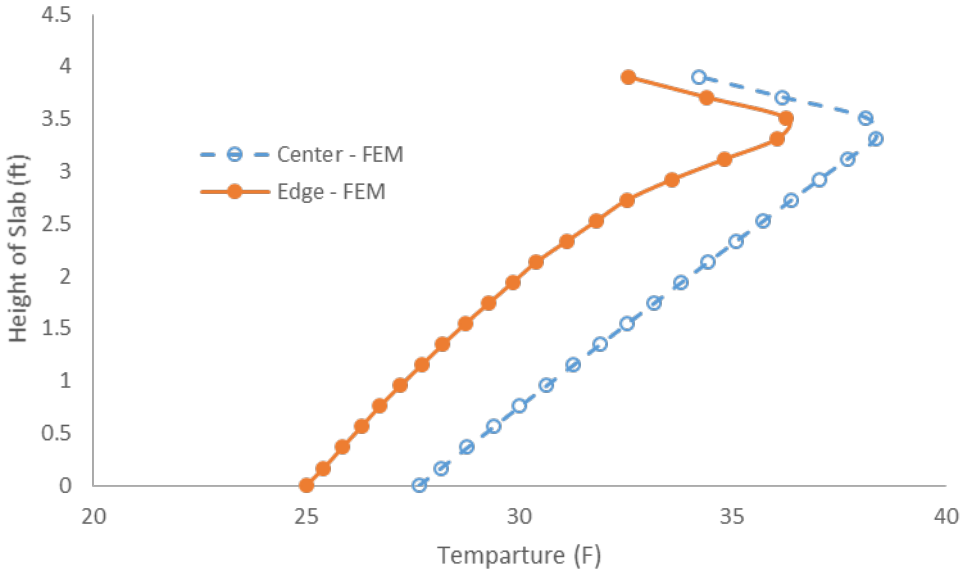

Figure 3.27. Finite element model results for center and edge point (110F supply temperature)

3.6Conclusion

In summary, the idea of saving thermal energy by mass heated concrete floor has been studied. The experiments show that 4 MBTU can be stored in the 118×46×1.22 m^3 mass floor after three heating cycle of 80°F, 90°F, and 90°F with 9 days long at each cycle. The thermal storage of mass floor can be applied in the building regarding the less energy usage. It actually provides the level of comfort and evenly temperature distribution in the buildings with a ground source system. Running the heating mass floor at nights and turning the heating system OFF at days would lead to save electricity plus saving thermal energy. The thermal behavior of the slab was investigated by a finite element model that shows that the temperature development of the slab after enabling the heating system is in good agreement with experimental data. The temperature variation inside of slab is independent on the ambient temperature. Therefore, other thermal loading on the piping system can be predicted by the FE model.

CHAPTER IV

COOLING PERFORMANCE OF THICK AND THIN CONCRETE RADIANT FLOOR SYSTEM WITH GROUND SOURCE SYSTEMS

4.1 Overview

The performance of radiant floor in the cooling mode with two ground source heat pump (GSHP) is evaluated in a newly constructed researchlaboratory at Oklahoma State University. The thickness of slabs are 7 in and 4 ft. The new approach of the thermal loading on the piping systemwas applied to optimize the energy consumption. The cooling floor has been running during the night time (8 P.M. to 8 A.M.) which carries off-peak rates for electricity. The result is compared with continuous cooling on the slabs. Then, a finite element (FE) model was applied to simulate the slab behavior in different loading conditions. A steady state thermal analysis is compatible with the temperature measurement from the building with the slab embedded piping system. The FE model is extended for other thermal loading patterns.

4.2Introduction

Radiant floor system with ground loop system is an efficient way to heat/cool the building in different seasons of a year. The recent research indicated that radiant floor system is able to provide thermal comfort and low energy consumption, and quiet operation [52, 53, 54, 55, 56]. There are additionalways to optimize and improve the performance of the radiant floor system such as using wind or solar energy combining with ground loop system [57]. Decreasing the heating or cooling load on the HVAC system is a cost effective way to minimize the energy cost of the building. Also, exterior and interior material selection, window type, and the building insulation are some options to reach this goal. Using mass concrete radiant floors may increase the efficiency of the heating/cooling system and reducing loading demand on the HVAC system. The mass floor construction and applying ground source heat pump to the radiant floor system would increase initial capital cost at of the building construction, but it is recovered within the initial years of energy conservation[58, 59]. Geothermal heat pumps would enhance the efficiencies of the heating/cooling radiant floor system by using the nearlyconstant temperature of fluid in contact with the earth. This efficient system isless energy intensive than one that draws the outdoor air, which is considerably warmer or colder in the hot or cold days. The heat pumps use less energy to absorb or provide heat from the underground fluid. The heat pumps have longer life span than conventional air conditioning system.

Thermal mass is a property of a material which can store heat and release large amount of thermal energy [41]. Massive concrete element in the building construction can possibly store heat due to low thermal conductivity and higher heat capacity. Other materials like wood do not provide appreciable heat storage properties. If thermal mass inside of building gains heat or cold, it could release this heat or cold gradually. Mass concrete floor in the residential building or laboratory can carry the heavy load and machines. The amount of heat storage in the concrete slabs with embedded piping system is a completely parallel application that does not interfere with the

structural properties. The piping position inside of slabs and slab height can be key elements to save thermal energy in the radiant floor system. If the piping system is too close or too far to the surface of the floor, the amount of thermal energy and efficiency of the system would be affected. To save energy and the energy usage is schedule based on off-peak 12 hours of enabling the cooling system releasing the thermal energy at day time.The mass floor is isolated from the external air temperature and this performance is most effective one [41]. The insulation in the floor foundation would be significant to reduce energy loss of the radiantly heated building [60]. Insulation for thin slabs would be necessary because the edges and around the heating pipe should be isolated from heat loss. Most of the heat loss happens at the surface of the mass radiant floor because radiant tubing in located 6 in below the surface, and bottom half of the mass floor does not affect by temperature change in the tubing system as much as near the surface does.

The supply piping temperature is an important key in designing the mass radiant floor for the building because it can provide the heating load for the whole building. The floor surface temperature in the most important factor which controls the heating/cooling capacity of the system [61]. Regarding the thermal comfort and condensation, the floor surface temperature should be controlled over a certain range of 19-29°C (66.2-84.2ºF) during summer until winter season [62].For the cooling floor in the summer, the surface temperature should not be less than 19ºC, the indoor thermal environment to comply with standard rules [63]. However, if part time heating or cooling is considered, this range could be different.The floor type and lifestyle of residents in the building are important [64, 65, 66]. In this case study, most of the time during the day, occupants wear shoes and stable temperature is favorable for experiments sensitive to temperature change.

Due to complicated nature of heat transfer through the concrete and reinforcement combination, some software engineering and technology may results in higher accuracy temperature distribution for the modeling. By simplifying the model, the accuracy of results should be in a

reasonable range. Some numerical methods such as finite difference have been used for modeling the heat transfer in different materials. For example, AzreeOthumanMydin was used one-dimensional finite difference method to resolve the heat conduction problem in the multi-layer panels [67]. However, the model validation needs to be completed by the physical model. Jin, X et al. [68] has studied a finite volume model for a radiant floor cooling system regarding the effects of the pipe thermal resistance and water velocity on the performance of the system. It was noted that the effect of water velocity in the radiant floor system is not great and the performance of radiant floor will be affected by low thermal conductivity of the piping system. Sattari and Farhanieh [52] studied a finite element model of radiant floor system and they concluded that thickness of the radiant floor system are the most important parameters in the radiant floor design. In order to test the different parameters on the performance of the system, a finite element model is used to have better understanding of the slab thermal behavior.

4.3Experiment

The ground source loop is composed of 36 boreholes of 400ft in depth. The supply and return temperature to GSHP system, indoor and outdoor temperature, flow rate of heat transfer fluid, and the input power by the system were measured.

Two ground source water-water heat pumps were applied to inject the chilled fluid to the radiant floor system working with three pumps after heat pumps. Based on the loading demand on the heat pump, either one or both is working to generate the supply temperature to the radiant floor system. The heat transfer fluid is water + 30% ethylene glycol to prevent the freezing the fluid and better heat transfer to the floor.

The average monthly temperature of the ambient temperature in Stillwater, Oklahoma is shown in Figure 4.1. The maximum average temperature is about 30°C (86ºF) in July and the minimum average of temperature was happened about 3°C (37.4ºF) in January. The floor cooling was

enabled in July until October 2016. To study the performance of the mass floor, different plans for cooling system were selected. The comparison between the different systems was conducted to optimize the floor cooling based on the days of running the system and energy consumption of the radiant floor system combined with ground source system. For the first 9.5 days of constant cooling the systems was operated started from 07/18until 07/27 followed by 9.5 days of rest. The chilled floor was enabled again for 19 days of continuous cooling from 08/05 until 05/24followed by19 days of rest. The floor cooling was enabled again for one week of night cooling from 09/12until 09/19. The final cooling cycleswas conducted from 09/23until 10/12. The supply temperature for the radiant floor system was 60°F (15.55ºC) for all cooling loading in the piping system. The whole cooling schedule for summer season is illustrated in Table 4.1.

Table 4.1. Cooling schedule for summer season

Time	Load Temperature	Condition
06/10/2016, 10:00 AM	67°F (19.44ºC)	ON for 9.5 days
06/20/2016, 8:30 AM		OFF for 9.5 days
06/29/2016, 01:00 PM	60°F (15.55ºC)	ON for 9.5 days
07/08/2016, 4:00 PM		OFF for 9.5 days
07/18/2016 8:15 AM	60°F	ON for 9.5 days
07/27/2016, 12:00 PM		OFF for 9.5 days
08/05/2016, 4:00 PM	60°F	ON for 19 days
08/24/2016, 4:00 PM		OFF for 19 days
09/12/2016, 4:00 PM	60°F	ON for 1 week (Cyclic)
09/19/2016, 4:00 PM		OFF for 4 days
09/23/2016, 4:00 PM	60°F	ON for 19 days (Cyclic)
10/12/2016, 4:00 PM		OFF

The cooling period of 9.5 days was chosen because the temperature in the slab at different elevation was almost stable. Then, 19 days selected to see any possibility of thermal storage of the slab in the cooling mode. Two periods, one week and 19 days of night cooling, were examined based on the saving the energy at night and using the cooled slab on the next day of enabling the system.

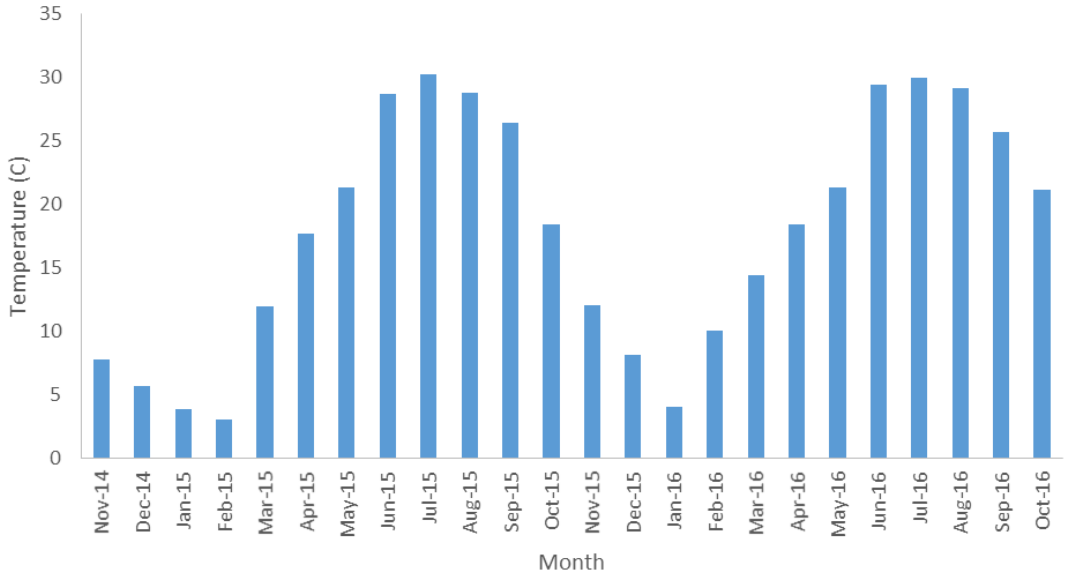

Figure 4.1. Temperature variation during the year 2015-2016

The moisture level and humidity are measured by moisture and humidity sensors in North and South section of the building. The moisture sensor operates based on the water detection on the surface of the slab which is connected to a detection alarm in the online system (Figure 4.2).

Figure 4.2 Water Detector Sensor on North (right picture) and South (left picture)

These sensors can be monitored by online system of Cooper lab which is shown in Figure 4.3.

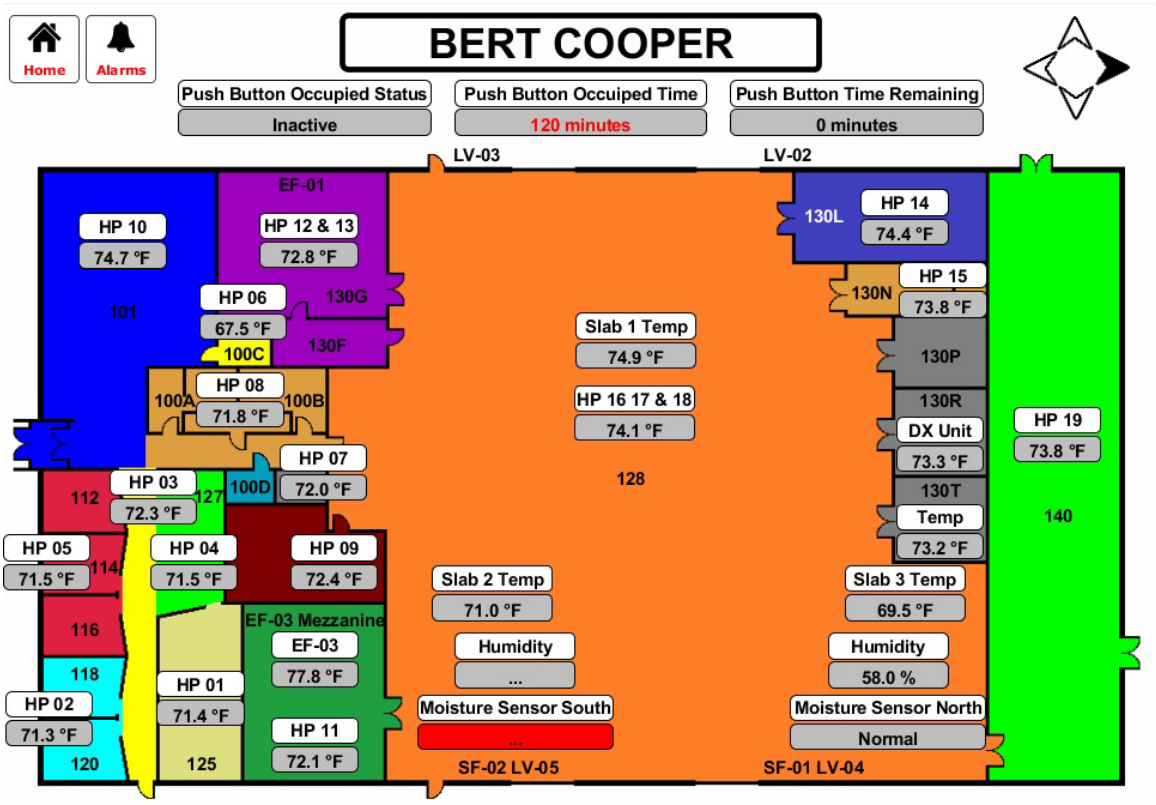

Figure 4.3 Online monitoring of radiant floor temperature and moisture sensors

The surface heat flux is measured by a FluxTeq device to monitor the surface temperature and heat flux delivered to the air by the radiant floor system [69]. Heat flux measurement is very important to characterize and control many thermal systems [70]. Two sensors installed on the center point of the mass floor and the 7 in slab. The sensor sensitivity for mass floor location is 6.588 ±0.020 μV/(W/m^2) and for thin slab is 6.926 ±0.020 μV/(W/m^2) at 20ºC. The heat flux should be recalibrated after 1 year to ensure reliability. The surface heat flux sensor is shown in Figure 4.4.

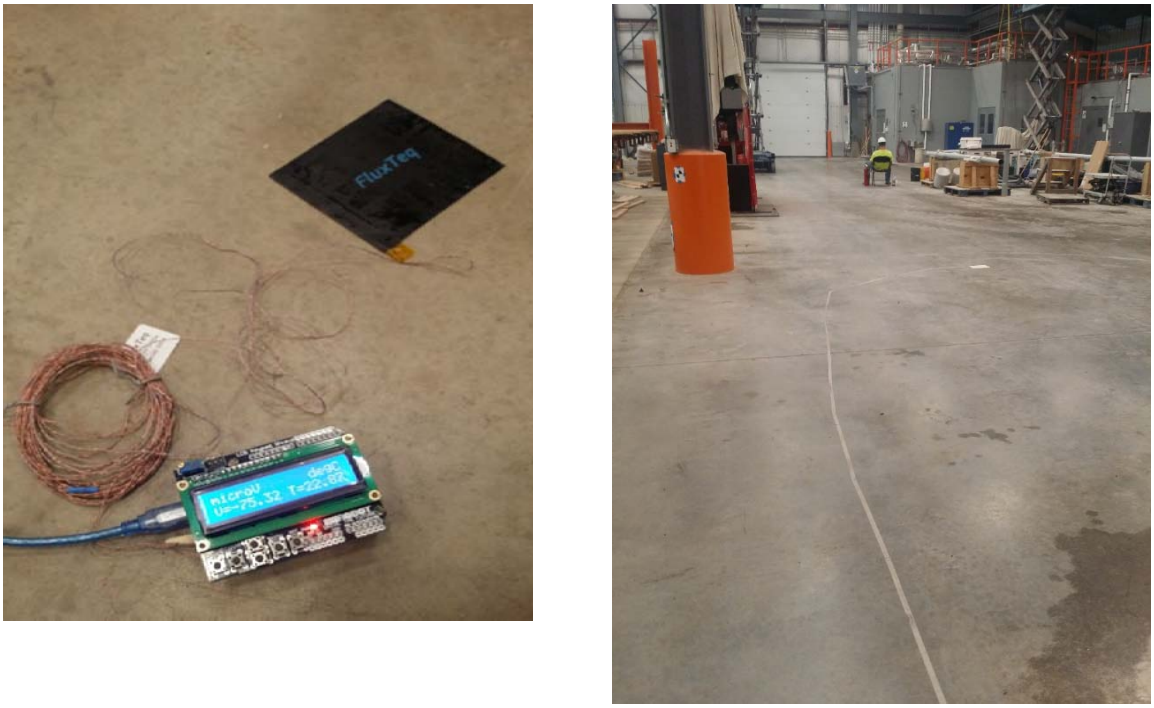

Figure 4.4. Surface heat flux before installation (left) and after installation (right)

4.4Results and Discussion

4.4.1 Site Result

The indoor temperature does not follow the outside weather condition when doors and openings are closed. The inside temperature of the slab is mostly affected by the pipe temperature and indoor air temperature. The ambient temperature and mass floor temperature is presented in

Figure 4.5. The measurements have been recorded from 10/01 which is shown with 5158 of hours at the origin of the graph on X-axis every 15 minutes. It should be mentioned that the time at zero is January first. The indoor temperature is controlled with an online monitoring system to provide comfortable temperature for residents in the research laboratory.

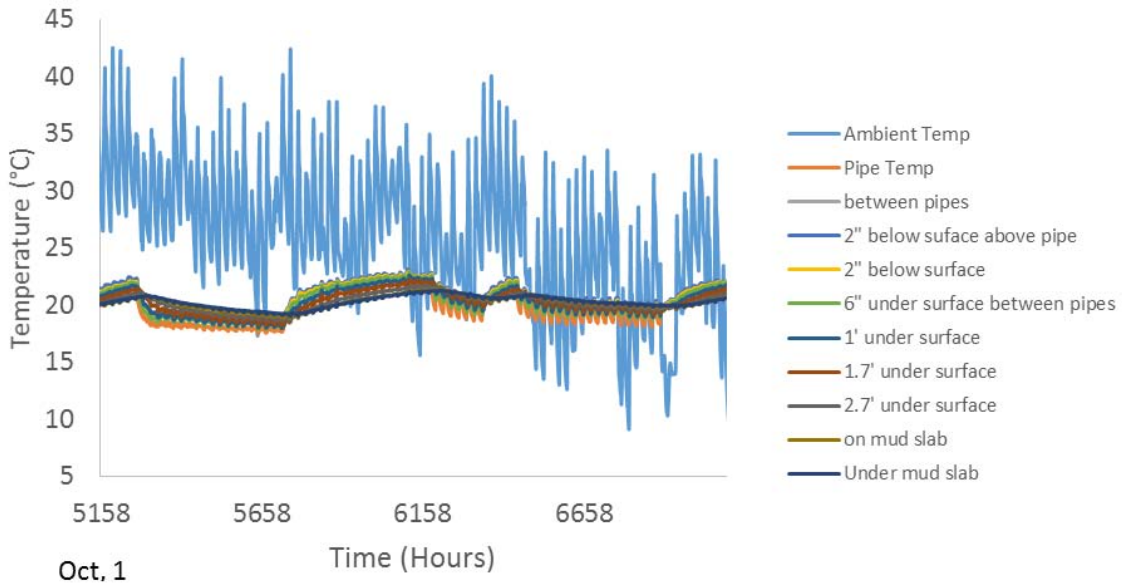

Figure 4.5. Ambient Temperature during the different stages of cooling operation

The ambient temperature is not shown to have a better resolution of temperature gradient inside of the mass floor because the ambient temperature range is higher than temperature profile of the mass floor cooling at nights has two advantages:

1 Weather is colder, so the slab gets colder faster because weather condition is important to affect the process of heating/cooling the floor.

2 Electric power is less expensive

The first cooling schedule in the summer started with supply temperature of 67ºF (19.44ºC) at 06/10 followed by another cooling load of 60ºF (15.55ºC) on 06/29. Temperature variation in the

mass floor and thin slab for the center point are illustrated in Figure 4.6 and Figure 4.7 respectively.

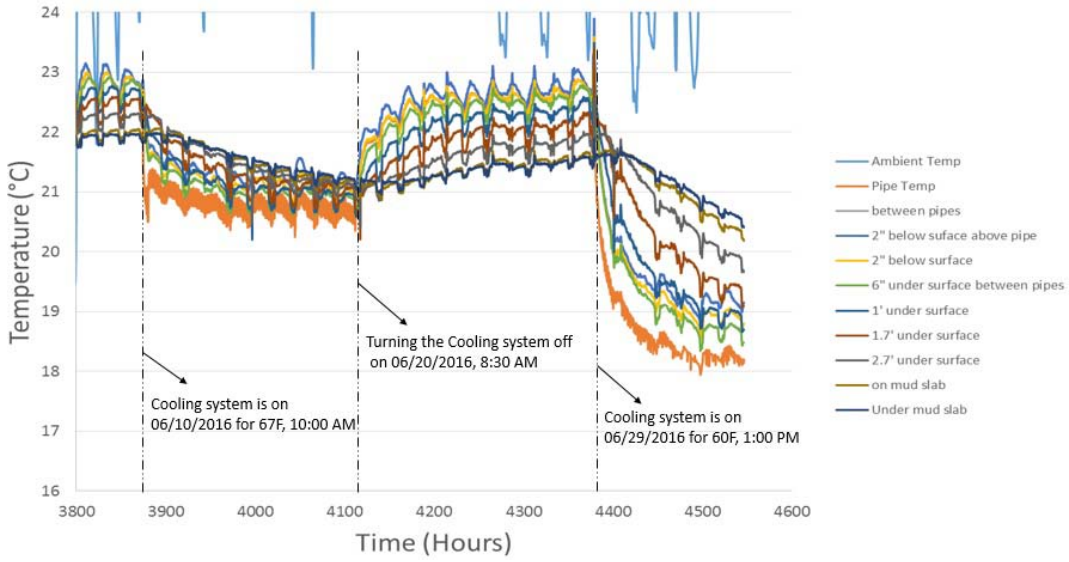

Figure 4.6. Temperature profile in the mass floor for 67ºF and 60ºF cooling load

After disabling the floor cooling, the temperature of the slab gradually returns to the initial temperature before enabling the cooling system. However, the cooling system for 60ºF has a steep slope of decreasing trend in comparison with 67ºF loading. Temperature of the mass floor would be less when the floor cooling set at colder supply temperature of radiant system. Therefore, it takes more time for the floor to return to its' initial temperature before running the cooling system.

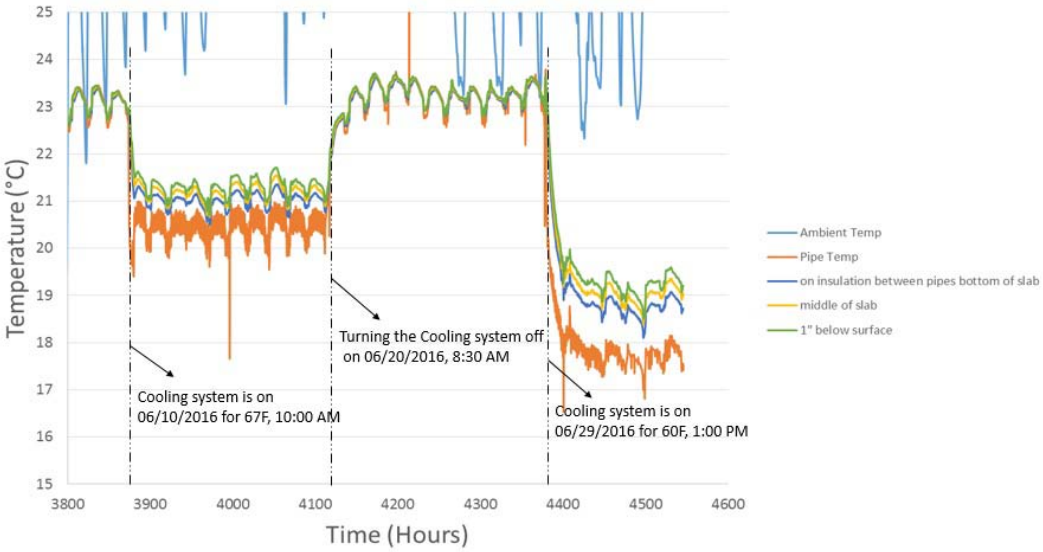

Figure 4.7. Temperature profile in the thin floor for 67ºF and 60ºF cooling load

Because the 7 in slab has less capacity to save the thermal energy, the temperature of the thin slab fully recovered to the initial condition after disabling the cooling mode. Therefore, the slab should be kept cold enough to become more effective in terms of providing lower indoor air temperature.

It should be mentioned that the night cooling (8 P.M. to 8A.M.) was scheduled in the online monitoring system of Bert Cooper laboratory. Figure 4.8illustrates the supply temperature is about 60ºFand return temperature is 66.3ºF. If cooling system in the radiant floor system makes the building too cold (below the minimum limit), it must be OFF to prevent enabling the air heating system. The floor cooling and heating air system are programmed to not work simultaneously. When the floor cooling system is ON, the demand on air conditioning system will be lower.

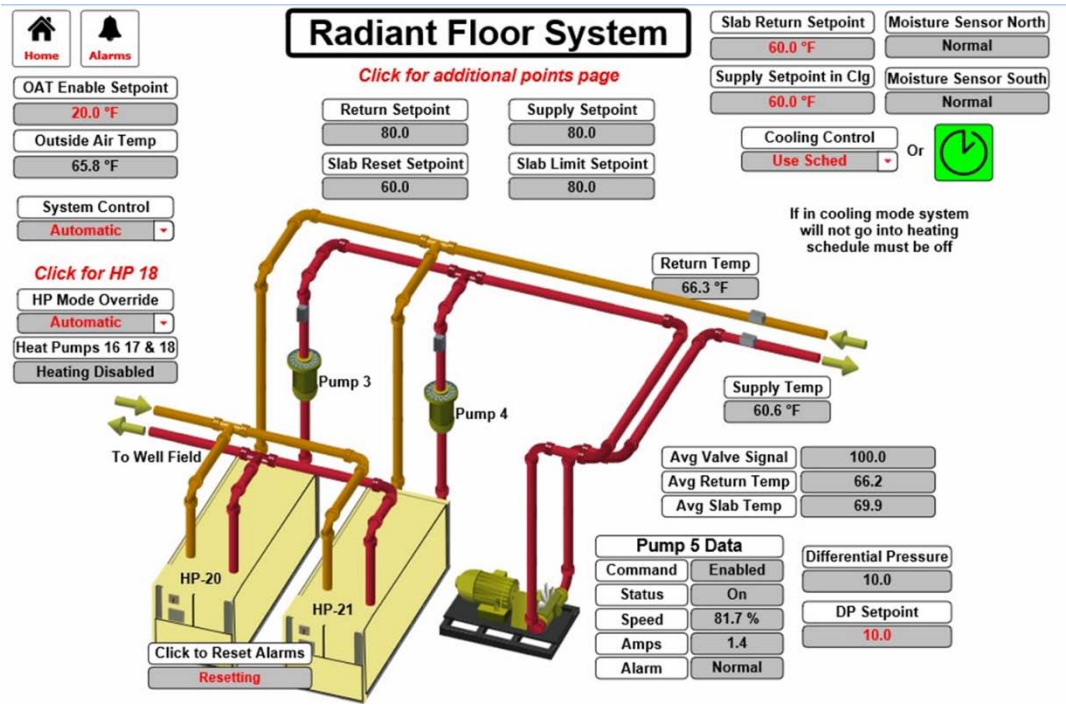

Figure 4.8. The online monitoring system for night cooling

Temperature profile in the center point of mass floor and thin slab for 1 week of night cooling (8P.M. to 8 A.M.) for 60ºF is shown in Figure 4.9 and Figure 4.10.

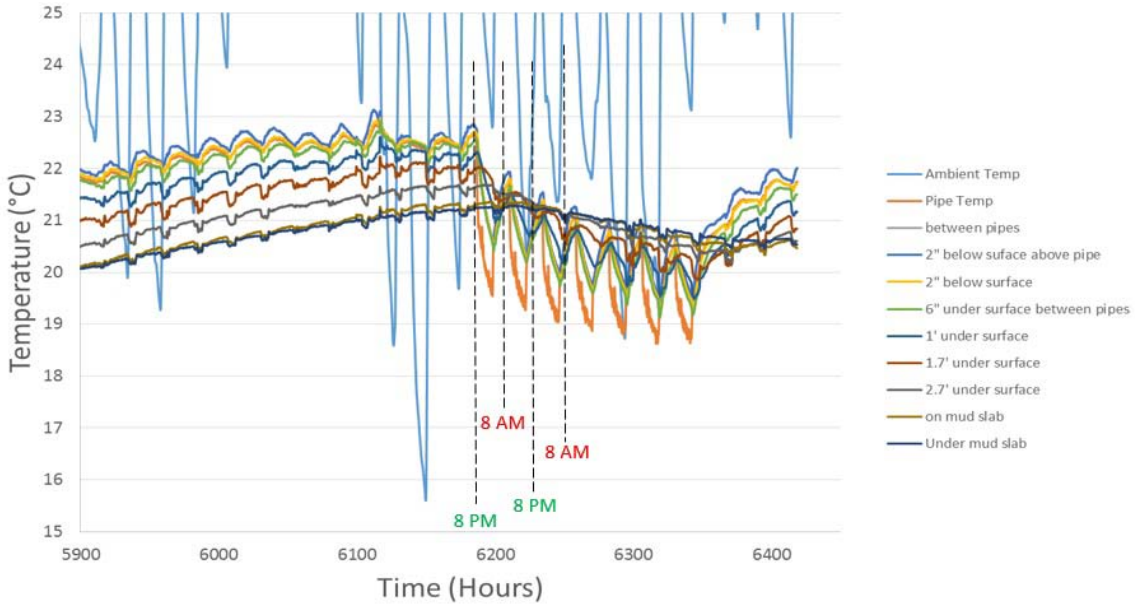

Figure 4.9. Temperature profile in mass floor for 1 week of night cooling (Center point)

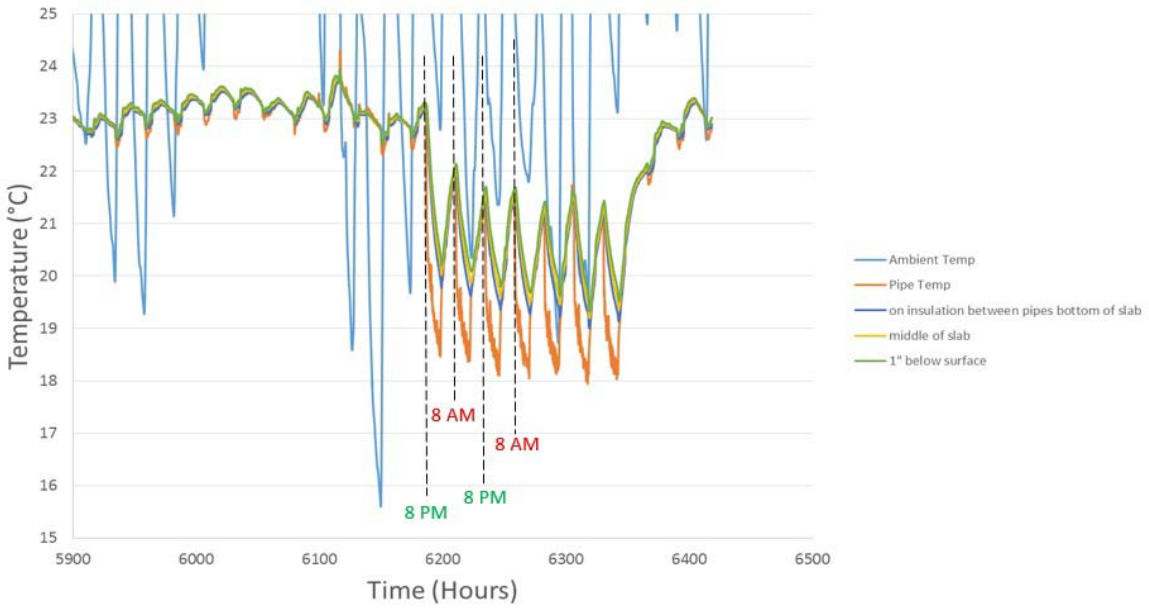

Figure 4.10. Temperature profile in thin floor for 1 week of night cooling (Center point)

The cooling system is enabled for 19 days to quantify theamount of temperature reduction for a double cooling period. The results are compared with 19 days of night cooling between 8 P.M. to 8 A.M. The night cooling has lower electricity consumption. The electricity price at the day time is 16 cent/kwh and at the night time is 4 cent/kwh [71].For condensation potential, the supply temperature was kept 60ºF. The different stages of the cooling mode including the continuous 19 days, 1 week of night cooling, and 19 days of night cooling in the mass floor are shown in Figure 4.11.

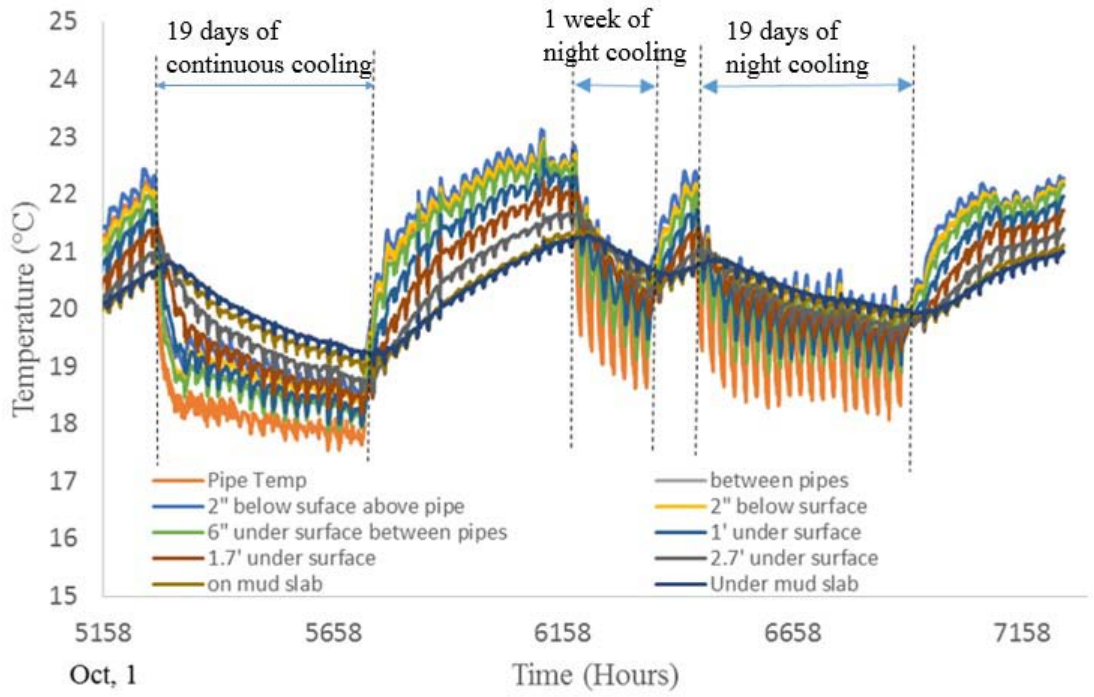

Figure 4.11. Three Different Cooling mode (continuously 19days, 7, 19 days of night cooling)

The same results are shown for the mass floor at the edge point is shown in Figure 4.12.

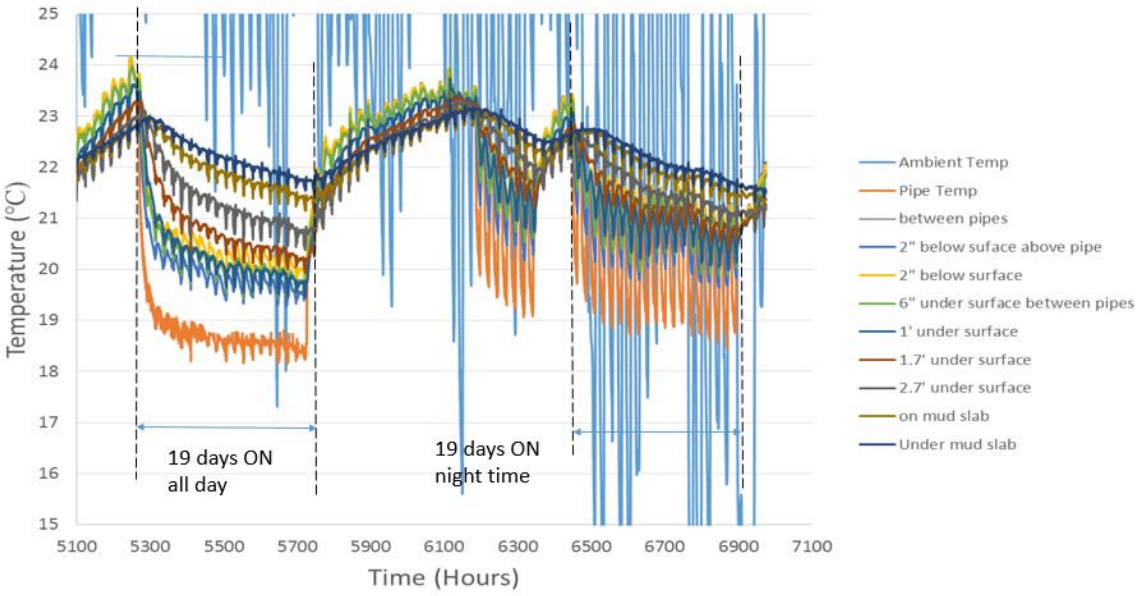

Figure 4.12. The floor cooling for 19days of continuous cooling and night cooling (edge)

Because the edge of slab is closer to the building façade, the initial temperature before enabling the cooling system would be higher than the center of slab. Also, the piping temperature at the edge point is lower than center point because of heat transfer loss.

The same graphs for the thin slab at center and edge points are shown in Figure 4.13, and Figure 4.14 respectively.

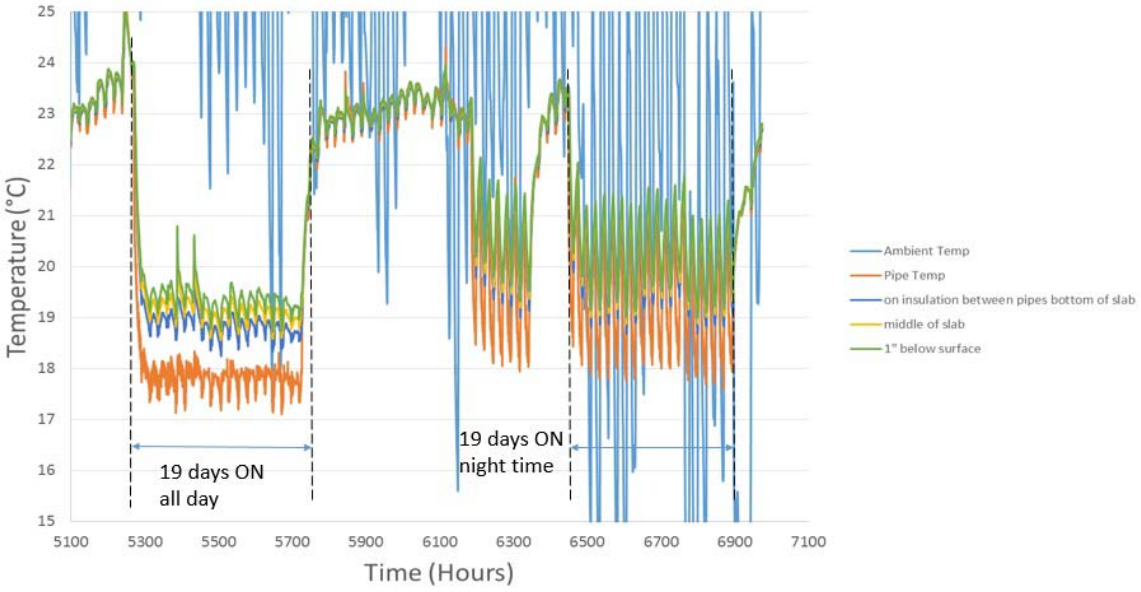

Figure 4.13. The floor cooling for 19days of continuous cooling and night cooling (7 in slab, center)

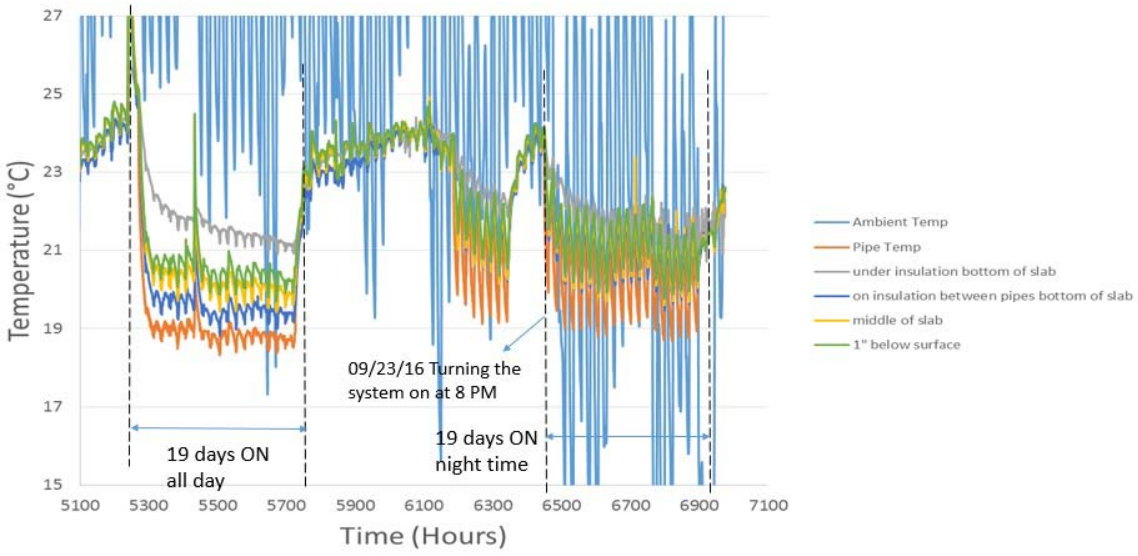

Figure 4.14. The floor cooling for 19days of continuous cooling and night cooling (7 in slab, edge)

Based on the above graphs, it is evident that the piping system at the edge point of slab feels higher temperature than the center for the same reason of mass floor's temperature drop. Both center and edge point of thin slab show that temperature drop has suddenly happened after enabling the cooling system and they are not able to store the thermal energy provided by the cooling system.

The heat flux measurements at the bottom of 7 in slab are shown in Figure 4.15.

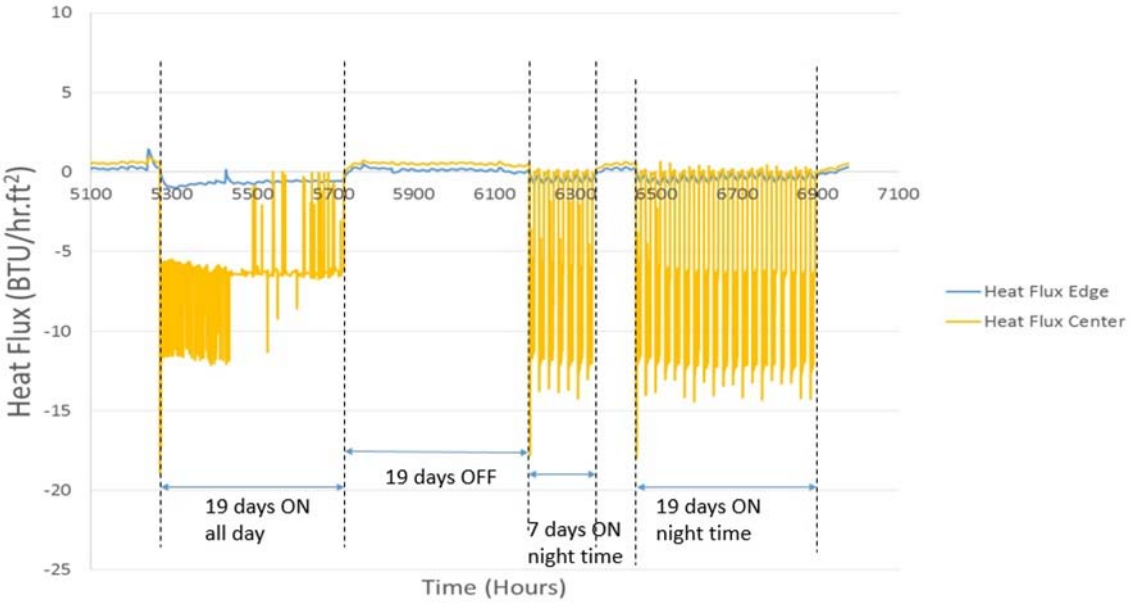

Figure 4.15. Heat Flux measurement at the bottom of 7 in slab (Edge, Center points)

Heat flux is about -7BTU/hr.ft^2 when the 60ºF cooling system is enabled and it is about zero when the cooling system is disabled. Also, the heat flux for the edge point shows that there is no appreciable heat transfer between the bottom of thin slab and underneath. The heat flux sensors at the surface of slab can measure the heat flux between the indoor air and surface of the slab due to temperature difference. Higher heat flux values indicate more convection between the indoor air and surface of the slab. Surface heat fluxes at mass floor and 7 in slab are shown in Figure 4.16.

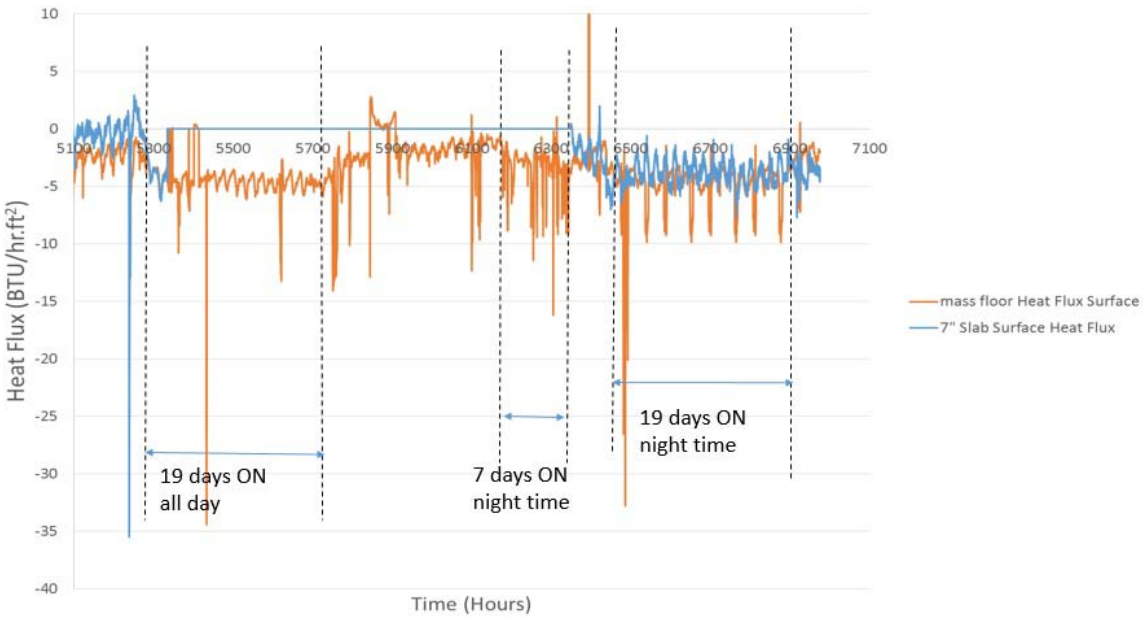

Figure 4.16. Surface heat flux sensors at mass floor and thin slab (center)

When the cooling system is enabled the amount of heat flux for the mass floor or thin slab is almost the same as -5BTU/hr.ft^2. Also, it can be seen that even the cooling system is OFF, we still have heat flux exchange between the indoor air and surface of the slab. Because the heat flux sensors are installed right on the surface of the slab, the wire is taped to the surface which is exposed to human walk and passing way of vehicles. The sensor wires are extended to a data logger box at the east side of the building. For a while, the wire for heat flux sensor at the 7 in slab were damaged and the records were missed for that period of time.

The heat flux measurement for continuous cooling on 06/29 to 07/08 and 07/18 to 07/27 are shown in Figure 4.17.

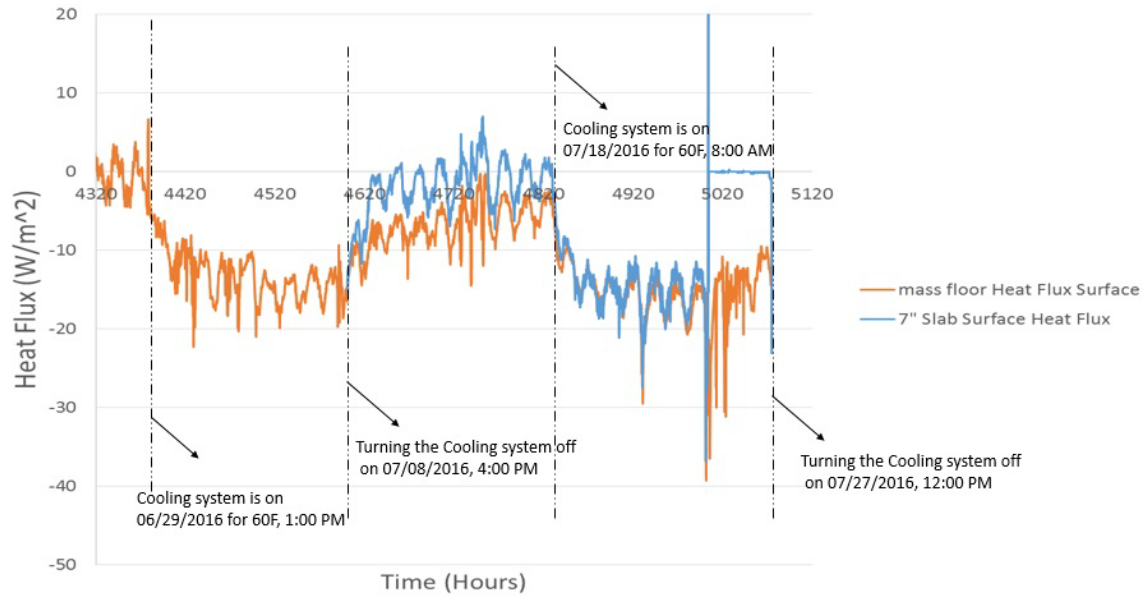

Figure 4.17. Surface heat flux in W/m^2

The results of comparison between continuous and night cooling for 19 days are shown in Figure 4.18 for the mass floor center point. This experiment has been completed to see the performance of radiant floor system in the night cooling system.

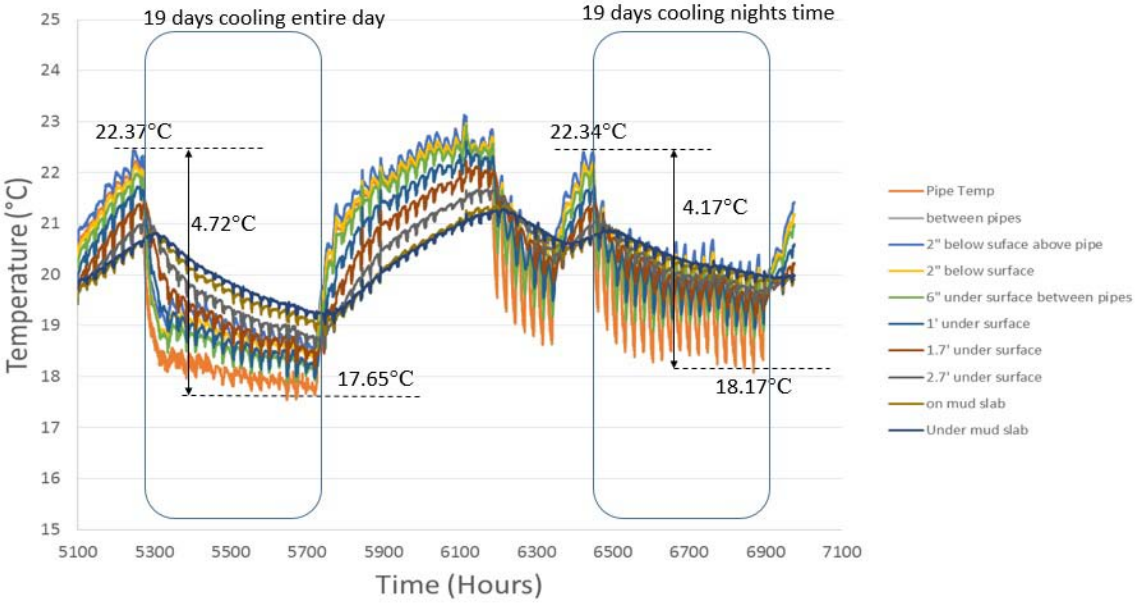

Figure 4.18. The floor cooling for 19days of continuous cooling and night cooling (edge)

Both tests have been started at the same initial temperature of 22ºC. Because continuous cooling happened for all 24 hours of the day, it could make the slab colder. However, the night cooling has a lower temperature drop in comparison with continuous cooling. The difference between maximum and minimum temperature in the mass floor for 19 days of continuous cooling is 4.72ºC while this difference is about 4.17ºC for night cooling system. It means the 4 foot slab could save the thermal energy provided at the night time. The summary of temperature comparison is shown in Table 4.2.

Table 4.2. Comparison between 19 days of cooling vs 19 days of night cooling

	Continuous cooling	Nights cooling (8pm-8am)
Maximum temperature of slab	22.37ºC (72.27ºF)	22.34 ºC (72.21ºF)
Minimum Temperature of slab	17.65ºC (63.77ºF)	18.17 ºC (64.71ºF)
Temperature difference	4.72 ºC	4.17 ºC
Highest temperature point	2 in below the surface above pipe	2 in below the surface above pipe

In addition to the previous test, the experiment was repeated for 9.5 and 19 days of continuous cooling. The result of this experiment is illustrated in Figure 4.19.

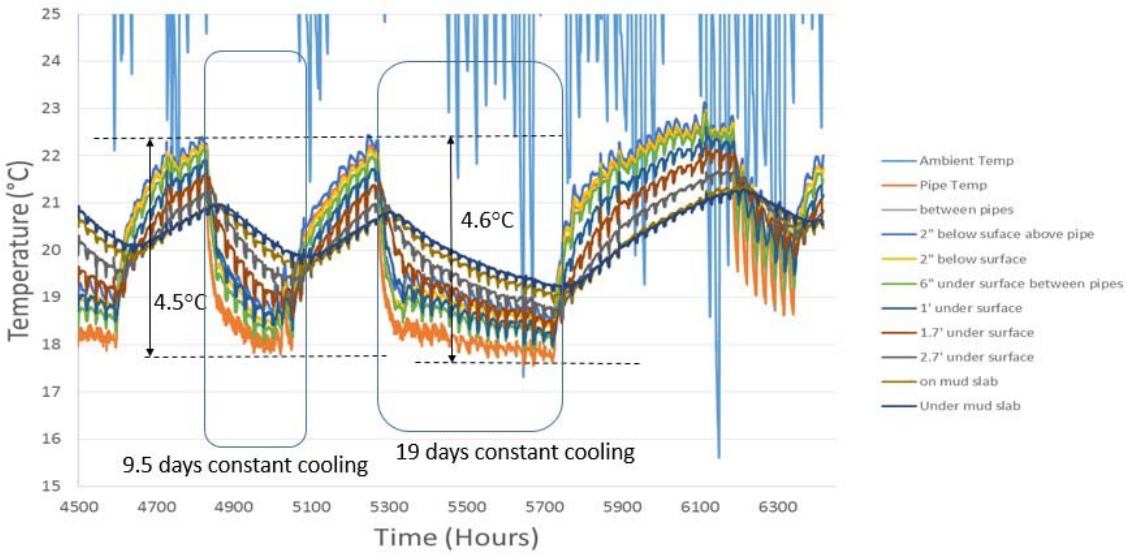

Figure 4.19. 9.5 days cooling Vs. 19 days Constant Cooling (60°C)

The maximum temperature difference in the mass floor of center point is almost the same for 9.5 days and 19 days of continuous cooling. It elaborates that the slab can achieve the thermal equilibrium in 9.5 days and running the cooling system on for longer time just keep the slab cold. However, even the supply temperature at heat pumps is 60ºF (15.5ºC), the piping temperature at the center of slab is not lower than 17.8ºC (64ºF).

Another test has been done to compare the results of cooling system for 1 week of continuous cooling and night cooling which is shown in Figure 4.20.

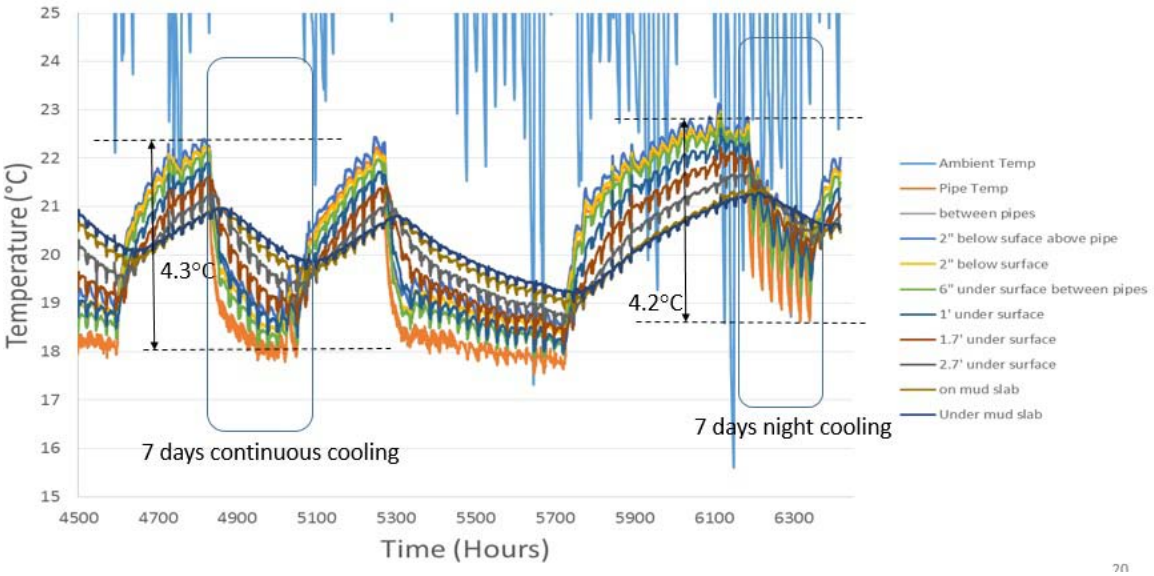

Figure 4.20. 7 days continuous cooling Vs. 7 days night cooling (60°C)

The temperature difference between the maximum and minimum temperature of the mass floor at the center point is 4.3ºC for 1 week of continuous cooling and 4.2ºC for 1 week of night cooling. However, this difference would be higher for longer time of running the cooling system. This difference for 19 days of continuous cooling is 4.72ºC and it is 4.17ºC for 19 days of night cooling (Table 4.2).

The moisture sensors are in normal condition during the floor cooling system. The humidity is between 50-58% during this testing. The only time that floor experienced the wet surface was when humid outdoor air brought to the building by the exhaust fans during floor cooling. Because of high humidity of the outdoor air, the surface of the slab experienced the lower temperature than dew temperature. Therefore, condensation would be an issue for floor cooling in the summer season if the supply temperature for the radiant floor is too low. However, if the inside of the building insulated from the humid outdoor air, it is not a common or serious problem. We need to maintain the slab from high humid outside air to blow on the surface of the concrete. Humidity North sensor was 86% and humidity South sensor was 79% during this period. Wet surface is shown in Figure 4.21. To resolve this effect, the floor cooling system was disabled and dry air was blown on the surface on the concrete. The radiant cooling system would work effectively if it used in conjunction with a ventilation system [72].The floor cooling system should be designed to prevent the condensation at the surface of the radiant floor [73]. The surface of the slab could potentially be in warning for condensation during the summer time if humid outdoor air is brought to the laboratory. If we use dehumifier system, we will not have this problem or it happens much less. As the surface temperature goes below the dew point temperature, we will have condensation issue. As we do not have this system, when the doors are open on hot/humid days, condensation will be a problem and we will have wet surface.

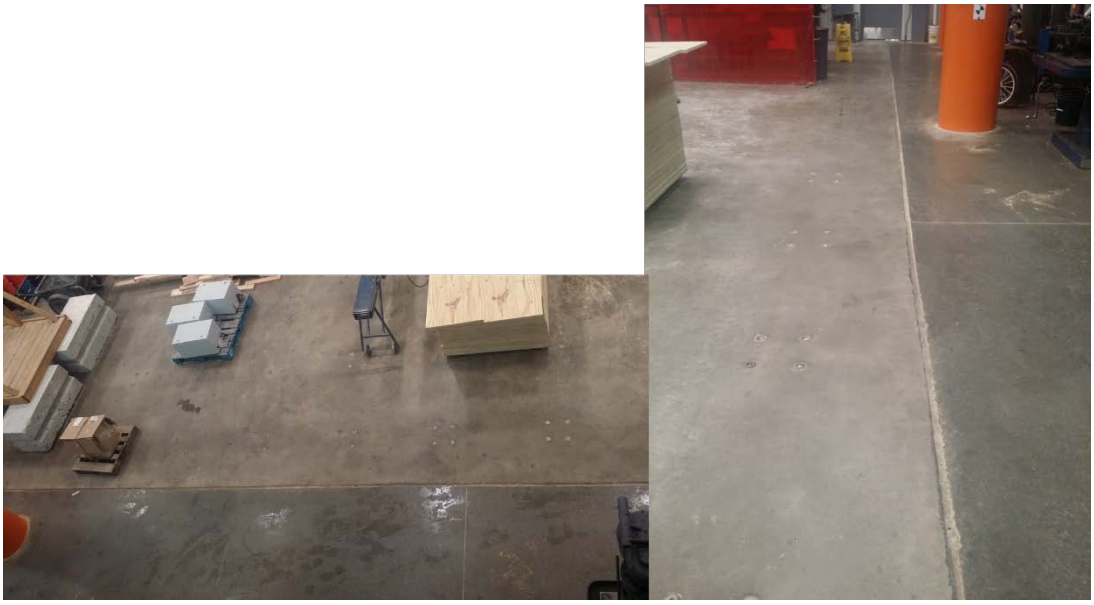

Figure 4.21. Condensation at the surface of radiant floor system

To have a better understanding of performance of the radiant floor system for night cooling, the temperature profile graph in the slab before and after enabling the cooling system would be helpful. These selected days are shown in Figure 4.22.

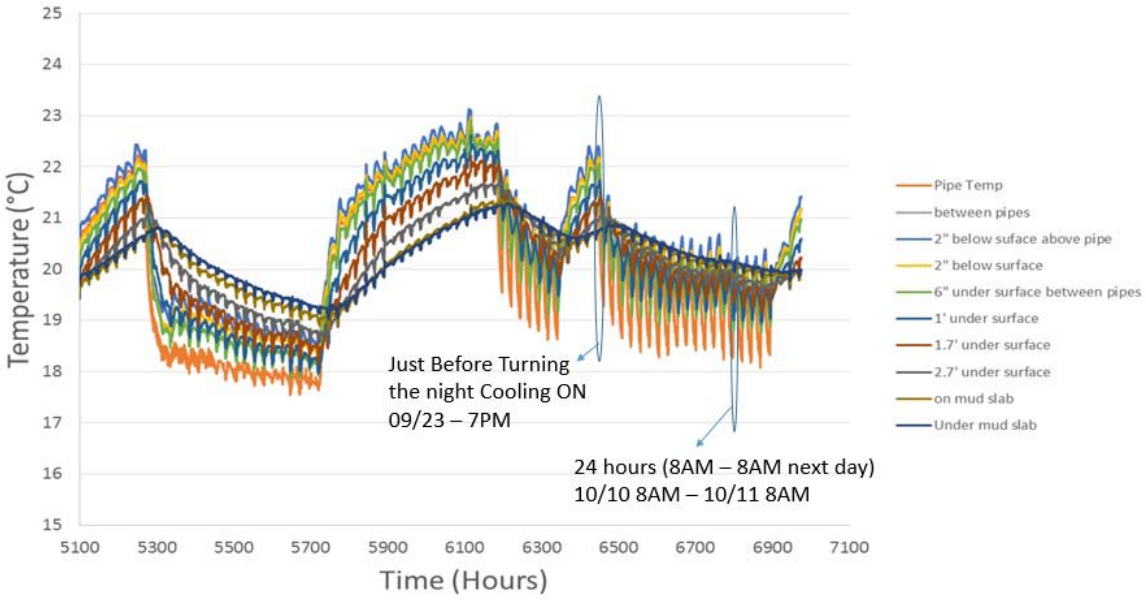

Figure 4.22. Selecting a day before enabling the night cooling and 1 day after some cyclic night cooling

The profile of slab temperature in two consecutive days of night cooling every 6 hours and just before enabling the system (09/23) is shown in Figure 4.23. The days 10/10 and 10/11 were selected when the cooling mode was almost stable in terms of temperature variation inside of the mass floor.

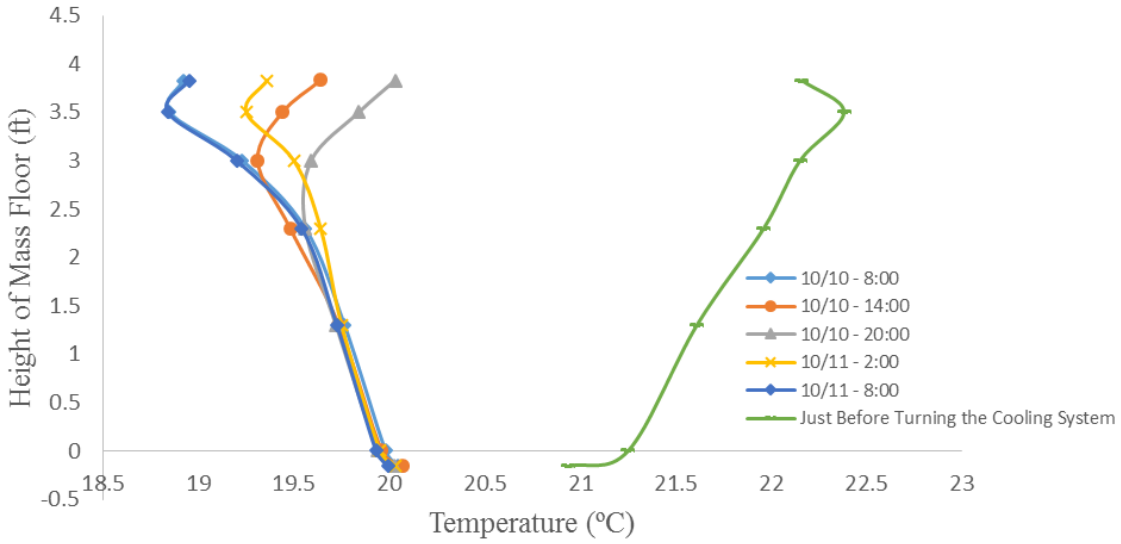

Figure 4.23. The temperature profile across the mass floor before and after (nights cooling)

It can be observed in Figure 4.23 that turning the night cooling system ON kept the overall mass floor temperature low enough to make the indoor air cold regarding the less consumed energy at nights. The vertical steel anchors in the mass floor inhibit the floor from remaining cool for a long periodafter disabling the cooling system. Enabling the cooling system at night and disabling at day time would be efficient for having the cold slab in comparison with all days running of the cooling system. The mass floor does not have time to get back to the initial condition of temperature when the mass floor is running again for the next night. From the five temperature profiles in the mass floor at the left side of the graph and one temperature profile at the right side, enabling the cooling system would result in a temperature drop at different elevations. However, the temperature drop after enabling the system is not considerable for the bottom half of the slab height. The temperature changes near the top of the slab because of embedded tube temperature. The cold slab decreases the demand on the air condition system of the building. The cooling

capacity of the building has been reduced by 50% if high thermal mass is used as radiant floor system [74].

The temperature variation in the mass floor for the center point of measurement is shown in Figure 4.24.

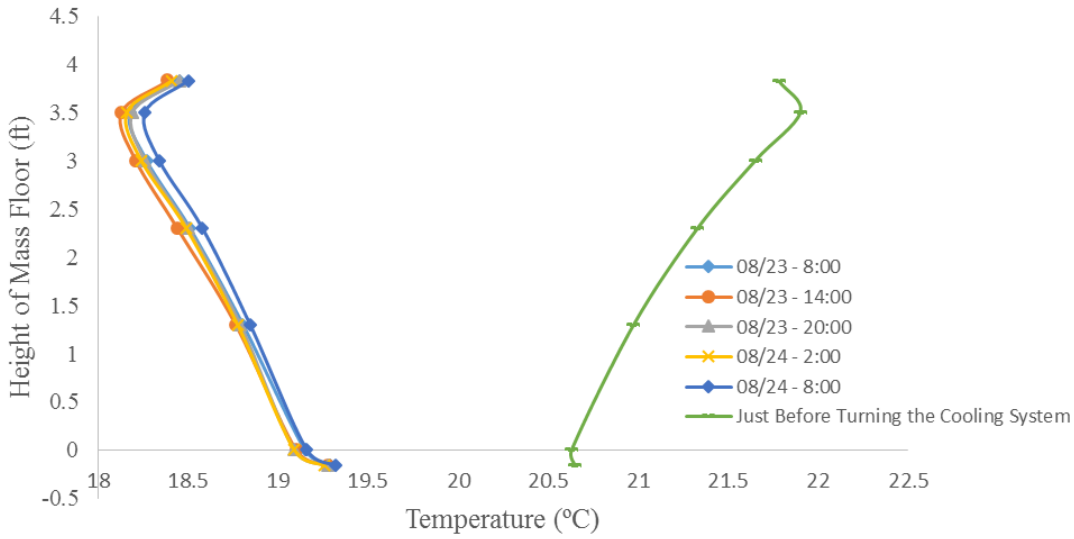

Figure 4.24. Temperature profiles across the mass floor before and after (continuous cooling)

The performance of the cooling tube in the mass floor for 19 entire days and 19 days of only night running by the average temperature profiles is shown in Figure 4.25, Figure 4.26for the edge and center of mass floor.

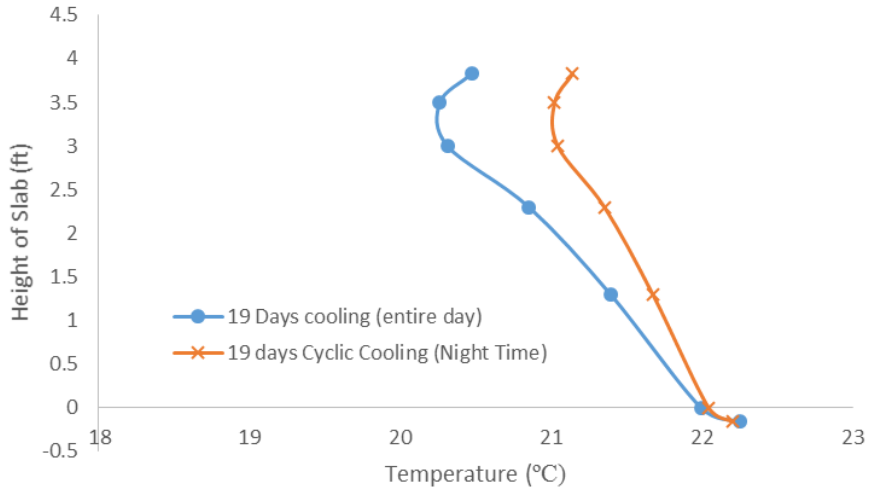

Figure 4.25. Average Temperature in mass floor (Edge)

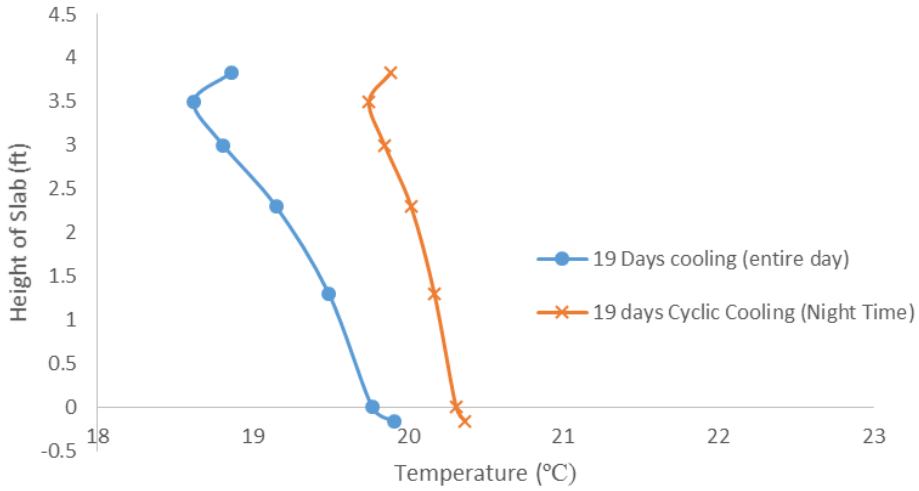

Figure 4.26. Average Temperature in mass floor (Center)

The quantitative data of average temperature inside of the mass floor for the edge point and center point are illustrated in Table 4.3 and Table 4.4.

Table 4.3 Average Temperature in the mass floor (Edge) for 19 days of continuous cooling and 19 days of night cooling

Thermocouple position	19 Days continuous Cooling	Nights Cooling
Pipe	20.21ºC (68.38ºF)	18.76 ºC (65.77ºF)
2 in under surface above pipes	19.97 ºC (67.95ºF)	20.87 ºC (69.57ºF)
2 in under surface between pipes	20.47ºC (68.85ºF)	21.14 ºC (70.05ºF)
6 in under surface between pipes	20.26 ºC (68.47ºF)	21.02 ºC (69.84ºF)
1ft under the surface	20.31 ºC (68.56ºF)	21.04 ºC (69.87ºF)
1.7ft under the surface	20.85 ºC (69.53ºF)	21.35 ºC (70.43ºF)
2.7ft under the surface	21.39 ºC (70.5ºF)	21.67 ºC (71.00ºF)
4ft under the surface on mud slab	21.99 ºC (71.58ºF)	22.04 ºC (71.67ºF)
4ft under the surface under mud slab	22.25 ºC (72.05ºF)	22.20 ºC (71.96ºF)

The temperature profile at different elevations for the 19 entire days of cooling is lower than the same profile with 19 days of night cooling. However, this difference is less than 1.5°C at different thermocouples spots.

Table 4.4 Average Temperature in the mass floor (Center) for 19 days of continuous cooling and 19 days of night cooling

Thermocouple position	19 Days continuous Cooling	Nights Cooling
Pipe	18.17 ºC (64.71ºF)	19.47 ºC (67.05ºF)
2 in under surface above pipes	19.05 ºC (66.29ºF)	20.06 ºC (68.11ºF)
2 in under surface between pipes	18.86 ºC (65.95ºF)	19.89 ºC (67.8ºF)
6 in under surface between pipes	18.62 ºC (65.52ºF)	19.75 ºC (67.55ºF)
1ft under the surface	18.81 ºC (65.86ºF)	19.85 ºC (67.73ºF)
1.7ft under the surface	19.15 ºC (66.47ºF)	20.02 ºC (68.04ºF)
2.7ft under the surface	19.49 ºC (67.08ºF)	20.17 ºC (68.31ºF)
4ft under the surface on mud slab	19.77 ºC (67.59ºF)	20.31 ºC (68.56ºF)
4ft under the surface under mud slab	19.91 ºC (67.84ºF)	20.37 ºC (68.67ºF)

4.4.2 Modeling Result

The finite element model in section 3.4 is used for modeling the thermal load on the mass floor for 60ºF (15.55ºC). The verification of the modeling with job site data is shown in Figure 4.27.

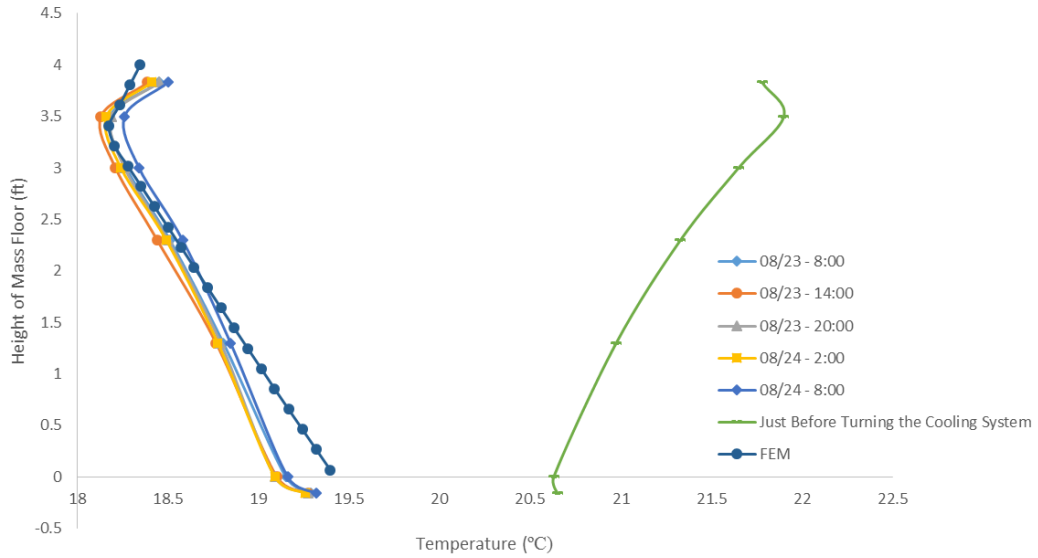

Figure 4.27. Finite element results for 60ºF continuous cooling loading at the center

The modeling shows good agreement with thermocouple measurement at the thermal equilibrium of the mass floor.

For modeling the thin slab, a 3D model including concrete and piping system is used. The element type for concrete is thermal solid 70 (3-D 8-node Thermal Solid) and for heating pipe is fluid 3D th-fl pipe 116. The heat transfer fluid is a mixture of water and 30% ethylene glycol. This mixture has a density of 8.603 lb/gal (1030 kg/m^3), a specific heat of 0.88 btu/lb.F(3680 J/Kg.K) and a thermal conductivity is 0.097 Btu (IT) foot/hour/foot^2/ºF (0.168 W/m.K). The heating tube is located at the bottom of 7 in slab. The concrete slab block and layout pattern of radiant floor tubing is shown in Figure 4.28. The bottom of slab is insulated from heat transfer because of 1 in insulation. The initial temperature in the modeling is assumed 24ºC based on the site measurement. The mesh convergence was examined by trying different mesh size.

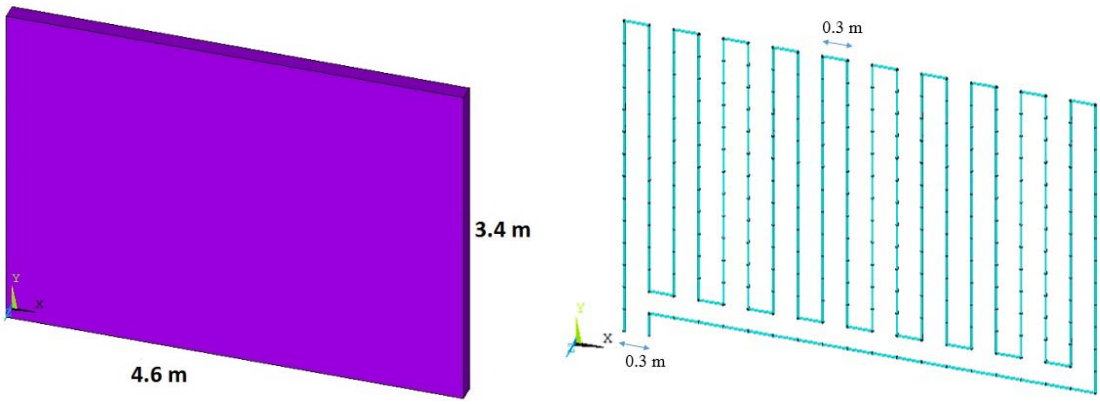

Figure 4.28. Concrete slab (left), piping system layout (right) in FE modeling

The whole slab and piping system is shown in Figure 4.29 as a 3D view and front view. The concrete slab dimension is 3.4×4.6 m^2 (11.15×15.1 ft^2) regarding the symmetry of actual size in the building. Height of concrete slab is 7 in or 0.18 m. piping diameter is ¾ in or 0.01905 m and flow rate is 33 gal/min based on the flow rate meter measurement. The 0.3 m distance between the tubes is selected based on the radiant floor layout.

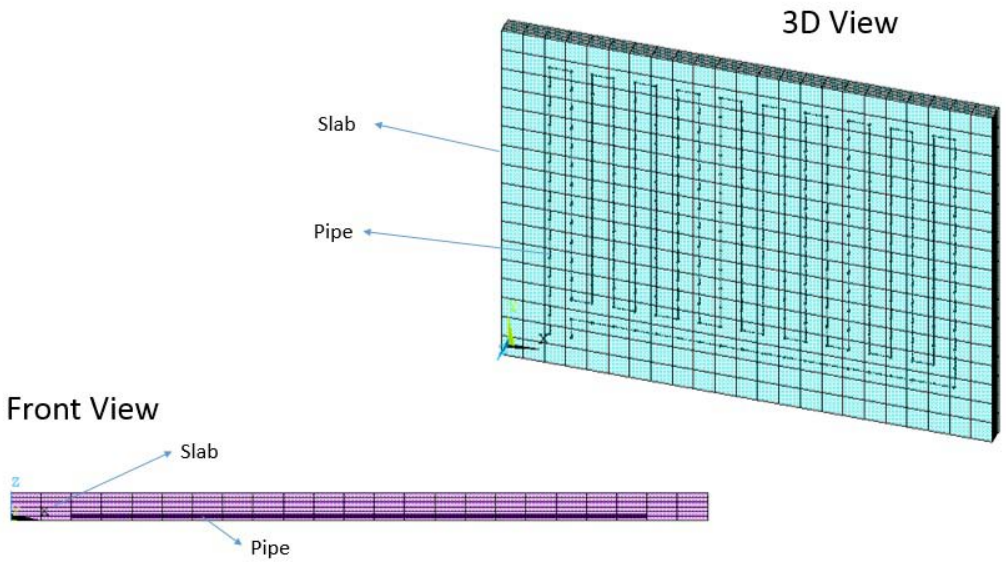

Figure 4.29. 3D and front view of the thin slab

Thermal loading of 60ºF (15.55ºC) at the left side of the concrete slab is inserted to the thin slab. The result of finite element modeling is shown in Figure 4.30.

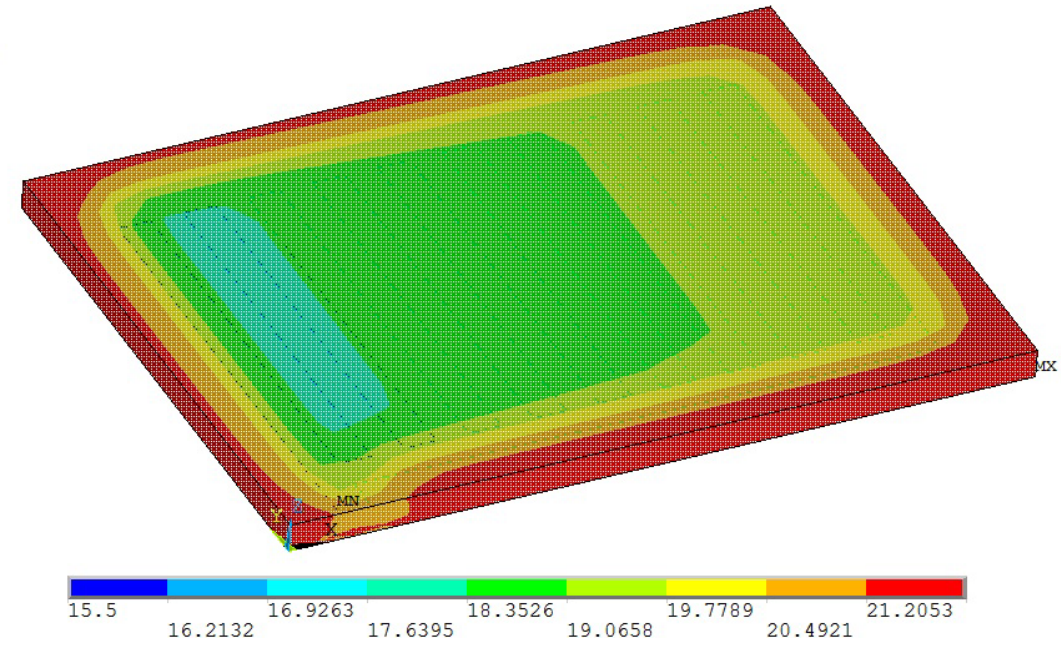

Figure 4.30. Finite element modeling of 7 in slab for 60ºF floor cooling

The higher temperature is concentrated on the left side of the concrete slab due to higher temperature of input fluid. The temperature range in the modeling is from 15.5ºC (60ºF) (temperature of pipe for the cooling system) to 21.2ºC (70ºF) (temperature of slab around the edges). The temperature around the edges of the thin slab is higher than other area of the slab because of greater distance from the chilled tubes. The comparison between temperature profile at the center point of 7 in slab from finite element modeling and job site data is shown in Figure 4.31. The green line at the right side of the graph shows the initial temperature of the thin slab before enabling the floor cooling and five other lines at the left side of graph show the temperature of the slab after thermal equilibrium. The blue dashed line shows the temperature profile from the finite element analysis which is close to site measurement.

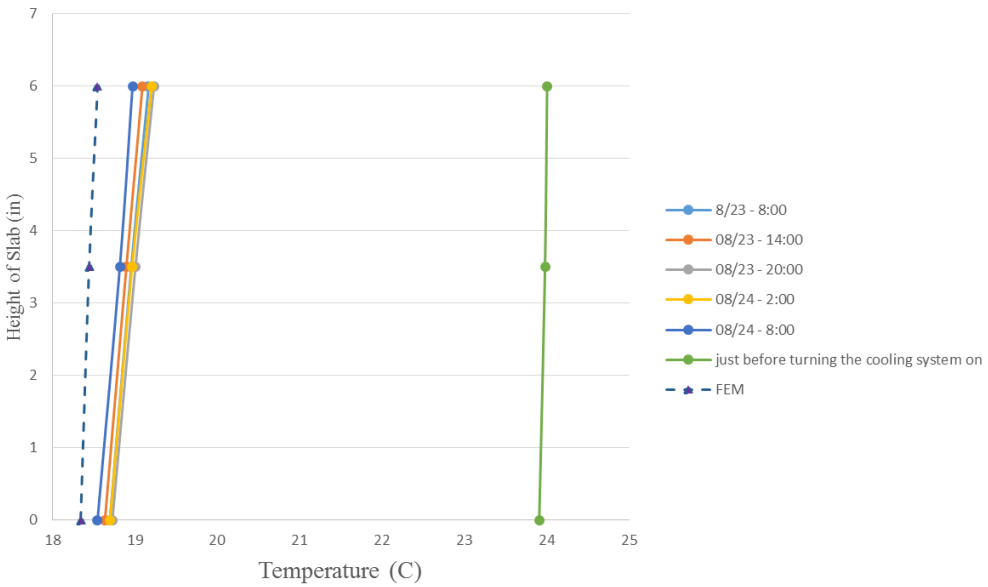

Figure 4.31. Temperature profile in thin radiant floor system (FEM and experimental data)

After verifying the model with experimental data, the new supply temperature of 50ºF or 10ºC is applied for finite element model. The result of temperature distribution is shown in Figure 4.32.

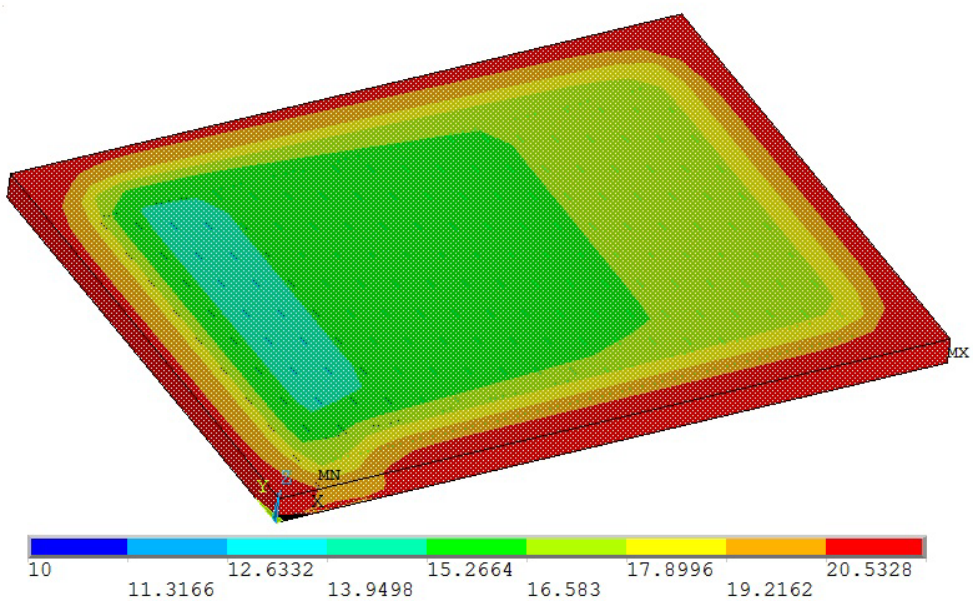

Figure 4.32. Modeling the floor cooling in 7 in slab for 50ºF (10ºC)

The general temperature distribution is similar to 60ºF (15.55ºC) cooling load. However, the temperature range inside of the thin slab is lower than the 60ºF model due to colder input temperature of piping system.

4.5 Conclusion

In summary, two cooling methods are examined to see the differences between the continuous and night cooling of 4 foot mass concrete radiant floor. The supply temperature for the thermal loading was 60ºF. Because of low thermal conductivity of concrete and high thermal lag, the supply chilling by ground source heat pump can be kept inside of the slab even by night cooling system. In addition, the amount of temperature drop in the mass floor for continuous cooling is 5-10% more than night cooling between 8 P.M. to 8 A.M. However, electricity savings can be achieved by running the mass floor cooling at night time which is energy off-peak time. The temperature profiles of continuous cooling system show that 10 days is the thermal equilibrium of 4 ft mass concrete floor with supply temperature of 60ºF. In addition, bare surface of the concrete floor should be kept out of outdoor humid air to prevent condensation and wet surface.

CHAPTER V

AN EFFICIENT APPROACH FOR USING THE MASS RADIANT FLOOR WITH GROUND SOURCE HEAT PUMPS

5.1 Overview

The concept of a thermal battery refers to storing supplied radiant heat and releasing this heat next day through convection. In this chapter, an innovative approach is introduced to examine the thermal battery idea. The heating radiant floor was turned ON at night time between 8 P.M. to 8 A.M., and the air conditioning system was disabled for 24 hours during the test period. Indoor air temperature shows 100ºF (37.78ºC) supply temperature at ground source heat pump would be enough to have stable warm temperature during cold days. Two weather conditions in the winter time were selected to do the test. The second test has a colder ambient temperature. However, the indoor air temperature showed that the night heating system performs well for both cases because it is maintained at constant temperature for entire day even at day time which every heating units are off. Also, the coefficient of performance of heat pumps and heating system is studied. COP of the heating system including heat pumps and pumps is 10% lower than COP of the heat pumps.

5.2Introduction

Longer life buildings have a much greater impact through operational reductions of greenhouse gases. A ground source heat pump is an option for high energy efficiency performance. In addition, radiant heating and cooling systems have been extensively used in residential and non-residential buildings such as airports, terminals, etc in Korea, China, Germany and Denmark [75, 76, 77].

Researchers have studied some strategies to control the radiant heating systems [78, 79]. Using the mass radiant floor has some benefits for the building regarding the thermal mass of concrete. The thermal mass of a structure is critical for passive storage of thermal energy [80]. Controlling the floor heating system is more challenging than the forced-air system because the large mass floor responds slowly to changes in heat input [81]. The heating/cooling radiant floor systems provide the heating/cooling by combination of radiation and convention and forced-air system work through the convection process [82, 83]. Also, the generated heat in the embedded pipe of radiant floor transfers to the surface of the slab by conduction.

The radiant heating floor system can provide an even distributed and vertical temperature gradient for the 2.5 m above the surface of the floor [84, 85]. The radiant floor is a silent way to heat the building and it would lead to less air movement inside of the building. It potentially decrease cold draught because of excessive air movement [86 ,87]. However, the surface temperature of the radiant floor should be controlled by the supplied temperature of the heat pumps to prevent discomfort for occupants and over-heating the building. The recommended temperature for surface of the radiant floor is between 17ºC to 29ºC in ASHRAE Standard 55 and ISO EN 7730 [88, 89].

It is feasible to combine the radiant heating/cooling system with renewable energy like solar energy or a ground source geothermal system [90, 91, 92].In this study, the radiant floor system works with a geothermal system which makes the heating system more efficient.

The use of high thermal mass is in an effective way to reduce energy demand peak of usage [93, 94, 95, 96]. Regarding this chapter, the mass floor should provide enough thermal heat storage to release it for one or more operationaldays. If the slab is not warm or cold enough during the night time, it cannot provide a sufficient thermal load for the day time. It is critical to run the radiant mass floor to take maximum advantage of thermal mass. If the pump operated during the night time in water distribution system, there would be a significant reduction of electricity cost [97, 98]. The whole slab would be warmer after certain cycles of heating at nights, and the building would be above a heat source all 24 hours a day.

5.3Experiment

The performance of the radiant floor has been tested for 5 days of night heating without any forced air system from 12/26 to 12/30. All overhead and man doors in the construction laboratorywere kept closed in this period to prevent the outside air exposure. The floor heating system was operatingat night between 8 P.M. to 8 A.M., and a forced-air system was disabled for 24 hours. The only heating unit in the building was the radiant floor system which was working at night time. The supply temperature at heat pumps was set at 100ºF, and the return temperature was set at 90ºF. The supply temperature and return temperature after two heat pumps and three pumps were measured over time every 15 minutes. However, due to heat loss from moving the fluid inside of the pipes, the actual temperature in the embedded pipes of the radiant floor system is less than 100ºF. The thermocouple attached to the piping system showsthe actual temperature felt by the piping system.

An electric meter was installed on the heat pumps and pumps to obtain the coefficient of performance (COP) of the heat pumps and COP of the heating system. All electricity meters are connected to a data acquisition system to record the data at 15 minute intervals (Figure 5.1). The electricity measurement would be helpful to compute the cost of heating floor performance.

Figure 5.1 Electricity meter (left picture) and data acquisition system (right picture)

The electricity usage was measured for two water-water heat pumps and five pumps (two pumps for ground system and three pumps for radiant floor system) as shown in Figure 5.2 as a schematic of the heating system including the radiant floor system with a ground loop system.

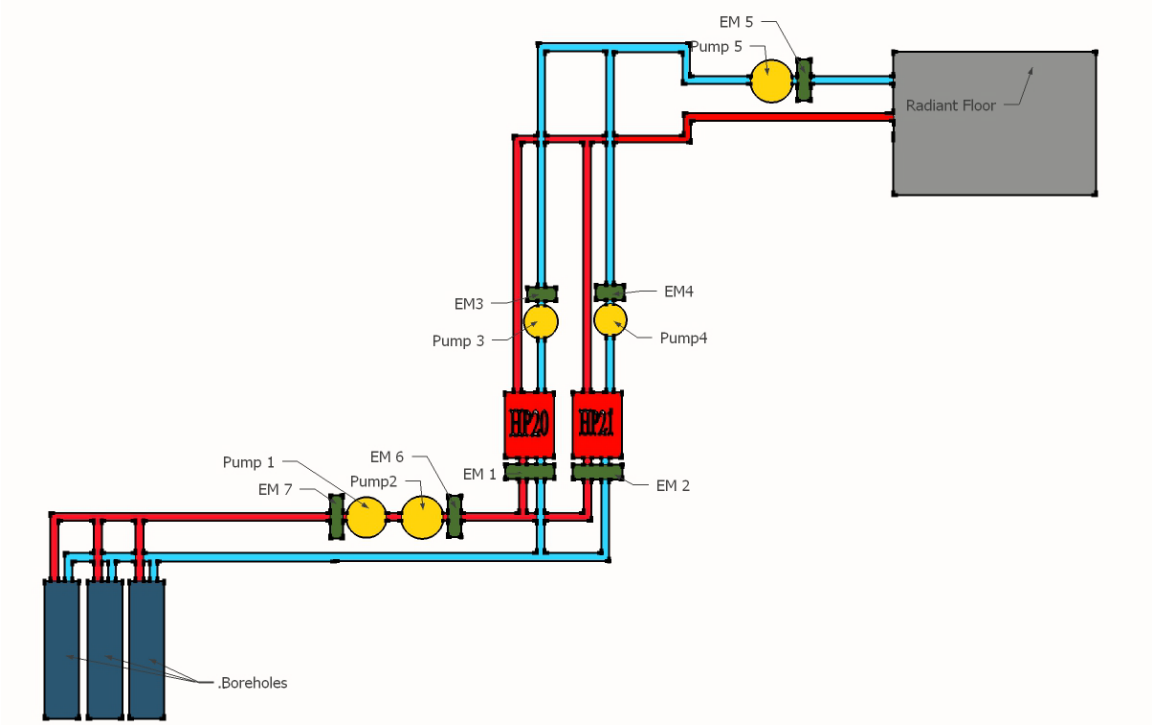

Figure 5.2.Schematic diagram of heating system

COP is a number to show the heat pump's efficiency. It is defined by dividing the output energy of the heat pump by the provided electrical energy needed to run the heat pump at a specific temperature. Greater COP number means higher efficiency.

$COP = h_h / h_w$

h_h = heat produced (Btu/h),

h_w = equivalent electric energy input (Btu/h) = 0.2931 P_w

P_w = electrical input energy (W)

Based on the properties of heat transfer fluid which is composed of water and 30% ethylene glycol, the density of the mix is 8.603 lb/gal, specific heat is 0.88 btu/lb.F. Therefore, the mass flow rate with 35 gal/min flow rate is 18066.3 lb/hr. System delivered BTU is calculated based on multiplying the mass by specific heat by temperature change between supply and return

temperature to the radiant floor system. Additionally, the electricity meters measure the electricity usage by heat pumps and pumps in kwh.

5.4Results and Discussion

The radiant floor system in this research program worked with a ground source heat pump (GSHP). The higher temperature of ground water is provided by a well system out of the building and the underground water heat will be transferred to the radiant floor fluid by the heat pump operation. Then, heated fluid is inserted to the floor pipes to make the concrete slab warm and is returned to the heat pump in a closed loop. Input supply temperature and return temperature of the pipes are measured over time to control the radiant floor system. These measurements were used as input parameters for the modeling of the radiant floor system. All measurements have been carried out over step time of 15 minutes and they are used for modeling of the heated slab. This measurement is representative of the supply and return temperature in the radiant floor system. Supply and return temperatures are shown in Figure 5.3 from 12/25 at 8:00 PM to 12/31 at 8:00 AM. Therefore, zero time is 12/25 at 8:00 PM.

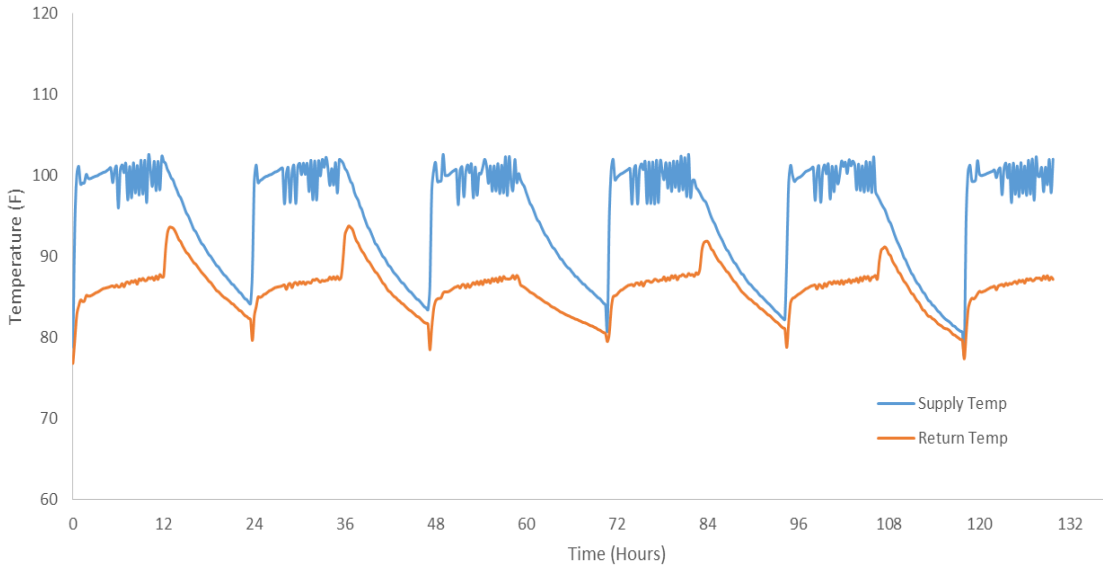

Figure 5.3. Supply and return temperature into the radiant floor system

This temperature trend shows a temperature drop after disabling the floor heating at 8 A.M. of every day. However, this temperature drop did not happen suddenly and the temperatureof the piping system decreased gradually over time. It can be seen that the supply temperature decreased from 100ºF to 84ºF in 12 hours until the next day. The heat pumps were needed to increase the piping temperature from 84ºF to 100ºF. There is less demand on the heat pumps when there is a lowerneed to provide atemperature difference. The return temperature in the slab shows that the temperature can increase every cycle of heating at night time. It is recommended that the average of supply and return temperature be controlled according to outdoor or indoor air temperature which can lead to accurate control of thermal output to the building [99].

The indoor air temperature should be compared with the outdoor air temperature to conclude how much the radiant floor can actually perform during the test. If the temperature does not drop during the day when all heating units are disabled, the test would be successful. However, the supply temperature in the radiant floor should be enough to maintain the indoor air temperature. If the surface temperature of the radiant floor remains warm enough with respect to thermal energy storage capacity of mass floor and conduction by vertical steel anchors, the indoor temperature would be potentially kept at a comfortable level. The same amount of heat flux will be delivered to space by radiant floor at a given surface temperature and indoor temperature regardless of the embedded radiant system type [100]. The indoor and outdoor air temperature during the first test are shown in Figure 5.4. It should be mentioned that zero time is 12/25 at 8:00 P.M. and end of experiment is 12/31 at 8:00 A.M.

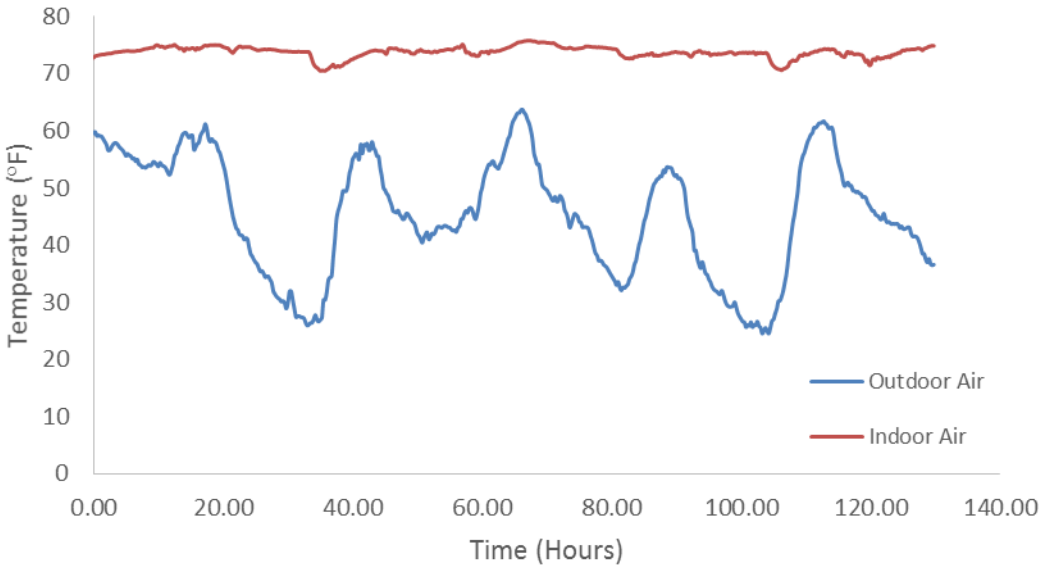

Figure 5.4. Indoor and Outdoor temperature (Test # 1)

The indoor air temperature is stable during the first test. The outdoor air temperature is between 26-63°F (-3.3-17.2ºC); however, the indoor air temperature range is between70.5-74.5°F (21.4-23.6ºC). As a result, the floor heating at night can keep the indoor air temperature at a desirable constant condition for the building for whole 24 hours of a day. To quantify the graph results, an average temperature of every day and night during the test is helpful. The average temperature of the heating system from 8 P.M. to 8A.M. and the average temperature from 8 A.M. to 8 P.M. are shown in Figure 5.5. The vertical axis is the temperature in degrees Fahrenheit and the horizontal axis represents the day and night of the test.

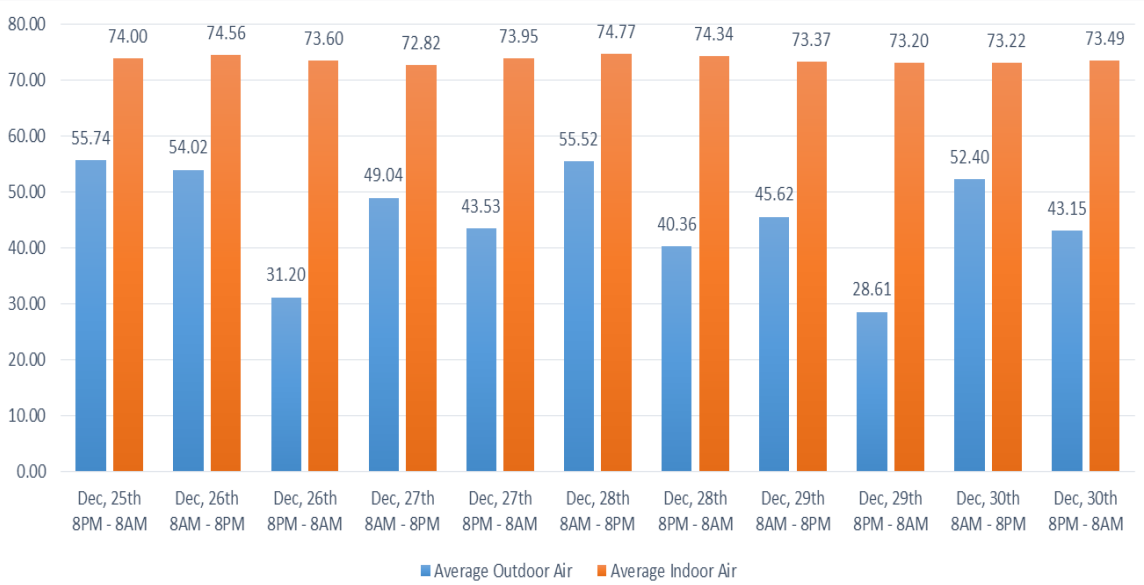

Figure 5.5. The average of Indoor and Outdoor temperature during day and night of the test

The average temperature of outdoor air at nights is lower than days. However, the indoor air temperature during the day time is stable. The constant temperature inside of the laboratory building would be great for some temperature sensitive experiment.

Extracting heat from the underground water to the heat transfer fluid in the radiant floor has been completed by two water-water heat pumps. In the ground loop system, the temperature of the water during the winter season is nearly64°F (17.8ºC). This temperature of water provides a more efficient system in comparison with a radiant floor system using domestic water. The temperature change in the ground loop system is shown in Figure 5.6.

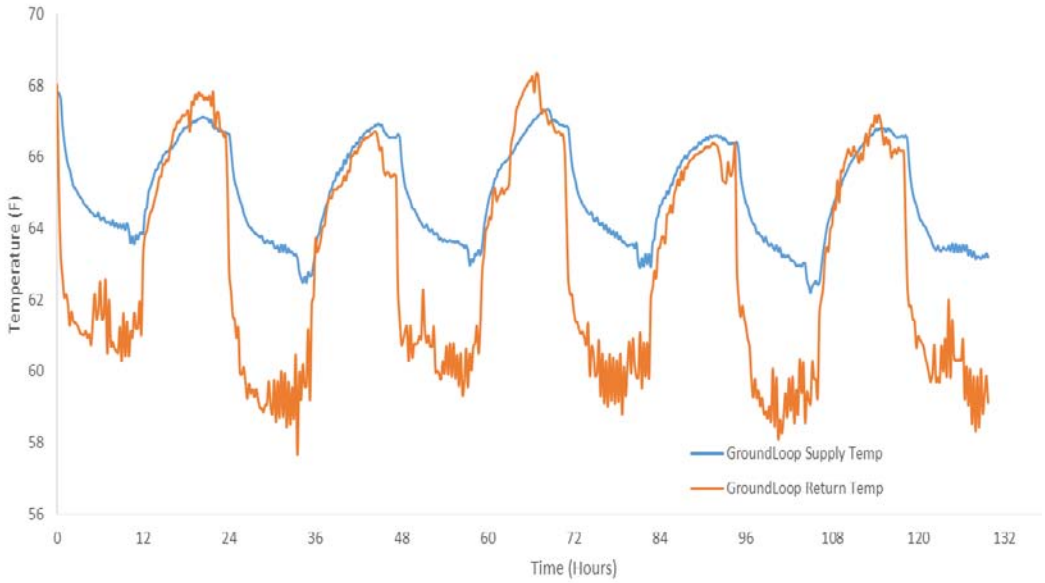

Figure 5.6. Ground Loop Supply and Ground Loop Return Temperature

The average temperature of the provided supply and return temperature of the ground loop system for the radiant floor system for each day and night of the test is shown in Figure 5.7. The vertical axis is temperature in degrees Fahrenheit, and the horizontal axis is day or night period of every day during the test.

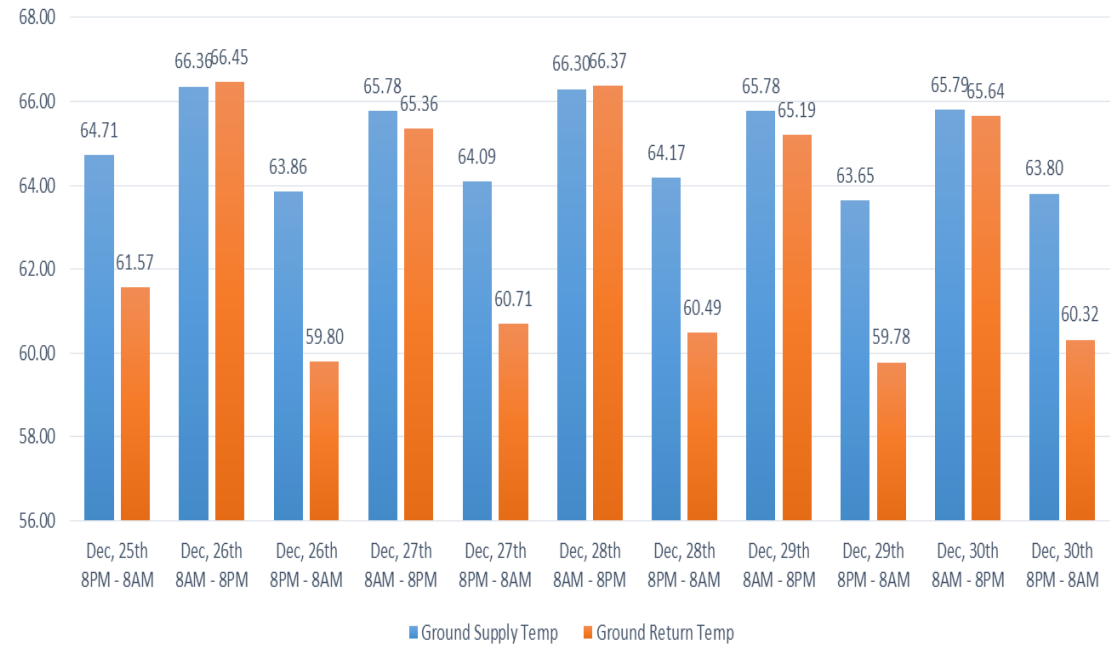

Figure 5.7. Average Ground Loop Supply and Return Temperature (Test #1)

The return temperature is lower than supply temperature during the heating cycle at night time and they are almost the same during the day time. The difference between the supply and return temperature of ground loop system is shown in Figure 5.8.

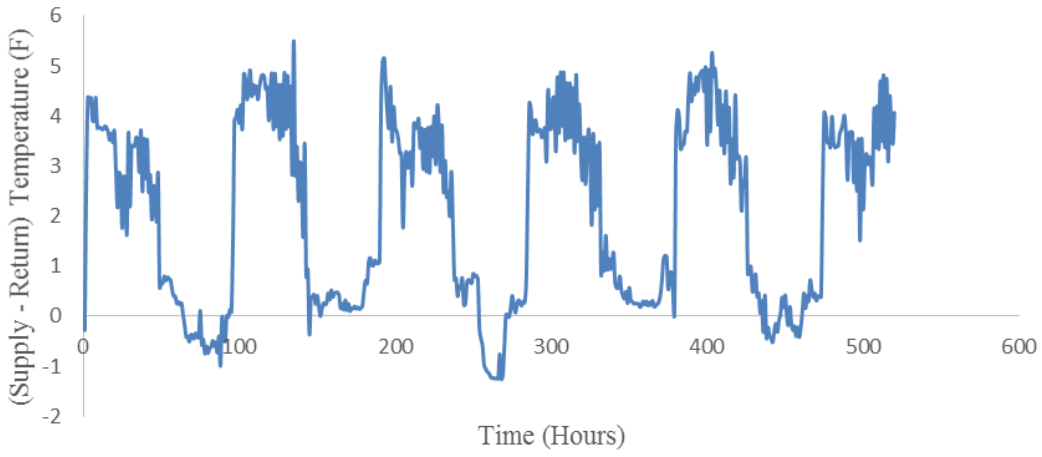

Figure 5.8. Difference between supply and return temperature in ground loop system

The maximum of temperature difference between the input and output temperature of supply and return temperature of the ground loop system is 4-5ºF.

The electricity usage by ground source heat pump during test # 1 is shown in Figure 5.9.

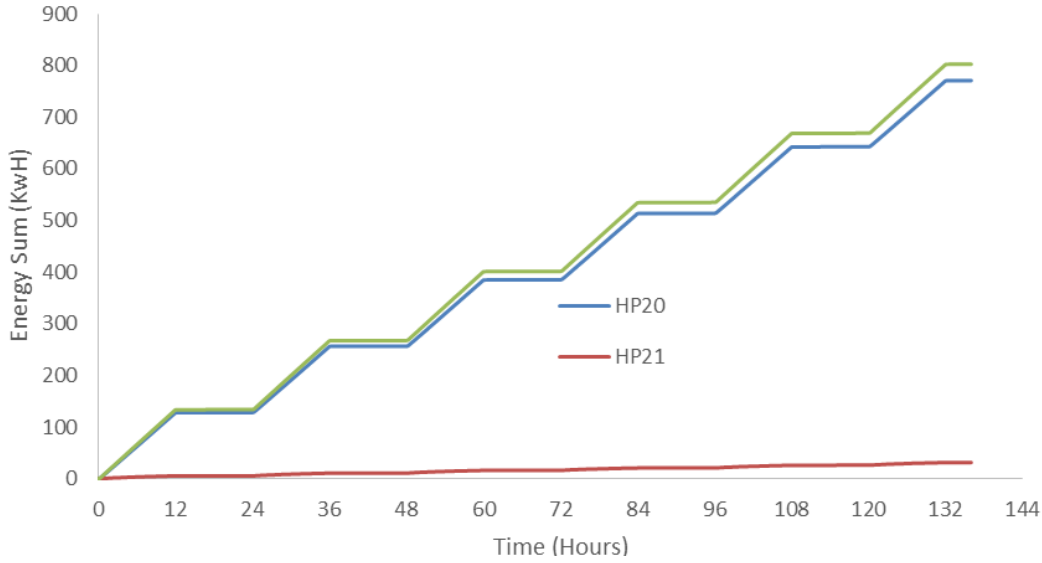

Figure 5.9. Electricity usage by two ground source heat pumps (test #1)

Every heating cycle at night time for 12 hours between 8 P.M. to 8 A.M. uses 133 kWh of electricity usage by two heat pumps. And during the day time between 8 A.M. to 8 P.M., electricity usage is nearly zero.

Another test was repeated for a colder period called test # 2 to verify the obtained data in test #1. The indoor air temperature vs outdoor temperature is shown in Figure 5.10. The average of indoor and outdoor temperature during day and night is shown in Figure 5.11. Ground loop supply and ground loop return temperature and average ground loop supply and return temperature for test # 2 are shown in Figure 5.12 and Figure 5.13, respectively. Finally, electricity usage by two ground source heat pumps is shown in Figure 5.14.

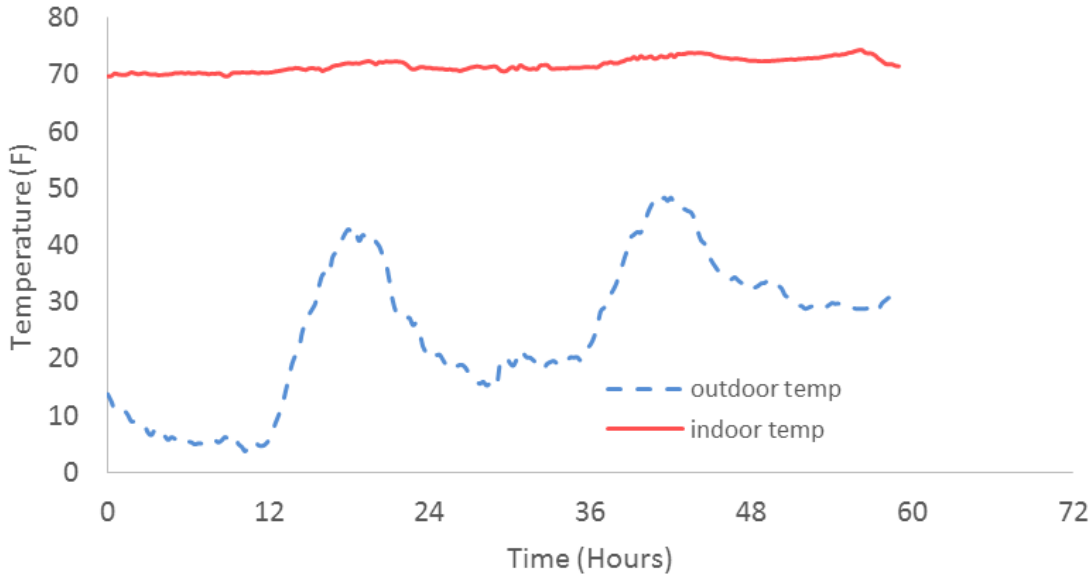

Figure 5.10. Indoor and Outdoor temperature (Test # 2)

The outdoor air temperature is between 4-48°F(-15.6-8.9ºC) which is colder than ambient temperature of test # 1, however the indoor air temperature range is around 70.5-74.5°F (21.4-23.6ºF).

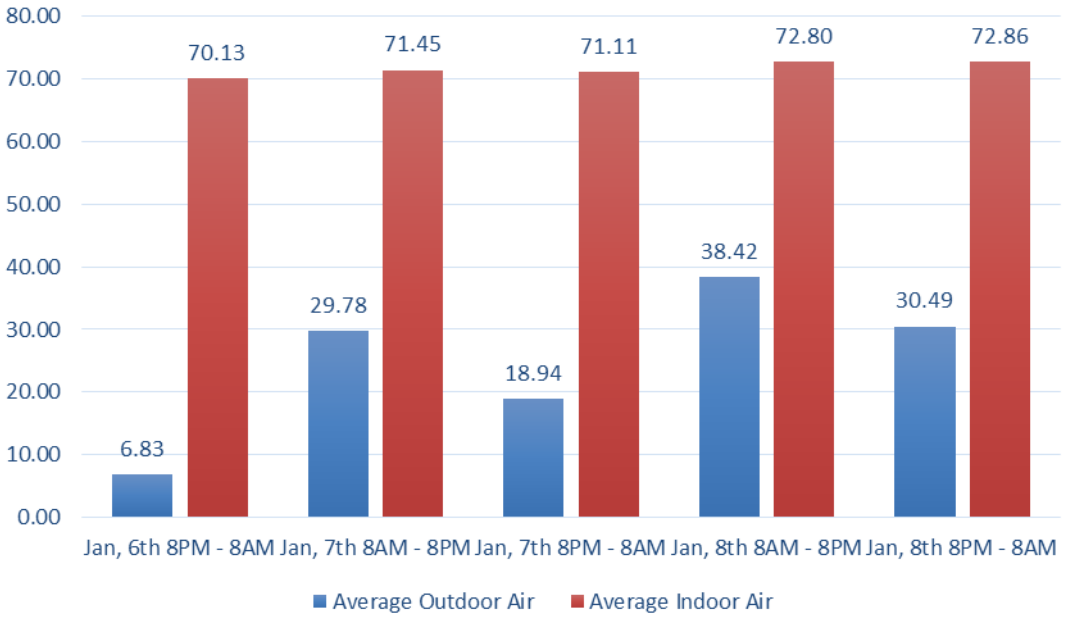

Figure 5.11. The average of Indoor and Outdoor temperature during day and night of the test #2

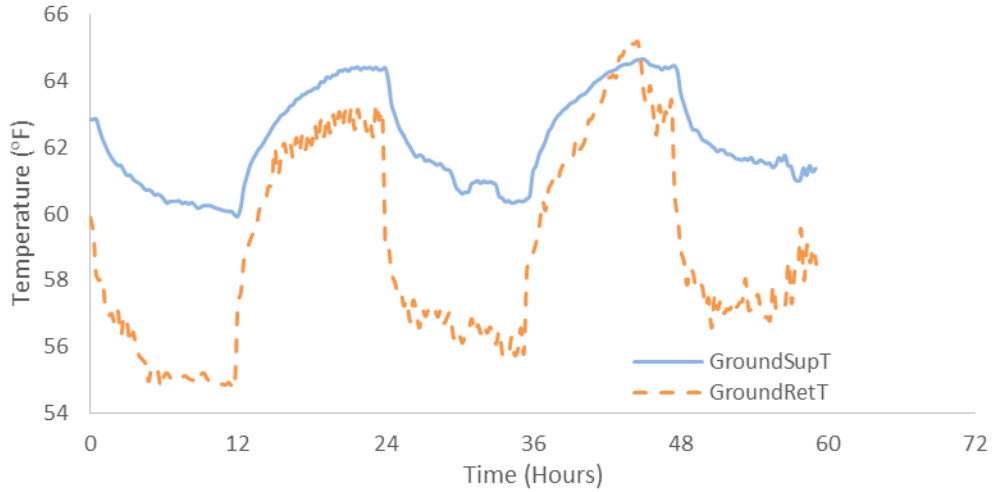

Figure 5.12. Ground Loop Supply and Ground Loop Return Temperature (Test # 2)

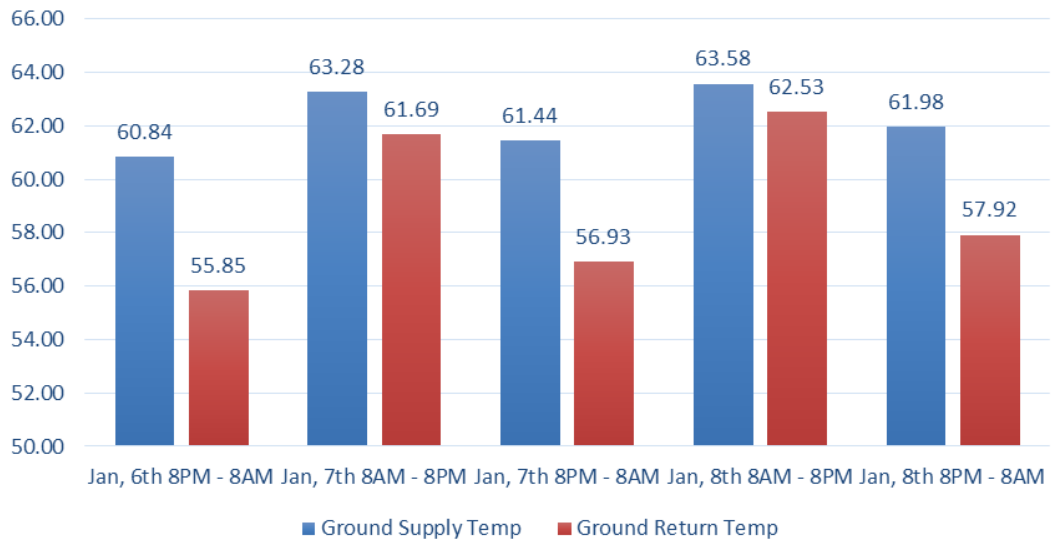

Figure 5.13. Average Ground Loop Supply and Return Temperature (Test #2)

A summary of results in terms of comparison between Test # 1 and Test # 2 about average indoor and outdoor air temperature and average supply and return ground temperature are illustrated in Table 5.1 and Table 5.2, respectively.

Table 5.1. Comparison of average indoor and outdoor temperature between Test 1, Test 2

	Test # 1 (12/26 – 12/30)	Test # 2 (01/06 – 01/08)
Average Outdoor Temp Night time (8 P.M. – 8 A.M.)	40.43ºF (4.68ºC)	18.75ºF (-7.36ºC)
Average Outdoor Temp Day time (8 A.M. – 8 P.M.)	51.32ºF (10.73ºC)	34.10ºF (1.17ºC)
Average Indoor Temp Night time (8 P.M. – 8 A.M.)	73.76ºF (23.2ºC)	71.37ºF (21.87ºC)
Average Indoor Temp Day time (8 A.M. – 8 P.M.)	73.75ºF (23.19ºC)	72.13ºF (22.29ºC)

Table 5.2. Comparison of average supply and return ground temperature between Test 1, Test 2

	Test # 1 (12/26 – 12/30)	Test # 2 (01/06 – 01/08)
Average Outdoor Temp Night time (8 P.M. – 8 A.M.)	64.05ºF (17.81ºC)	61.42ºF (16.34ºC)
Average Outdoor Temp Day time (8 A.M. – 8 P.M.)	66.00ºF (18.89ºC)	63.43ºF (17.46ºC)
Average Indoor Temp Night time (8 P.M. – 8 A.M.)	60.44ºF (15.8ºC)	56.90ºF (13.83ºC)
Average Indoor Temp Day time (8 A.M. – 8 P.M.)	65.80ºF (18.78ºC)	62.11ºF (16.73ºC)

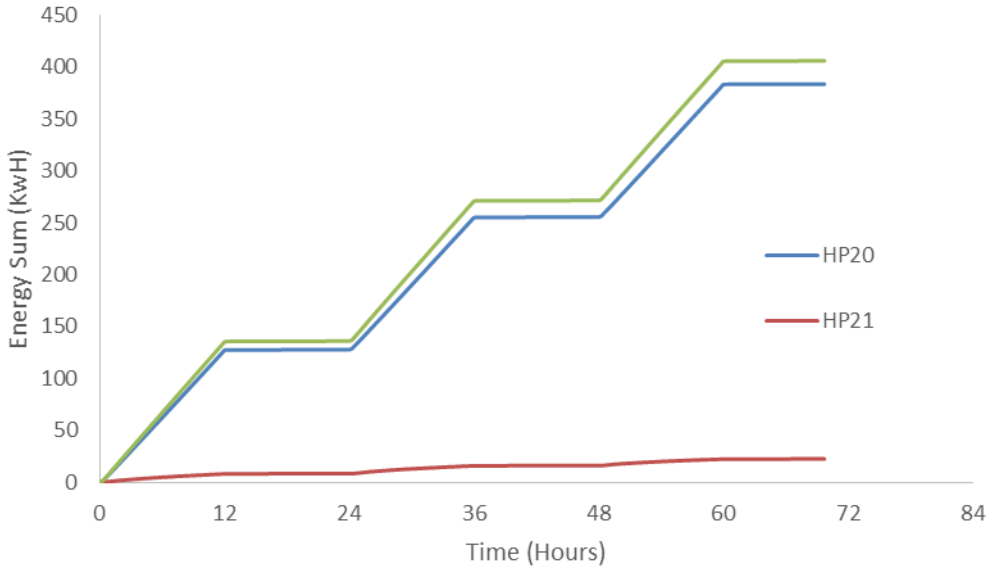

Figure 5.14. Electricity usage by two ground source heat pumps (Test # 2)

Electricity usage by heat pumps is the same as test #1 for each cycle of night heating which means the electricity usage only depends on supply temperature demand.

It should be mentioned that running the radiant floor system at 80ºF uses 50 kWh for two heat pumps during 12 hours of night heating. Also, the electricity usage for continuous 24 hours of heating mode on 80ºF is 90 kWh for two heat pumps. Electricity price for 24 hours of night heating and continuous heating at different supply temperature of heat pumps is shown in Table 5.3. The electricity price is estimated based on Stillwater electricity rate which is 16 cent/kwh at the day time and 4 cent/kwh at the night time.

Table 5.3. Electricity usage comparison of night heating and continuous heating at different supply temperature in the heat pumps

	Electricity usage	Price
80ºF night heating	50 kWh	$2
80ºF continuous heating	90 kWh	$8.87
90ºF night heating	110 kWh	$4.4
100ºF night heating	133 kWh	$5.32

The electricity cost of heat pump for continuous 24 hours heating is 4 times of electricity cost of heat pump for 12 hours of night heating. COP of the heat pumps and COP of heating system including two heat pumps and five pumps during test # 1 are shown in Figure 5.15, 5.16.

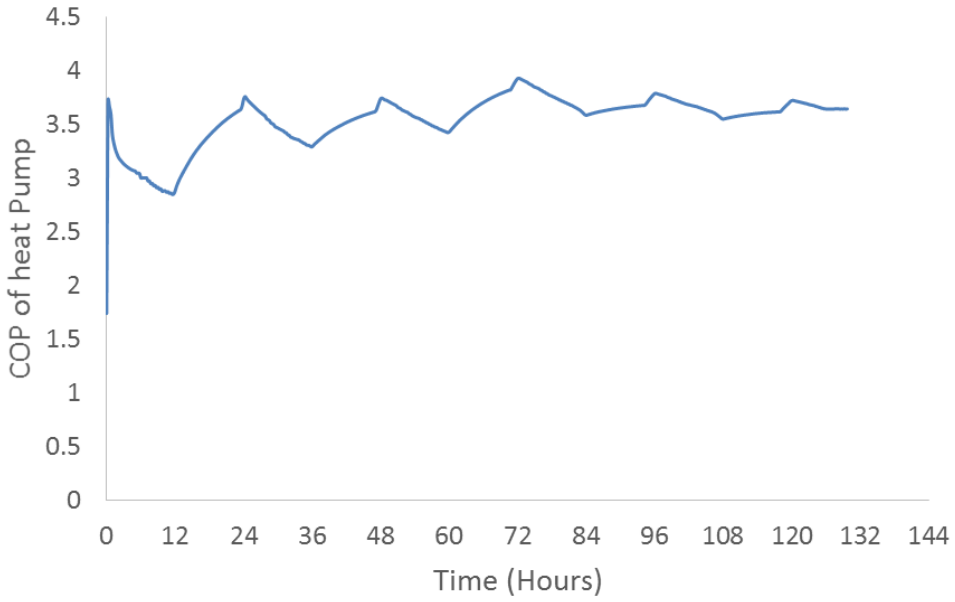

Figure 5.15. COP of heat pumps (Test # 1)

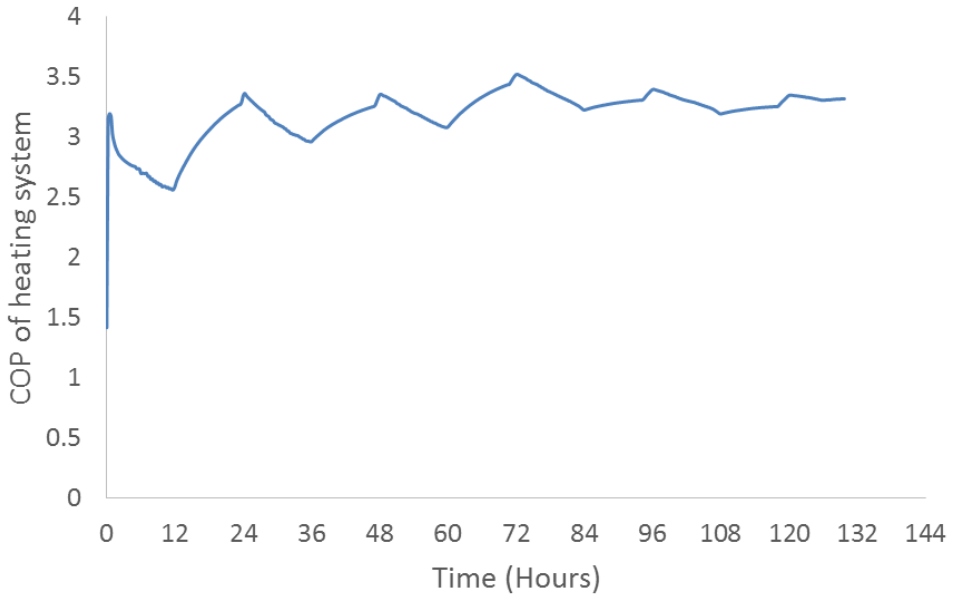

Figure 5.16. COP of heating system (Test # 1)

The temperature profile in the mass concrete floor is illustrated in Figure 5.17 and Figure 5.18 for the center and edge point, respectively. The slab temperature could be used as a controlled parameter to increase energy efficiency or prevent discomfort [101, 102].

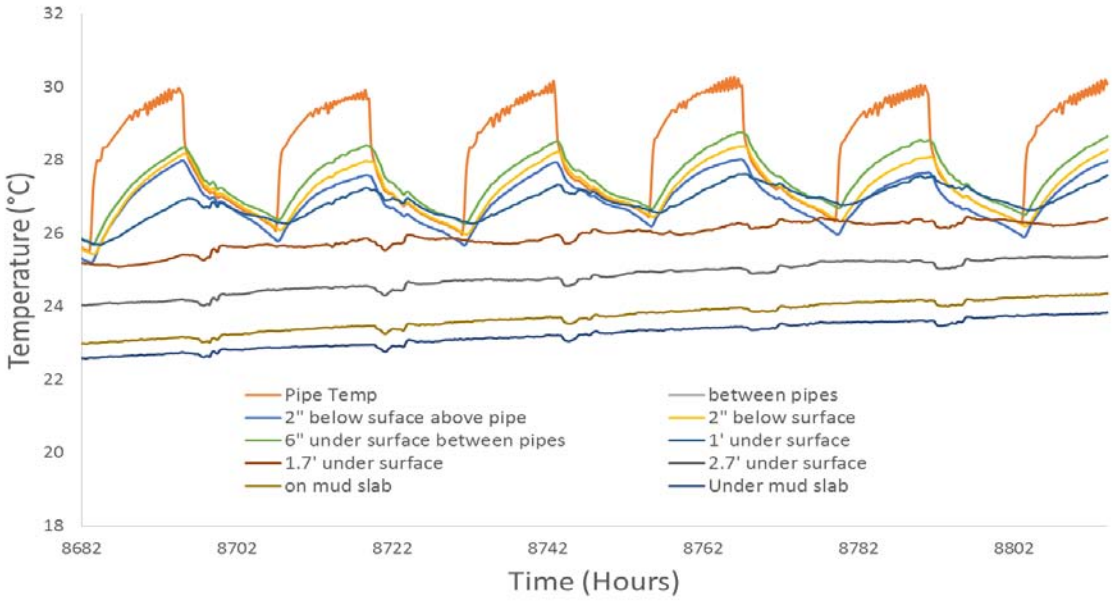

Figure 5.17. Temperature profile inside of mass floor (Center)

The vertical axis shows the temperature range of 18-32ºC (64.4-89.6ºF). The orange color trend shows the piping temperature during test # 1. The maximum temperature is nearly 30ºC (86ºF) at end of every heating cycle at night time. Because the piping system is located at 6 in below the surface, the temperature sensor at 6 in under the surface indicates the highest temperature after piping temperature. The temperature at 2 in below the surface between the pipes is higher than temperature at 2 in below the surface and above the piping system. The bottom half of mass floor temperature does not follow the cyclic heating load on the piping system. However, the temperature trends at 1.7 ft under the surface, 2.7 ft under the surface, on the mud slab (bottom of slab), and under the mud slab (ground temperature) is slightly rising during test # 1.The slab can store the thermal energy after heating cycles at night time. The overall temperature of the slab increases and foundation of the building is warmer and it acts like a thermal battery of the building. The vertical steel anchor inside of mass floor can conduct the heat at the bottom of slab to the surface in contact with indoor air. Because the thermal conductivity of steel is significantly higher than thermal conductivity of concrete.

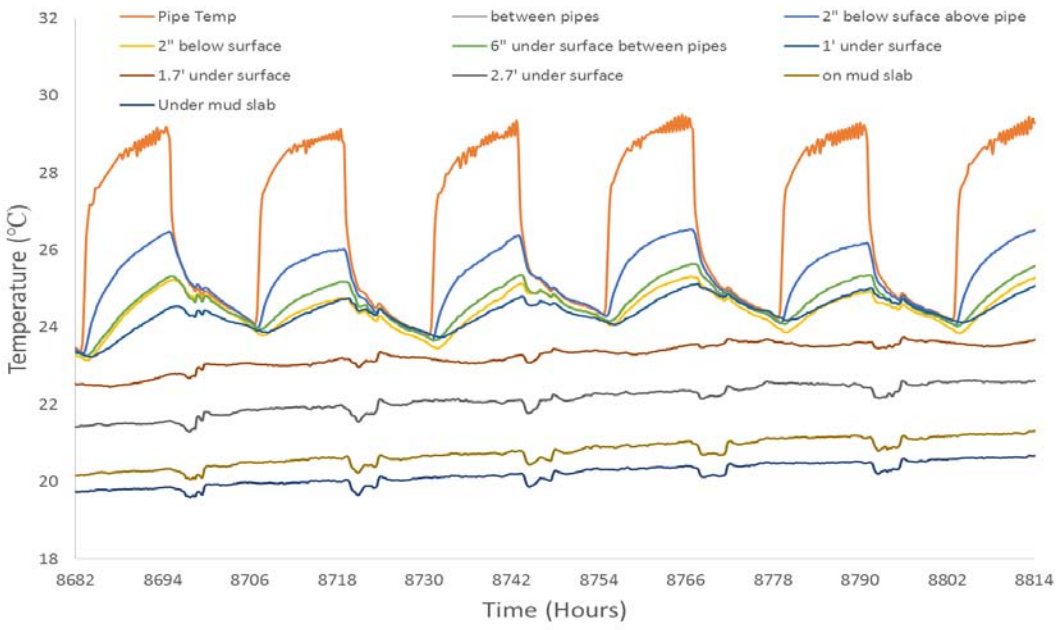

Figure 5.18. Temperature profile inside of mass floor (Edge)

In general, the temperature at the center of slab is higher than slab temperature at the edge point for 2ºC. The edge point is closer to the building wall, and it is more affected by cold weather. However, the temperature trends at the center and edge point follow the same pattern at different elevations throughout the slab height. The temperature at the center point and edge point of the mass floor is about 23-28°C (73.4-82.4ºF) and 20.2-26.4°C (68.36-79.52ºF), respectively. The heat is more stored at the center of the mass floor.

The temperature at 7 in slab for center and edge points during test # 1 is shown in Figure 5.19 and Figure 5.20.

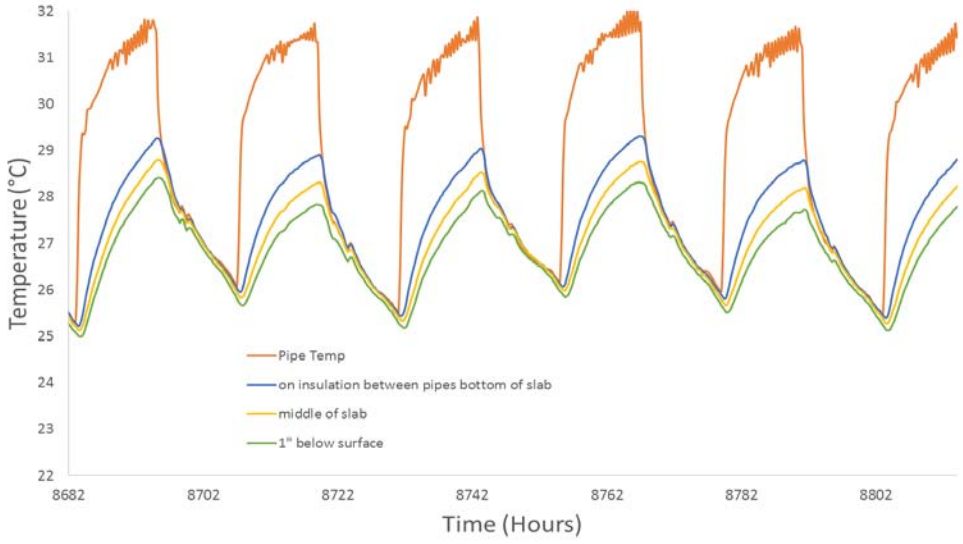

Figure 5.19. Temperature profile inside of thin slab (Center)

As mentioned earlier, the thin slab is not performing like thermal mass because of low height in comparison with 4 ft mass floor. The temperature profiles in the thin slab for the edge point is shown in Figure 5.20.

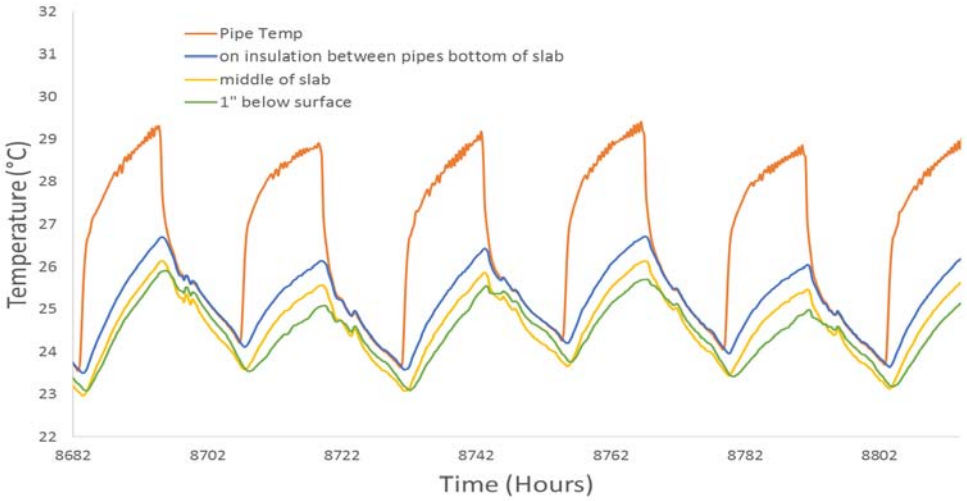

Figure 5.20. Temperature profile inside of thin slab (edge)

The piping temperature is higher in the center point because it is closer to manifold which provides the supply temperature. The edge point is near the outside wall of the building and feels the outside cold air. Therefore, the overall temperature at the edge point of thin slab is less than temperature profile at the center of slab. One day of test # 1 period is selected to monitor the temperature profile with 6 hours interval from 12/27, 20:00 to 12/28, 20:00. These five temperature profiles are shown in Figure 5.21.

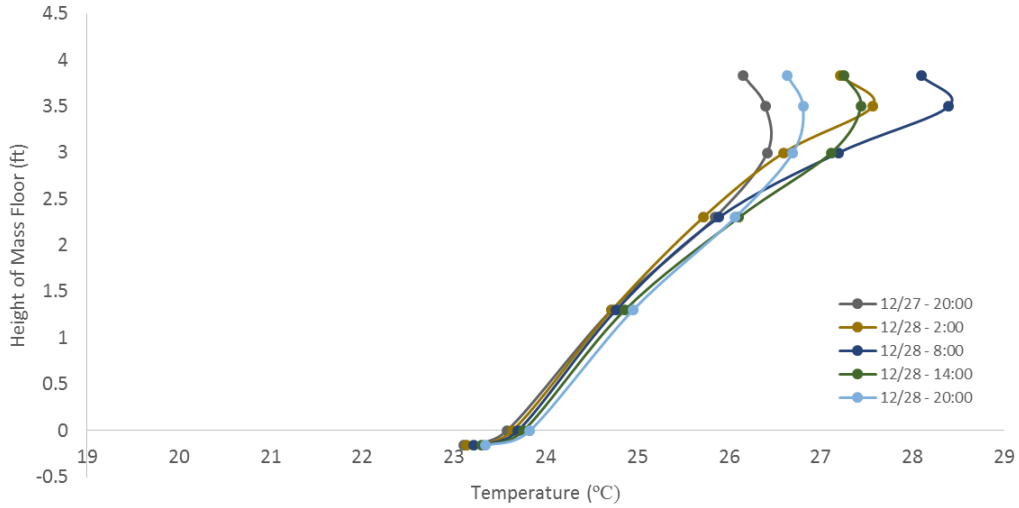

Figure 5.21. Temperature profile in the mass floor

The minimum surface temperature is 12/27, 20:00 which is the starting time of night heating and maximum surface temperature is 12/28, 8:00 which is end of night heating. It means the slab surface reaches 28.4ºC(83.12ºF) at day time which is all heating units are disabled. This surface temperature would be sufficient to keep the indoor air warm from 8 A.M. to 8 P.M.

5.5 Conclusion

In this chapter, an efficient approach of using the mass radiant floor has been introduced that running the heating system at night time between 8 P.M. to 8 A.M. would be enough to have a constant temperature inside of the building for whole 24 hours in a day. The mass radiant floor actsas a thermal battery of the building. The heat at the night time by a ground source heat pump was released on the next day when the all heating units are disabled. The supply temperature for radiant floor was set at 100ºF (37.78ºC). The results of two tests are presented in a cold period of time in winter with average outdoor air temperature of 40.43ºF (4.68ºC) and 18.75ºF (-7.36ºC) at night time and 51.32ºF (10.73ºC) and 34.10ºF (1.17ºC) at day time are presented. For these two tests, average of indoor temperature of 73.76ºF (23.2ºC) and 71.37ºF (21.87ºC) at the night time and 73.75ºF (23.19ºC) and 72.13ºF (22.29ºC) at day time have been recorded. In addition, the temperature gradient inside of mass concrete floor proves that heat can be stored in the concrete slab during the test of night heating. Regarding the electricity cost saving, this method would be applicable to other similar large bay area building by running the mass radiant floor at night time which energy is less expensive. COP of the heating system including heat pumps and pumps is 3.3 and unit COP of the heat pumps is 3.7.

CHAPTER VI

CONCLUSION

The research presented in this dissertation is divided by three phases. In the first phase, the temperature rise due to limestone blended cement hydration in the mass floor system has been studied. A finite element model was used to predict this temperature rise and the results were compared with ASTM cement type I-II. In the second phase, heating and cooling performance of the radiant floor system with ground source heat pumps have been studied. Thermal energy storage by thermal mass of concrete floor has been investigated. Also, the outcomes of cyclic night cooling with continuous cooling were compared. At last phase, the thermal battery concept has been verified with two tests of night heating.

The main conclusions of the dissertation are as following:

6.1 Heat of Hydration in a concrete slab-on-grade floor with limestone blended cement

- Different cements have different cement hydration properties
- Limestone blended cement is not available in most of temperature predication commercial software as a default value
- Maximum temperature at the job site occurred at 42.94°C (109.29ºF) after 51.75 hours,
- Maximum temperature for FEM model predicted at43.03°C (109.45ºF) after 56.7 hour,

- Maximum temperature for commercial software with ambient temperature of the job site predicted 39.08ºC (102.34ºF) after 72 hours
- The software is applicable as an estimation of temperature rise prediction
- Finite element model with calorimetry result is more accurate
- The finite element results verified by the job site measurements
- Maximum temperature of cement IL+25%FC would occur at 43.03°C (109.45ºF) after 56.7 hours and would be 39.86°C (103.75ºF) after 59.3 hours for cement I-II+25%FC
- Higher maximum temperature of cement IL hydration than cement I-II is probably because of high finer particle and greater cement Blaine
- Calorimetry and measured weather data would be needed to generate the hydration information for Concreteworks and FEM model

6.2 Heating performance of mass concrete radiant floor system with ground source pipe systems

- 3ºC temperature rise in the mass floor after three cycle of heating
- 4 MBTU can be stored in the 118×46×4ft^3 mass floor after three heating cycle of 80°F (26.67ºC), 90°F (32.22ºC), and 90°F with 9 days period at each cycle
- Saving thermal energy by mass heated concrete floor
- Vertical steel in the slab conduct the heat from bottom of slab to the surface
- Heat cannot be stored in thin slab as much as mass floor
- A full 3D finite element model of mass floor is in good agreement with job site data.

6.3 Cooling performance of thick and thin concrete radiant floor system with ground source pipe systems

- Temperature drop in the mass floor for continuous cooling is 5-10% more than night cooling between 8 P.M. to 8 A.M.
- 9.5 days is the thermal equilibrium of 4 ft mass concrete floor with supply temperature of 60ºF (15.55ºC).
- Bare surface of the concrete floor should be kept out of outdoor humid air to prevent condensation.
- Night cooling can keep the surface temperature low.

6.4 An efficient approach for using the mass radiant floor with ground source heat pumps

- An efficient approach to use the mass radiant floor as a thermal battery of the building by running the floor heating from 8 P.M. to 8 A.M. for 100ºF (37.78ºC) supply temperature
- Two test results show that indoor air temperature is constant and warm with just running the radiant floor at night time.
- First test shows average outdoor air temperature of 40.43ºF (4.68ºC) and 18.75ºF (-7.36ºC) at night time with indoor temperature of 73.76ºF (23.2ºC) and 71.37ºF (21.87ºC) at the night time.
- Second test shows average outdoor air temperature of 51.32ºF (10.73ºC) and 34.10ºF (1.17ºC) at day time with indoor temperature of 73.75ºF (23.19ºC) and 72.13ºF(22.29ºC) at day time.
- Thermal comfort and silent heating method
- Storing heat by thermal mass concrete floor during night heating

6.5 Future Work

In this dissertation, the research has concentrated on saving thermal energy and application of using a mass concrete radiant floor system combined with ground source heat pumps. However, to study more about this system in the building, the following list suggested:

- Investigation on indoor air quality regarding CO_2 emission of vehicles in the lab, welding work, etc
- Applying the ventilation system with floor cooling system to prevent condensation on the surface of the floor
- Optimizing the working hours of radiant floor system with respect to outdoor and indoor air temperature
- Covering the steel caps to see the difference in performance of the radiant floor system
- Cost efficiency of the system

REFERENCES

[1] www.wbcsdcement.org, Recycling Concrete, Executive summary. The cement sustainability initiative. World Business Council for Sustainable Development.

[2] Korea Concrete Institute, Thermal Crack Control of Mass Concrete, Concrete Practices Manual, 2010.

[3] Shekarchizadeh, M., Tahersima, M., Hajibabaee, A., &Layssi, H. (2008). Concrete Mix Proportions with Ultra-High Electrical Resistivity. In 11DMBC International Conference on Durability of Building Materials and components.

[4] BentzA, D. P., IrassarB, E. F., BucherC, B., &WeissC, W. J. Limestone Fillers to Conserve Cement in Low w/cm Concretes: An Analysis Based on Powers' Model.

[5] Bonavetti, V., Donza, H., Menendez, G., Cabrera, O., &Irassar, E. F. (2003). Limestone filler cement in low w/c concrete: a rational use of energy. Cement and Concrete Research, 33(6), 865-871.

[6] Barker, A., & Cory, H. P. (1991). The early hydration of limestone-filled cements. In blended cements in construction. papers presented at the international conference, university of sheffield, uk, 9-12 september 1991.

[7] Klemm, W. A., & Adams, L. D. (1990). An investigation of the formation of carboaluminates. In Carbonate Additions to Cement. ASTM International.

[8] Bensted, J. (1983). Further hydration investigations involving Portland cement and the substitution of limestone for gypsum. World cement, 14(10), 383-392.

[9] Campiteli, V. C., &Florindo, M. C. (1990). The influence of limestone additions on optimum sulfur trioxide content in Portland cements. In Carbonate additions to cement. ASTM International.

[10] Rahhal, V. F., Irassar, E. F., Trezza, M. A., &Bonavetti, V. L. (2012). Calorimetric characterization of Portland limestone cement produced by intergrinding. Journal of thermal analysis and calorimetry, 109(1), 153-161.

[11] Ramezanianpour, A. A., Firoozmakan, S., Tahersima, M., & Ebadi, T. (2011) Effects of Nano-Silica on Mechanical Properties of Mortars, 9th International Congress on Advances in Civil Engineering.

[12] Cement and Concrete Terminology, ACI 318 Farmington Hills, ACI, 2005.

[13] Hunt, J. G. (1971). A laboratory study of early-age thermal cracking of concrete (No. TR 42.457 R&D Rept.).

[14] Tahersima, M., &Tikalsky, P. (2017). Finite Element Modeling of Hydration Heat in a Concrete Slab-on-grade Floor with Limestone Blended Cement. Construction and Building Materials.

[15] Ayotte, É.,Massicotte, B., Houde, J., &Gocevski, V. (1997). Modeling the thermal stresses at early ages in a concrete monolith. ACI Materials Journal, 94(6), 577-587.

[16] Tahersima, M., Ley, T., &Tikalsky, P. (2017). Hydration Heat in a Mass Concrete and a Thin Slab with Limestone Blended Cement, International Journal of Materials Science and Engineering, 5(2), 79-86.

[17] Babiak, J., Olesen, B. W., &Petras, D. (2009). Low temperature heating and high temperature cooling. Rehva., Brussels, 2009.

[18] ISO, ISO 11855-2:2012(E) Building Environment Design-Design, Dimensioning, Installation and Control of Embedded Radiant Heating and Cooling Systems. Part 2: Determination of the Design Heating and Cooling Capacity, International Organization for Standard, Gen_eve, Switzerland, 2012.

[19] Handbook, A. S. H. R. A. E. (1996). HVAC systems and equipment. American Society of Heating, Refrigerating, and Air Conditioning Engineers, Atlanta, GA.

[20] da Amorim Coelho, N., Pedroso, L. J., da Silva Rêgo, J. H., & Nepomuceno, A. A. (2014). Use of ANSYS for Thermal Analysis in Mass Concrete. Journal of Civil Engineering and Architecture, 8(7).

[21] http://www.holcim.us/en

[22] Document provided from Holcim Inc. Ada, OK.

[23] ANSYS academic research, release 15.0

[24] Gurney, L., Bentz, D., Sato, T., & Weiss, W. (2012). Reducing Set Retardation in High-Volume Fly Ash Mixtures with the Use of Limestone: Improving Constructability for Sustainability. Transportation Research Record: Journal of the Transportation Research Board, (2290), 139-146.

[25] http://www.engineeringtoolbox.com

[26] Tahersima, M., Yeganeh-Bakhtiary, A., & Hajivalie, F. (2011). Scour pattern in front of vertical breakwater with wave overtopping. *Journal of Coastal Research*, (64), 598.

[27] Concreteworks, www.texasconcreteworks.com

[28] Riding, K. A. (2007). Early age concrete thermal stress measurement and modeling. ProQuest.

[29] Lawrence, A. M. (2009). A finite element model for the prediction of thermal stresses in mass concrete (Doctoral dissertation, University of Florida).

[30] Cost, V., Howard, I., & Shannon, J. (2013). Improving concrete sustainability and performance with use of portland-limestone cement synergies. Transportation Research Record: Journal of the Transportation Research Board, (2342), 26-34.

[31] Tennis, P. D., Thomas, M. D. A., & Weiss, W. J. (2011). State-of-the-Art Report on Use of Limestone in Cements at Levels of up to 15%. Illinois, accessed November, 9, 2015.

[32] Lothenbach, B., Le Saout, G., Gallucci, E., & Scrivener, K. (2008). Influence of limestone on the hydration of Portland cements. Cement and Concrete Research, 38(6), 848-860.

[33] Bilgen, E., & Richard, M. A. (2002). Horizontal concrete slabs as passive solar collectors. Solar Energy, 72(5), 405-413.

[34] The concrete center, Utilization of thermal mass in non-residential buildings, UK, 2006.

[35] Baumert, K. A., Herzog, T., & Pershing, J. (2005). Navigating the numbers: Greenhouse gases and international climate change agreements.

[36] EIA. Annual energy review 2004. In: E.I.A. U.S. Department of Energy, editor. Washington, DC: Energy Information Administration; 2005.

[37] Urchueguía, J. F., Zacarés, M., Corberán, J. M., Montero, A., Martos, J., & Witte, H. (2008). Comparison between the energy performance of a ground coupled water to water heat pump system and an air to water heat pump system for heating and cooling in typical conditions of the European Mediterranean coast. Energy Conversion and Management, 49(10), 2917-2923.

[38] https://energy.gov/energysaver/geothermal-heat-pumps

[39] Shen, P., &Lukes, J. R. (2015). Impact of global warming on performance of ground source heat pumps in US climate zones. Energy Conversion and Management, 101, 632-643.

[40] Döring, B., Kendrick, C., & Lawson, R. M. (2013). Thermal capacity of composite floor slabs. Energy and Buildings, 67, 531-539.

[41] Walsh, R., Kenny, P., and Brophy, V. (2006) Thermal mass & sustainable building, Improving energy performance and occupant comfort. Irish Concrete federation.

[42] Choubane, B. and M. Tia, (1995), “Analysis and Verification of Thermal-Gradient Effects on Concrete Pavement,” Journal of Transportation Engineering, Vol.121, No. 1, pp. 75-81.

[43] http://nepuh.com/heat-pump-anatomy/

[44] Kavanaugh, S. P., & Rafferty, K. (1997). Ground-source heat pumps: design of geothermalsystems for commercial and institutional buildings. American Society of Heating, Refrigerating and Air-Conditioning Engineers.

[45] http://www.prostar-mechanical.com/radiant_floor/radiant_floor.htm

[46] http://www.findanyfloor.com/RadiantFloorHeating/RadiantHeatingInformation.xhtml

[47] “ANSYS Theory Reference: Analysis tools”, 001099, 9th ed. SAS IP, Inc.

[48] ANSYS Thermal Analysis: Tutorial for Rev. 5.0, DN-T031:50, 6., 1992.

[49] Dahmani, L. (2011). Thermomechanical response of LNG concrete tank to cryogenic emperatures. Strength of materials, 43(5), 526-531.

[50] Ozisik, M.N. (1985). Heat transfer: A basic approach. McGraw-Hill, London.

[51] Mattsson, I., & Fries, G. (1997). RADIANT HEAT WITH CONCRETE. Concrete Technology Today, 18(PL971. 01B).

[52] Niu, J. L., Zhang, L. Z., &Zuo, H. G. (2002). Energy savings potential of chilled-ceiling combined with desiccant cooling in hot and humid climates. Energy and Buildings, 34(5), 487-495.

[53] Feustel, H. E., &Stetiu, C. (1995). Hydronic radiant cooling—preliminary assessment. Energy and buildings, 22(3), 193-205.

[54] Imanari, T., Omori, T., &Bogaki, K. (1999). Thermal comfort and energy consumption of the radiant ceiling panel system: Comparison with the conventional all-air system. Energy and buildings, 30(2), 167-175.

[55] Stetiu, C. (1999). Energy and peak power savings potential of radiant cooling systems in US commercial buildings. Energy and buildings, 30(2), 127-138.

[56] Rhee, K. N., & Kim, K. W. (2015). A 50 year review of basic and applied research in radiant heating and cooling systems for the built environment. Building and Environment, 91, 166-190.

[57] Ma, H., Li, C., Lu, W., Zhang, Z., Yu, S., & Du, N. (2016). Investigation on a solar-groundwater heat pump unit associated with radiant floor heating. Renewable and Sustainable Energy Reviews.

[58] Hepbasli, A. (2002). Performance evaluation of a vertical ground-source heat pump system in Izmir, Turkey. International Journal of Energy Research, 26(13), 1121-1139.

[59] Hwang, Y., Lee, J. K., Jeong, Y. M., Koo, K. M., Lee, D. H., Kim, I. K., ...& Kim, S. H. (2009). Cooling performance of a vertical ground-coupled heat pump system installed in a school building. Renewable Energy, 34(3), 578-582.

[60] Weitzmann, P., Kragh, J., Roots, P., &Svendsen, S. (2005). Modelling floor heating systemsusing a validated two-dimensional ground-coupled numerical model. Building and Environment, 40(2), 153-163.

[61] Jin, X., Zhang, X., & Luo, Y. (2010). A calculation method for the floor surface temperature in radiant floor system. Energy and Buildings, 42(10), 1753-1758.

[62] Olesen, B. W. (2002). Radiant floor heating in theory and practice. ASHRAE journal, 44(7), 19.

[63] Lim, J. H., Jo, J. H., Kim, Y. Y., Yeo, M. S., & Kim, K. W. (2006). Application of the control methods for radiant floor cooling system in residential buildings. Building and Environment, 41(1), 60-73.

[64] ISO, ISO 11855-1:2012(E) Building Environment Design-Design, Dimensioning, Installation and Control of Embedded Radiant Heating and Cooling Systems. Part 1: Definition, Symbols, and Comfort Criteria, International Organization for Standard, Switzerland, 2012.

[65] Song, G. S. (2005). Buttock responses to contact with finishing materials over the ONDOL floor heating system in Korea. Energy and Buildings, 37(1), 65-75.

[66] Olesen, B. W., & Parsons, K. C. (2002). Introduction to thermal comfort standards and to the proposed new version of EN ISO 7730. Energy and buildings, 34(6), 537-548.

[67] MdAzreeOthumanMydin, (2013) Simplified Explicit Model to Measure Transient Heat Transfer in Foamcrete Panel System, Australian Journal of Basic and Applied Sciences, 7(7): 1-13. ISSN 1991-8178.

[68] Jin, X., Zhang, X., Luo, Y., & Cao, R. (2010). Numerical simulation of radiant floor cooling system: The effects of thermal resistance of pipe and water velocity on the performance. Building and Environment, 45(11), 2545-2552.

[69] http://www.fluxteq.com/

[70] Langley, L. W., Barnes, A., Matijasevic, G., & Gandhi, P. (1999). High-sensitivity, surface-attached heat flux sensors. Microelectronics journal, 30(11), 1163-1168.

[71] Meeting with Mr. Rosner (Director of Energy Management, Oklahoma State University) about rate structure of OSU/OG&E wind farm on 10/30/2015.

[72] Bean, R., &ArchD, K. W. K. (2010). Part 2: History of Radiant Heating & Cooling Systems. Ashrae Journal, 52(2), 50.

[73] Rhee, K. N., Olesen, B. W., & Kim, K. W. (2017). Ten questions about radiant heating and cooling systems. Building and Environment, 112, 367-381.

[74] Rijksen, D. O., Wisse, C. J., & Van Schijndel, A. W. M. (2010). Reducing peak requirements for cooling by using thermally activated building systems. Energy and buildings, 42(3), 298-304.

[75] Yeo, M. S., Yang, I. H., & Kim, K. W. (2003). Historical changes and recent energy saving potential of residential heating in Korea. Energy and Buildings, 35(7), 715-727.

[76] Zhuang, Z., Li, Y., Chen, B., &Guo, J. (2009). Chinese kang as a domestic heating system in rural northern China—a review. Energy and Buildings, 41(1), 111-119.

[77] Olesen, B. W. (2002). Radiant floor heating in theory and practice. ASHRAE journal, 44(7), 19.

[78] Zaheer-uddin, M., Zhang, Z. L., & Cho, S. H. (2002). Augmented control strategies for radiant floor heating systems. International journal of energy research, 26(1), 79-92..

[79] Chen, T. Y. (2002). Application of adaptive predictive control to a floor heating system with a large thermal lag. Energy and Buildings, 34(1), 45-51.

[80] Heier, J., Bales, C., & Martin, V. (2010). Energy Efficiency through Thermal Energy Storage-Evaluation of the Possibilities for the Swedish Building Stock, Phase 1. In Clima2010, Antalya, Turkiet, 9-12 maj, 2010.

[81] Reiss, E., Mears, D. R., Manning, T. O., Wulster, G. J., & Both, A. J. (2007). Numerical modeling of greenhouse floor heating. Transactions of the ASABE, 50(1), 275-284.

[82] CIBSE, CIBSE Guide B-heating, (2007). Ventilating, Air Conditioning and Refrigeration: the Chartered Institution of Building Services Engineers, London.

[83] Feustel, H. E., &Stetiu, C. (1995). Hydronic radiant cooling—preliminary assessment. Energy and buildings, 22(3), 193-205.

[84] Olesen, B. W. (2002). Radiant floor heating in theory and practice. ASHRAE journal, 44(7), 19.

[85] Tian, Z., & Love, J. A. (2008). A field study of occupant thermal comfort and thermal environments with radiant slab cooling. Building and Environment, 43(10), 1658-1670.

[86] Corgnati, S. P., Perino, M., Fracastoro, G. V., & Nielsen, P. V. (2009). Experimental and numerical analysis of air and radiant cooling systems in offices. Building and Environment, 44(4), 801-806.

[87] Lin, B., Wang, Z., Sun, H., Zhu, Y., & Ouyang, Q. (2016). Evaluation and comparison of thermal comfort of convective and radiant heating terminals in office buildings. Building and Environment, 106, 91-102.

[88] ANSI/ASHRAE. Standard 55, (2010). Thermal Environmental Conditions for Human Occupancy, American Society of Heating, Refrigerating, and Air-Conditioning

Engineers, Altanta, GA.

[89] ISO, ISO 7730: Ergonomics of the Thermal Environment-Analytical Determination and Interpretation of Thermal Comfort Using Calculation of the PMV and PPD Indices and Local Thermal Comfort Criteria, International Organization for Standardisation, Switzerland, 2005.

[90] Athienitis, A. K. (1997). Investigation of thermal performance of a passive solar building with floor radiant heating. Solar energy, 61(5), 337-345.

[91] Self, S. J., Reddy, B. V., & Rosen, M. A. (2013). Geothermal heat pump systems: Status review and comparison with other heating options. Applied Energy, 101, 341-348.

[92] Ren, J., Zhu, L., Wang, Y., Wang, C., &Xiong, W. (2010). Very low temperature radiant heating/cooling indoor end system for efficient use of renewable energies. Solar Energy, 84(6), 1072-1083.

[93] Koschenz, M., &Dorer, V. (1999). Interaction of an air system with concrete core conditioning. Energy and Buildings, 30(2), 139-145.

[94] Lehmann, B., Dorer, V., &Koschenz, M. (2007). Application range of thermally activated building systems tabs. Energy and buildings, 39(5), 593-598.

[95] Gwerder, M., Lehmann, B., Tödtli, J., Dorer, V., &Renggli, F. (2008). Control of thermally-activated building systems (TABS). Applied energy, 85(7), 565-581.

[96] Olesen, B. W., De Carli, M., Scarpa, M., &Koschenz, M. (2006). Dynamic Evaluation of the Cooling Capacity of Thermo-Active Building Systems. ASHRAE transactions, 112(1).

[97] Olesen, B. W., Sommer, K., &Duchting, B. (2002). Control of slab heating and cooling systems studied by dynamic computer simulations. ASHRAE Transactions, 108, 698.

[98] Olesen, B. W. (2012). Thermo active building systems using building mass to heat and cool. Ashrae Journal, 54(2), 44-52.

[99] Ryu, S. R., Lim, J. H., Yeo, M. S., & Kim, K. W. (2004). A Study on the Control Methods for Radiant Floor Heating and Cooling System in Residential Building. ASHRAE Transactions, 110(2).

[100] ARCHD, K. W. K., &Olesen, B. W. (2015). Part One: Radiant Heating and Cooling Systems. ASHRAE Journal, 57(2), 28.

[101] Shin, M. S., Rhee, K. N., Ryu, S. R., Yeo, M. S., & Kim, K. W. (2015). Design of radiant floor heating panel in view of floor surface temperatures. Building and Environment, 92, 559-577.

[102] Cho, S. H., &Zaheer-Uddin, M. (1999). An experimental study of multiple parameter switching control for radiant floor heating systems. Energy, 24(5), 433-444.

APPENDICES

Appendix: A

Mass Floor Modeling with Steel and without steel (60ºC heating load)

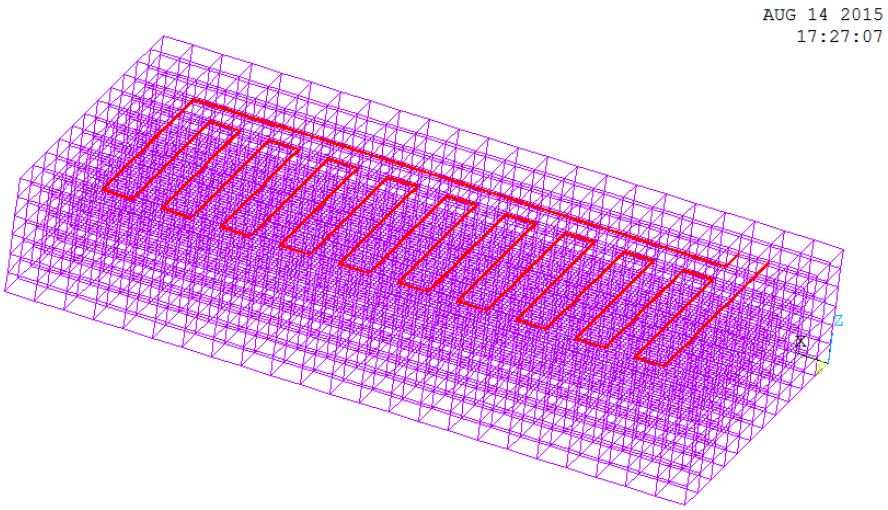

Fig A.1. Concrete and piping system modeling (No steel)

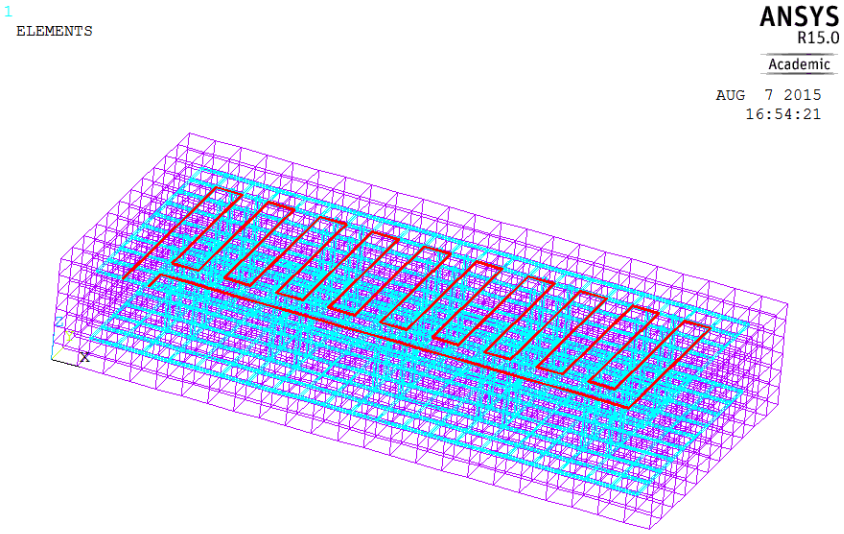

Fig A.2. Concrete, steel, piping system modeling

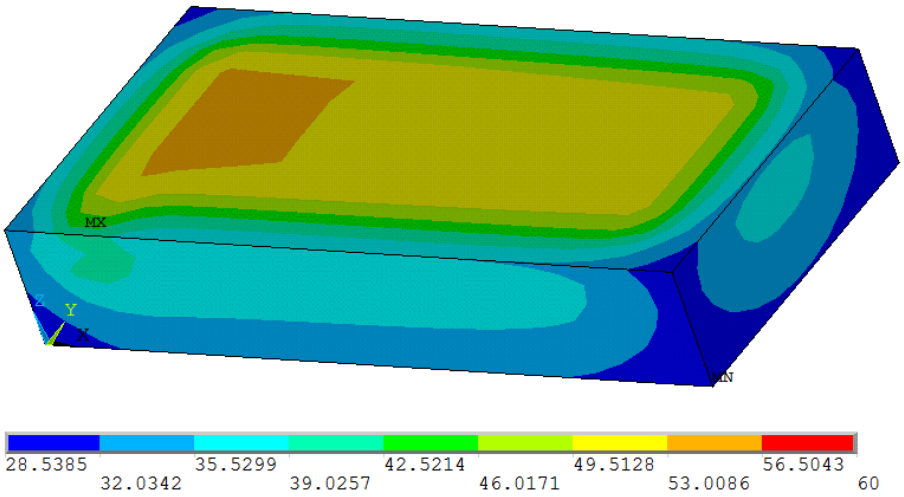

Fig A.3. Temperature distribution in Concrete and piping system modeling (No steel)

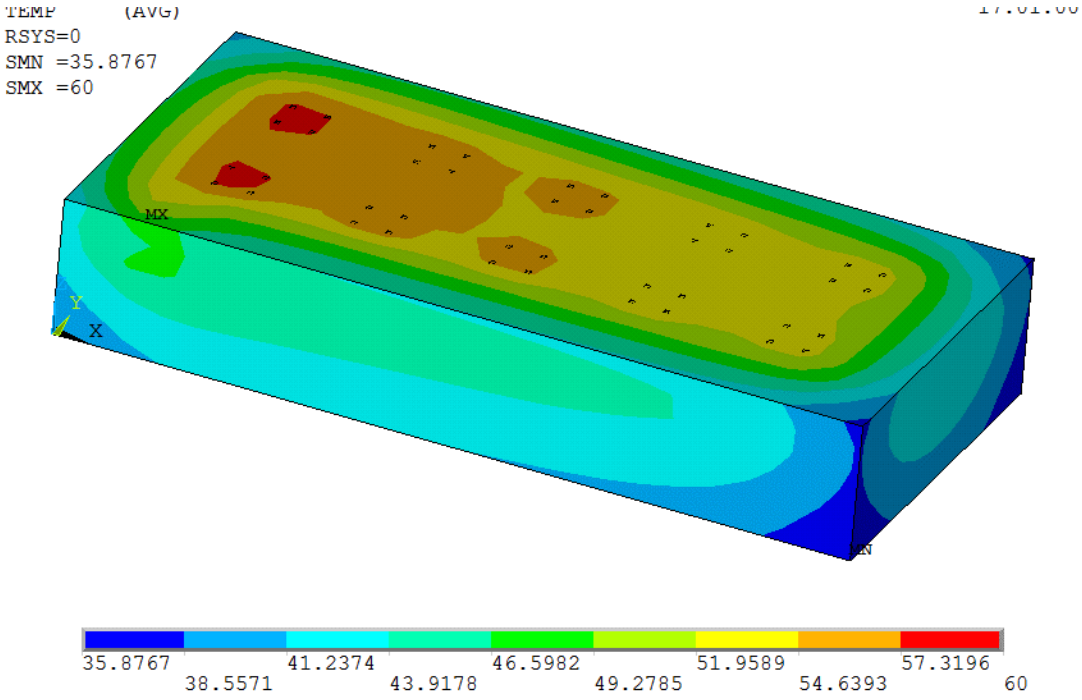

Fig A.4. Temperature distribution in Concrete, steel, piping system modeling

Appendix: B

Two different Layout Pattern on heating pipe system Heat Piping position in the slab (60ºC heating)

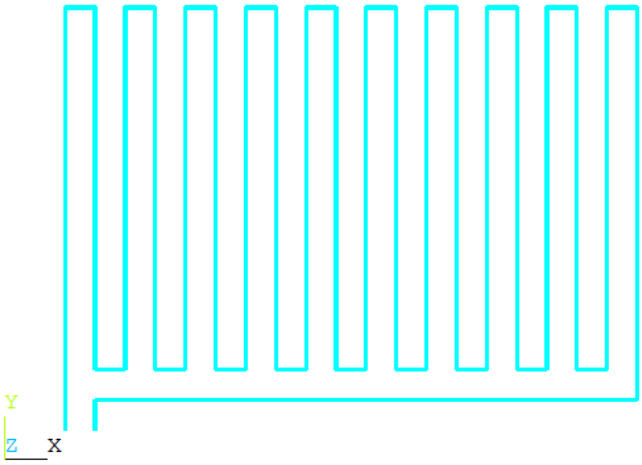

Fig B.1. Piping layout (Case 1)

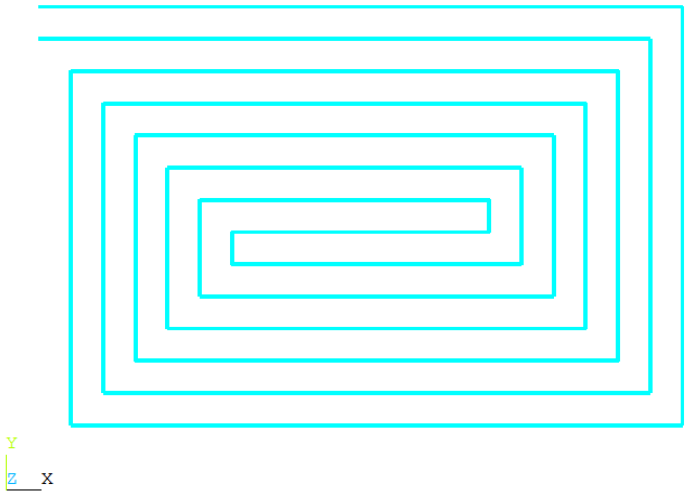

Fig B.2. Piping layout (Case 2)

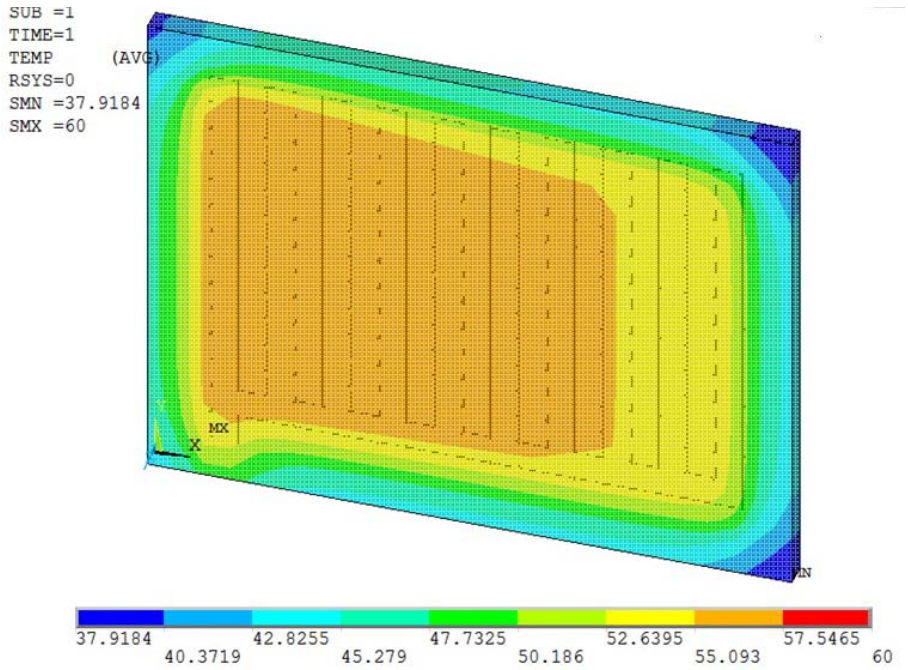

Fig B.3. Temperature distribution in the 7 in slab (Piping layout Case 1)

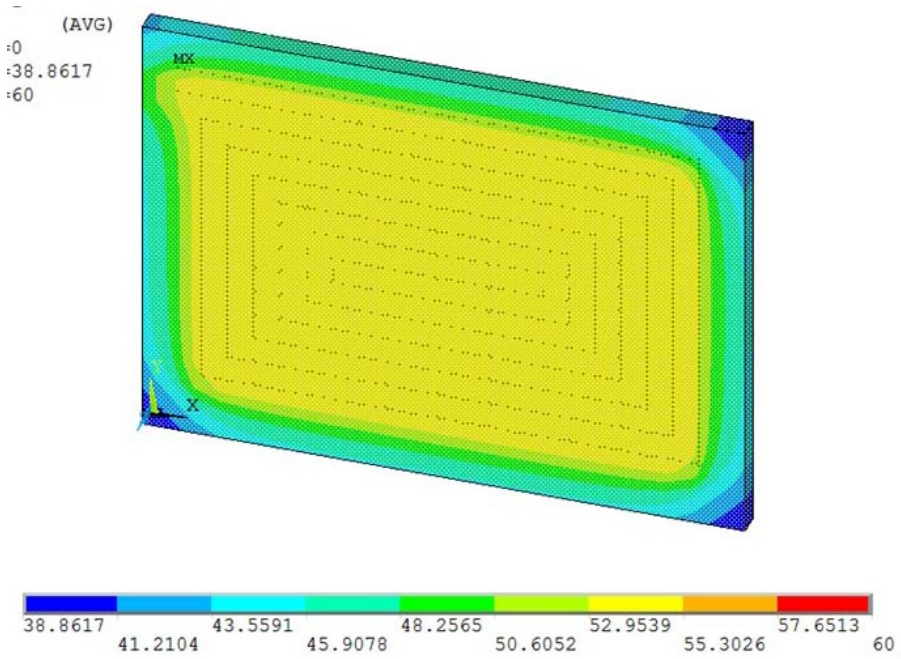

Fig B.4. Temperature distribution in the 7 in slab (Piping layout Case 2)

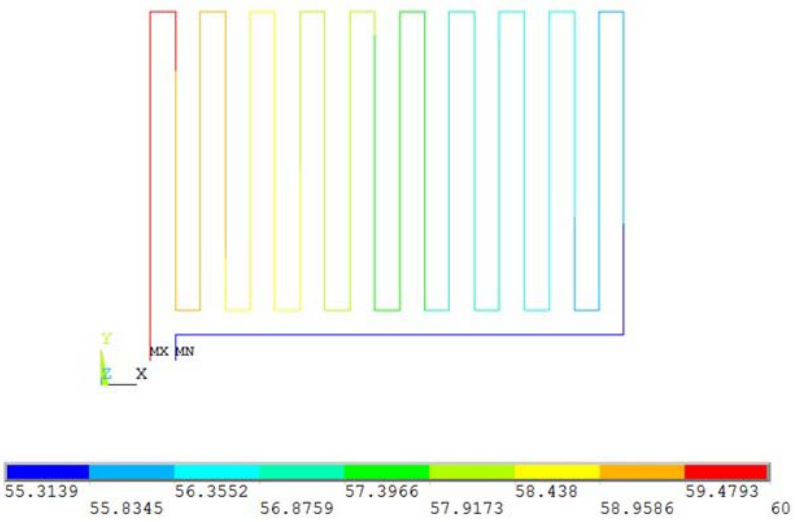

Fig B.5. Temperature distribution in piping system (layout Case 1)

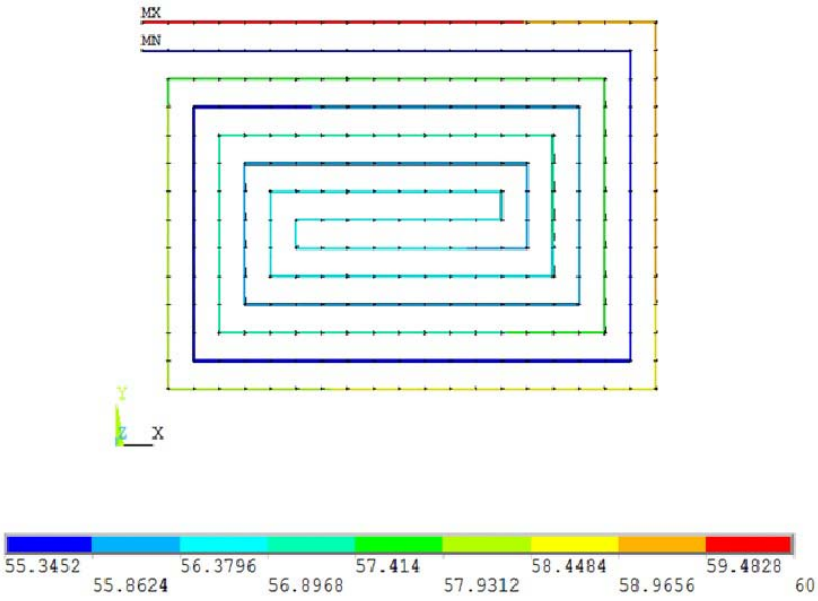

Fig B.6. Temperature distribution in piping system (layout Case 2)

Discussion:

- Case 2 has lower and higher pipe temp together. (Every two sequential pipes near each other).
- Case 1: Higher temperature concentration is happened at input and lower temperature at the outlet of the pipe system.
- Lowest temperature in Case 2 slab is higher than Case 1. It means the slab is heated more.
- Case 2 temperature is more evenly distributed at the surface.
- Case 2 has higher thermal flux. (13%)
- Case 2 has higher Energy. (2%)
- Case 2 has higher Heat Flow. (20%)
- Case 2 is recommended for heat tubing layout on the 7 in concrete floor.

Appendix: C

Concreteworks Results:

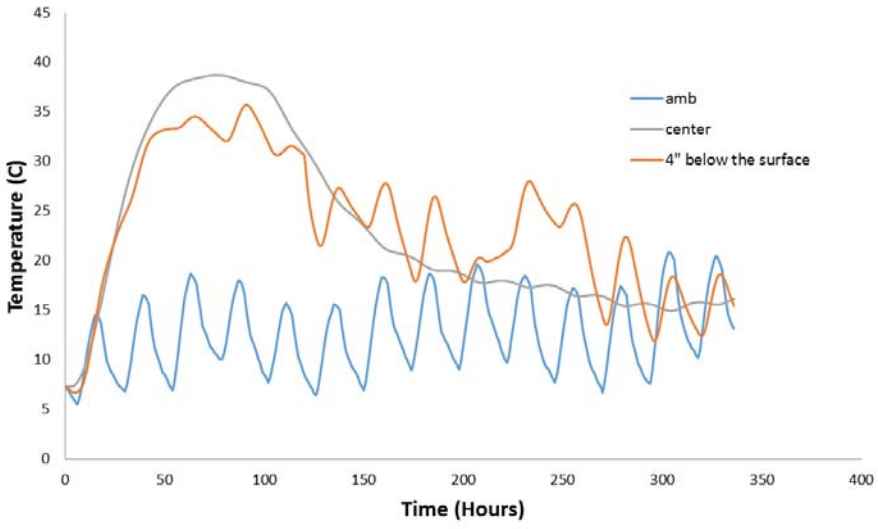

Fig C.1. Concreteworks temperature distribution with software weather data

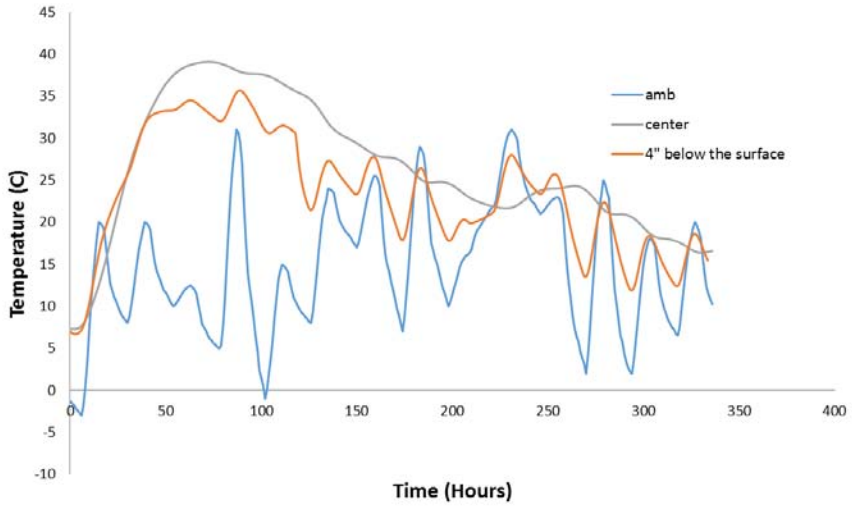

Fig C.2. Concreteworks temperature distribution with job site weather data

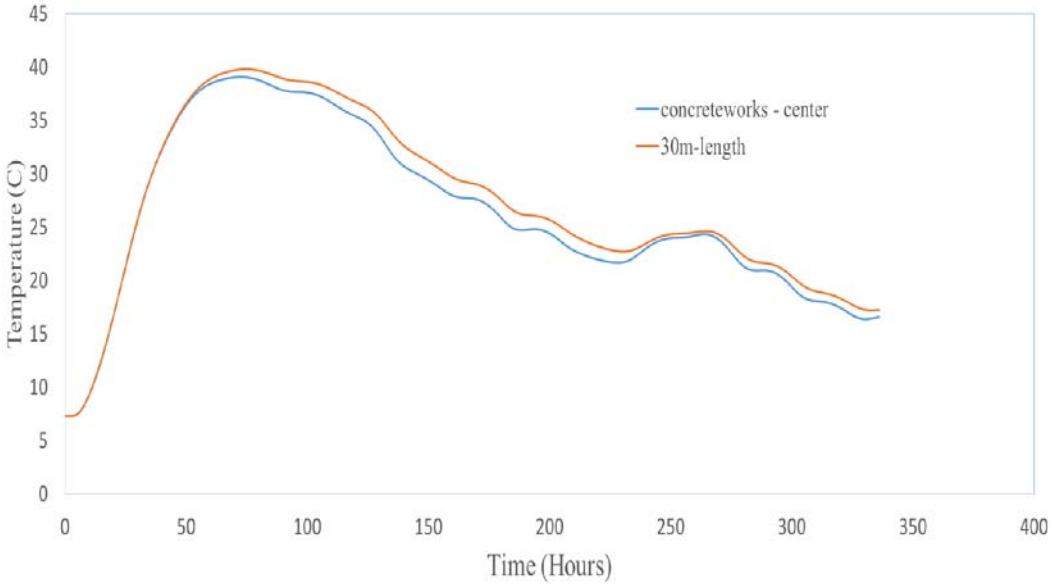

Fig C.3. Comparison of temperature gradient for center point (different length of 10m or 30m)

Appendix: D

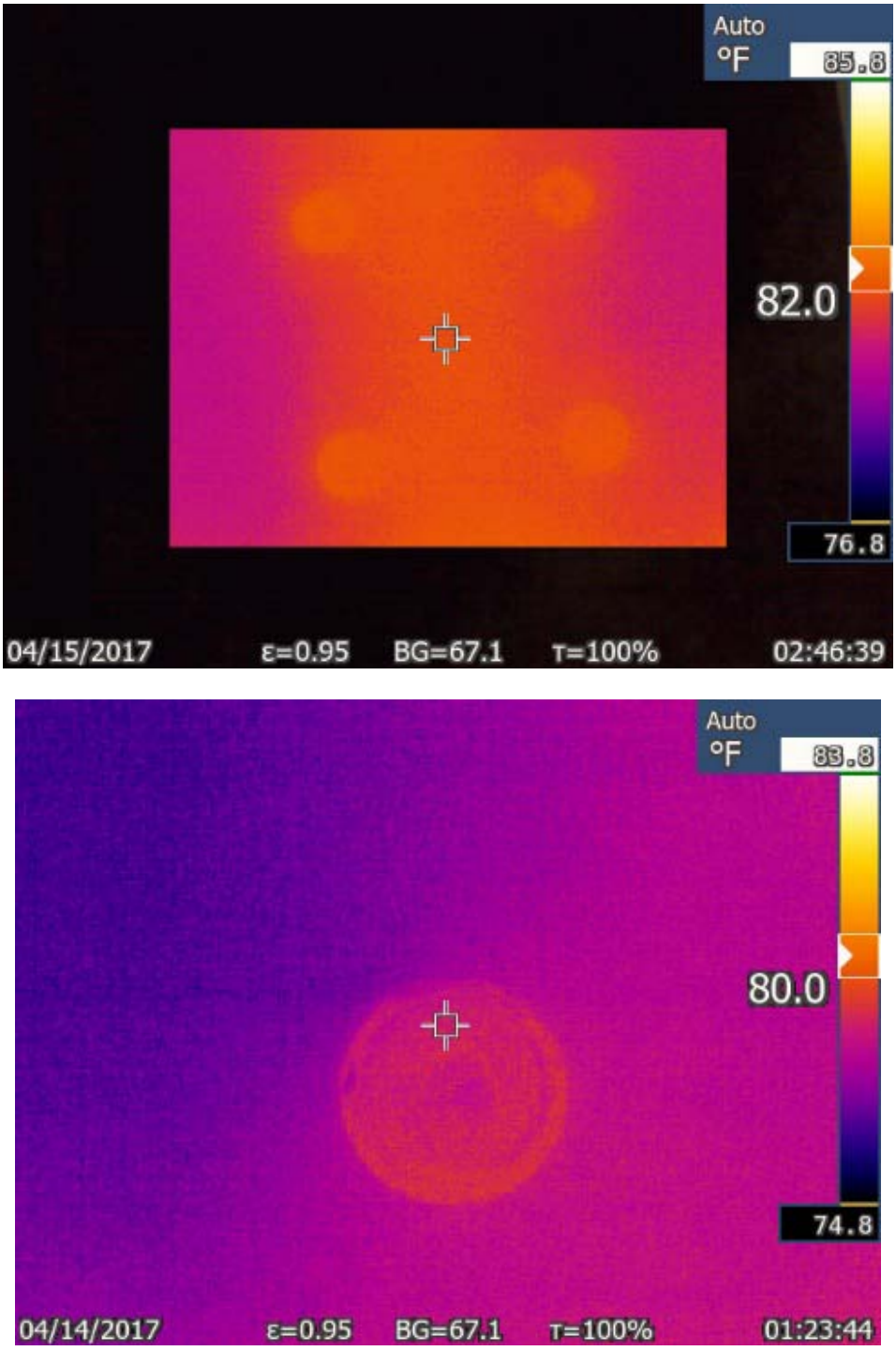

D.1. Thermal images of radiant floor

VITA

MOHAMMAD TAHERSIMA

Candidate for the Degree of

Doctor of Philosophy

Thesis: MODELING HEAT TRANSFER IN MASS CONCRETE FLOORS WITH RADIANT HEAT FROM GROUND SOURCE SYSTEMS

Major Field: Civil Engineering

Biographical:

Education:

Completed the requirements for the Doctor of Philosophy/Education in Civil Engineering at Oklahoma State University, Stillwater, Oklahoma in May, 2017.

Completed the requirements for the Master of Science in Civil Engineering at Iran University of Science and Technology, Tehran, in 2011.

Completed the requirements for the Bachelor of Science in Civil Engineering at University of Tehran, Tehran, in 2008.

Experience:

Member of American Concrete Institute (ACI)
American Society of Civil Engineering (ASCE)